Title

Modulation of neurophysiology at neuromuscular junctions: effects of the pesticide ziram and the role of glutamate in muscle contraction

Author

Jensen, Jenna L

Publication Date

2020

Peer reviewed|Thesis/dissertation

University of California

Los Angeles

Modulation of neurophysiology at neuromuscular junctions: effects of the pesticide ziram and the role of glutamate in muscle contraction

A dissertation submitted in partial satisfaction of the

requirements for the degree of Doctor of Philosophy

in Molecular Toxicology

by

Jenna Harrigan

2021

ABSTRACT OF THE DISSERTATION

Modulation of neurophysiology at neuromuscular junctions: effects of the pesticide ziram and the role of glutamate in muscle contraction

by

Jenna Harrigan

Doctor of Philosophy in Molecular Toxicology

University of California, Los Angeles, 2021

Professor David E. Krantz, Chair

Drosophila neuromuscular junctions are powerful models for the investigation of synaptic and neuronal circuit function as well as the regulation of muscle contraction. We have used the well- characterized larval neuromuscular junction (NMJ) as a model to investigate the neurophysiological effects of ziram and other pesticides linked to Parkinson's Disease. Using electrophysiology and calcium imaging, we show that ziram alters two separate aspects of neurophysiology by disrupting two distinct pathways. It causes an increase in synaptic vesicle release at least in part through disruption of the protein ubiquitination pathway. Secondly, ziram enhances excitability at both aminergic and glutamatergic neurons by blocking either directly or indirectly the *eag* family of potassium channels. We additionally use the adult reproductive tract NMJ to investigate the regulation of muscle contraction by the excitatory transmitter glutamate. We show that ionotropic and metabotropic glutamate receptors have a distinct pattern of expression on the reproductive tract muscle and in local neurons. Ionotropic receptors are expressed in the muscle cells and are important for the initial glutamate-induced muscle

contraction. By contrast, metabotropic glutamate receptors are expressed only in local cells extrinsic to the muscle and are important for the rhythmic pattern of activity underlying muscle contraction. We suggest that cells expressing the metabotropic receptor may relay signals from neurons to the muscle and be important for modulation of muscle activity.

This dissertation for Jenna Harrigan is approved.

Patrick Allard

Jeffrey Michael Donlea

David E. Krantz

Oliver Hankinson

Felix Erich. Schweizer

University of California, Los Angeles

2021

Table of Contents

List of Figures

List of Tables

Acknowledgements

First of all, I am very thankful for my mentors, **Dr. David Krantz and Dr. Felix Schweizer**. I was lucky enough to end up in the labs of two of the most intelligent and nicest human beings I know. I always learn something when I speak to them and they bring an enthusiasm to scientific experiments and concepts like no other scientists I have met. I enjoy that they constantly bring new creative ideas to the lab, and their enthusiasm is very contagious. Dr. Krantz has generously taken me into his lab with no prior neuroscience background and provided me the opportunity to work on interesting projects, to think about important questions, and thrive in his lab. He has provided me with the intellectual and material resources to learn and accomplish what I needed to become a toxicologist and neuroscientist. Dr. Felix Schweizer is one of the most genuine and caring person I ever met and he brings his excitement for neuroscience to the lab in a way that could convince anyone that a single experiment or analysis is the most exciting thing in the world. He has increased my confidence as a scientist, treating me as a colleague and encouraging discussion of ideas from neurons to food and travel. My mentors have taught me that you can make your own tools to achieve what you want with experiments and to get creative to constantly be improving upon your experimental design. They always welcomed questions with an “open door” policy that made them available for scientific discussion and insight.

I would like to acknowledge all of the members of my committee, **Dr. Jeff Donlea, Dr. Patrick Allard, and Dr. Oliver Hankinson**, as they have provided me with a high level of scientific feedback and guidance along my path as a doctoral student.

Dr. Sonali Deshpande taught me so much from dissections to giving presentations and that it is possible to be simultaneously a great mom and successful scientist. She believed in my

potential as a member of the lab and pushed me when I was ready to give up. She introduced me to the world of Drosophila and could always take the time to answer my questions. Sonali is a strong female role model to me and all the young scientists that she takes her time to mentor.

Daisy Brambila has been my experiment partner in crime, bringing lots of laughs and fun to lab every day. She is an observant and creative scientist and I am so proud of her on her way to becoming an amazing doctor. Her strong ability to learn any experimental technique quickly and ability to think about the results, even from “accident” experiments, accelerated our lab’s discoveries and pushed our publication forward. I have learned to be more thoughtful about my results from her and I strive to be as organized as she so effortlessly is.

Dr. Aditya Eamani is a very kind person who always supplied me with what I needed for experiments, prepared my flies, and taught me several techniques. Her support and kind words helped me on good and bad experiment days. **Dr. Meera Pratap** is a truly caring person who is a mentor to me, and to all the scientists in our lab and most other labs as well. She is inspirational as a skillful electrophysiologist and chef. Thank you to **Ethan Rohrbach, Dr. Shivan Bonano, Dr. Kathy Meyers, and Dr. James Asuncion** for your valuable suggestions in lab meetings and useful insights throughout my graduate career. I want to thank **Dr. Maureen Sampson** for alwys bringing a happy face into lab and being my Toxicology advisor. I am so grateful to have had **Dijana Vojnivic** work alongside me, motivating me to keep going while I watched her take on ten things at once and empathizing with me when the electrophysiology spirits were against us. Thank you **Julianne Yang** for making me take breaks, working with me at Starbucks, and the motivational talks when graduate school seemed too difficult. I had the opportunity to work with fantastic undergraduates as well: **Dake Huang** taught me the larval NMJ dissection and always brought a happy face to lab and started interesting conversation in the Schweizer lab, scientific or otherwise; **Deepna Chand** is always ‘stirring the pot’ and

keeping things interesting in lab and I enjoy seeing her quickly pick up any experimental technique; **Sarah Maraach** enthusiastically learned a dissection in a day that took me months to do well and gives 100% effort in all of her work, and is always happy to help with my experiments; **Elise Denghausen** has been a delight to conduct experiments with and I know she will excel in grad school; **Allen Chen** keeps me on my toes with thoughtful questions and a determination to improve upon his experiments.

I was very fortunate to have met and worked these and other amazing scientists who made me excited to come in to lab, encouraged me through days of failed experiments, and who made every little success that much more thrilling.

My sister **Holly** has always been a huge support in my life, and is the most understanding person. She encourages me to pursue my interests and be the “weird one” in our family. She is always happy to listen to every detail about my current projects despite not being in the sciences and is genuinely interested in new things I have learned. She reminds me that I am a strong woman scientist and how cool it is that I am going to be a doctor. Holly has always been there to help me with homework or any project I am working on late at night, especially if it involves an artistic touch, even if it is just staying up making me laugh while I work. I met my husband **Brent** at UC Davis in the college dorms and since then he has supported and helped me in all aspects of my academic journey. He always tells people that I am the “smart one” and truly believes in me as a scientist and academic. He enjoys discussing “science” with me and reminds me to enjoy all aspects of life outside of academia as well. Brent knows how to make bad days happy and makes me a more confident scientist and mother. He is the best husband and dad and I got very lucky with him. **Kibeth**, my hound, is a light in my life, and the best at-home working companion. I thank my **mom Juanita** for encouraging my love for biology by showing me how to care for several of my farm animals, bringing me to all my 4-H meetings,

and always being there to talk to. And last but certainly not least, I thank my **dad Mark** who supported me through school and always reminds me that he is proud of me going to college.

Vita

EDUCATION

2015- Anticipated 2020 Ph.D. Molecular Toxicology

University of California, Los Angeles, CA

2013-2015 M.S. Nutritional Sciences

University of Washington, Seattle, WA

2007-2011 B.S. Animal Sciences

University of California, Davis, CA

RESEARCH EXPERIENCE

2015- Current

Graduate Student

Department of Molecular Toxicology, University of California, Los Angeles

Advisor: David Krantz, M.D., Ph.D. and Felix Schweizer, Ph.D.

My Ph.D. dissertation focuses on the neurophysiological effects and mechanisms of pesticides linked to Parkinson's Disease risk. Using an open-ended approach to investigate novel pathways that may contribute to the etiology of Parkinson's Disease and other complex diseases, we found that the pesticide ziram increases excitability through inhibition of the *eag* family of potassium channels. A second focus aims to identify the role of glutamate in the coordination of visceral muscle contraction. We find that metabotropic and ionotropic glutamate receptors both contribute to the electrical activity of visceral muscle and suspect that metabotropic receptor- expressing cells on the muscle may regulate rhythmic activity similar to interstitial cells in mammalian smooth muscle.

2013-2015

Master's Student

Department of Nutritional Sciences, University of Washington, Seattle

Advisor: Michael Rosenfeld, Ph.D.

My M.S. thesis examined the role of diesel exhaust exposure *in-utero* on adult susceptibility to atherosclerosis in hyperlipidemic mice to test whether there are developmental origins of this disease with a restricted environmental exposure. We investigated whether toxicant exposure during a restricted time window of development rather than chronic exposure to a complex combination of environmental and genetic factors is sufficient to trigger long-term metabolic disease risk.

2012-2013

Research Assistant

Biosurg, Inc., Winters, CA

I monitored and recorded animal behaviors and health (vitals, food consumption, etc.) of laboratory animals used in trials for the safety and effectiveness of medical devices (pacemaker devices, satiation devices, etc.) and communicated with sponsors about animal health and technology operations. I assisted veterinarians with routine laboratory animal health care procedures (administer medicine, restraint, blood collections, etc.)

Introduction: **Basic principles in neurophysiology and modulation of neuromuscular junctions by pesticides and glutamate**

Basic Principles in Neurophysiology: Ion Channels and Neuronal Excitability in Drosophila

The Hodgkin-Huxley action potential model was the first to describe how voltage-dependent variability in ion permeability form the basis for neuronal communication (Barnett and Larkman, 2007; Barker, 2017). This permeability varies with the distinct set of ion channels in each cell membrane, setting both the resting membrane potential (RMP) of neurons and their ability to fire an action potential, or its excitability. The sodium (Na) and potassium (K) gradients are a product of active ion pumps that develop and maintain a large outward K and inward Na gradient. K channels are the primary channel open at rest and thus determine most neurons' RMP near the K equilibrium potential (Barker, 2017; Chen et al., 2018). Chloride (Cl) channels are also important contributors to the RMP and synaptic transmission in neurons. They are additionally important for inhibition of neurotransmission especially in the context of a neuronal circuit since they gate negative ions. Voltage-gated Na channels open as the cell depolarizes to cause the action potential upstroke (Barnett and Larkman, 2007). The action potential propagation down the nerve leads to opening of presynaptic calcium (Ca) channels, specifically of the *cacophony* Ca channels in flies that cluster close to the neuron's active zone where vesicles are released. Flies have four pore forming Ca channel subunit genes homologous to the vertebrate L-, N-, and T-type channels, but the main regulator of presynaptic release, *cacophony* (N-type Ca channel in vertebrates) Ca channels, surround vesicles ready at the active zone. Inflow of Ca, which binds to a calcium sensing protein, triggers neurotransmitter release. The spacing between these voltage gated Ca channels and vesicles ready to be released at the active zone strongly influences synaptic release properties (Sudhof and Rizo, 2011; Sudhof, 2013; 2020b). The tight coupling of calcium influx and electrical activity allow us to use the calcium indicator GCaMP as a proxy for neuronal activity. While GCaMP provides the advantage of cell type specificity and accessibility, the Ca handling dynamics and diverse Ca

signaling among different neuron types needs to be taken into account (Akerboom et al., 2012; Xing and Wu, 2018). By contrast, electrophysiological methods typically still provide better temporal resolution but lack the genetic precision of calcium imaging methods. While action potentials are generated by voltage-gated Na channels, thirty different types of K channels in flies (differentially regulated by several beta subunits) set the excitability properties of cells, which include the threshold potential, action potential time duration, after-hyperpolarization potentials, spontaneous depolarizations, or action potential bursting patterns. K channels fit these roles because there are several diverse types which differ in their gating properties, their voltage-dependence, and their modulation (Frolov, 2012; Jan and Jan, 2012). As key determinants of cell excitability, K channels provide stability and at the same time allow for plasticity within neuronal networks.

While an important function of all cells is communication, neurons have evolved unique abilities for fast, long distance, spatially complex communication via electrochemical signals. The action potential is a transitory reversal in the membrane potential polarity due to transient changes in ion permeability, which initiates at highly Na dense regions of neurons, typically at the axon initial segment, and travels down the axon to the terminals (Wicher et al., 2001; Ainsley, 2003). Since the initial depolarizing phase of the action potential is mediated by an increase in Na permeability, blocking of the Na channels with tetrodotoxin (TTX) prevents action potential initiation and only action potential- independent events can occur (MN et al., 2016). Action potentials can be evoked experimentally by applying a brief electrical current to the outside of the nerve, promoting a local disturbance in the axon membrane potential to induce an opening of a few Na channels and a depolarizing response. A few voltage-gated Na channels (flies have two pore-forming subunit genes which undergo alternative splicing to form 48 variants), open in response to a local depolarization of the cell since these channels are voltage sensitive, and the influx of Na adds to the depolarization. If the membrane potential depolarizes to a certain

amount, this leads to rapid regenerative recruitment of adjacent voltage-gated Na channels on the axon, and a full action potential is generated in an all-or-nothing fashion.

Neuromuscular junctions

Similar to neurons, muscle resting membrane potential is also set by K, Cl, Na, and Ca permeability through their respective channels (Wicher et al., 2001). However, the depolarizing muscle potentials are carried by voltage-gated L-type Ca channels rather than voltage-gated Na currents, and larval muscles generate graded rather than the typical fast action potentials of neurons (Peron et al., 2009). The larger number of K channels in these muscles decreases the Ca depolarizing effects to allow for only subthreshold regenerative potential spiking, which is a characteristic of the slow contracting supercontractile muscles at the NMJ.

Rather than “skeletal” or “smooth” muscle types, *Drosophila* muscle is all striated and can be categorized as tubular, indirect flight muscles (IFM), or supercontractile muscles. Most adult fly muscles are tubular, which connect different parts of the exoskeleton and are made up of rectangular myofibrils. IFMs are made up of circular myofibrils separated by large mitochondria. Supercontractile muscles make up the larval body wall muscles and all visceral organs and are unique in their ability to contract more than 50% below their resting length (Peron et al., 2009).

Although there are some ultrastructural feature differences between *Drosophila* larval muscles and vertebrate striated muscles, the molecular organization of the thick and thin filaments are comparable, indicating that the basic principles of contraction and its regulation are similar. The motor protein in larval muscle is a class II myosin and the main regulator of the contractile response is the *troponin complex* that mediates the thin-filament response to calcium when striated muscular contraction is initiated (Atwood et al., 1993; Peron et al., 2009). The contractile response in the myofibrils of larval muscles is stimulated via an increase of intracellular calcium following depolarization in the muscles. The increase of calcium in the

muscle cell results from an inward current through voltage-dependent calcium channels and to a release of calcium from intracellular stores, but the amount contributed from these two components is unknown. Following the increase in intracellular calcium, it will decrease by efflux through the membrane and by uptake into the sarcoplasmic reticulum through the action of SERCA. *Drosophila* express a single SERCA endoplasmic–sarcoplasmic reticulum calcium pump. The Ryanodine receptor is also critical for contraction in larval and other insect muscles (Peron et al., 2009).

Although the generation and propagation of peristaltic waves has not been fully investigated in *Drosophila*, experiments in insects indicate the essential role of central pattern generators in the central nervous system in most systems (Fox et al., 2006; Peron et al., 2009; Yoshikawa, 2016). The central pattern generator neuronal circuits that regulate rhythmic movements at the larval NMJ are made up of interneurons and motoneurons whose rhythmic activities cause a coordinated pattern of muscle contraction (Fox et al., 2006). These pattern generating neuronal circuits share many characteristics with other invertebrate and vertebrate neuronal systems, and thus may be a good model to investigate the link between neuronal circuits and behavior. Another similarity to mammals is the myogenic transmission of electrical activity in the absence of innervation, which has been demonstrated across the smooth muscle of most mammals and insects, but the mechanisms remain largely unexplored in insects. While visceral muscles in insects are striated, functionally they resemble vertebrate smooth muscles with their slow rhythmic contractions, sensitivity to mechanical stretch and often coordinated peristaltic waves (Miller, 1975). Visceral muscles like mammalian muscles are regulated by an excitatory transmitter- acetylcholine in mammals and glutamate in insects- and are modulated by monoamines and various peptides. In mammal visceral organs such as the gastrointestinal tract, neurons from the central nervous system can modulate muscle activity indirectly through signaling to various intermediary cells, such as Interstitial cells of Cajal, which were originally

described by the neuroscientists Ramon y Cajal and recently their critical functional role in muscle contraction has been illustrated (Klein et al., 2013; S et al., 2013; MG, 2020).

Drosophila models for studying synaptic and neuronal circuit function

The neuromuscular system of Drosophila melanogaster larvae is a well-defined, genetically accessible, and easy to visualize model to understand synaptic function and cell excitability. The system is made up of central pattern generator circuits that integrate inputs and drive output from about 36 motor neurons per ventral nerve cord (VNC) hemisegment innervating body wall muscles through 3 main nerve trunks to produce patterned motor behaviors (Brent et al., 2009; Peron et al., 2009). Each muscle is innervated by glutamatergic type I synapses that trigger contraction through ionotropic glutamate receptors on the muscle. Type I terminals consist of small and big types (Is and Ib) and contain mostly small clear glutamate containing vesicles, but other neuropeptides may be released as well. Type I axons innervate single specific muscle segments, allowing for fine tuning of muscle contraction. Post-synaptically the ionotropic glutamate receptors bind glutamate which depolarizes the muscle and initiates contraction. In contrast, type II synapses release octopamine (OA), analogous to norepinephrine in mammals, (and possibly glutamate) and innervate muscles 12 to 13 among others but not muscle 6 to 7. A third type III synapse that innervates muscle 12 contains large vesicles with insulin-like peptide and other peptides, which, like the amines, modulate contraction and motor pattern generation (Jia et al., 1993; Brent et al., 2009; Peron et al., 2009).

Larval locomotion is produced by waves of neuronal activity initiated by central pattern generating networks of cells. The biogenic amines, OA and tyramine, are thought to play a central role in initiation and regulation of these rhythmic patterns (Fox et al., 2006). Motor behavior is additionally modulated in the central nervous system by various types of interneurons including excitatory cholinergic and inhibitory GABAergic and glutamatergic inputs

as well as by sensory neurons like ppk-positive cells (Fox, 2006; Gorczyca, 2014). The larval NMJ is a powerful model to dissect the various pathways by which muscle activity can be modulated by environmental toxins.

A relatively more complex aminergic-glutamatergic circuit model consisting of direct and indirect pathways that control and coordinate muscle contractions at the reproductive tract is the *Drosophila* egg laying circuit (Rodriguez-Valentin et al., 2006). This system consists of a cluster of nine octopaminergic and two glutamatergic identified neurons in the abdominal ganglion of the ventral nerve cord (*Drosophila* central nervous system) that project to various regions of the reproductive organs (Garner et al., 2018). Target organs of both central and peripheral neurons include ovaries, lateral and common oviducts, uterus, and two types of sperm storage receptacles (Middleton et al., 2006). The reproductive tract regions are differentially innervated with distinct sets of receptors which regulate muscle contraction. The two ILP7 glutamatergic neurons lead to contraction of the common oviduct, while stimulation central octopaminergic neurons leads to contraction of the lateral oviducts. The central and peripheral receptors responsible for regulating these muscle movements is currently being investigated by our lab. There are also peripheral neurons, some of which express the gene pickpocket, and is expressed in mechano-sensory cells that are important for egg laying behavior, but its mechanisms are not fully understood (Lee et al., 2016). The previously proposed “simple” model circuit regulating egg laying behavior is that octopamine leads to relaxation of the reproductive tract muscle while glutamate causes contraction (Rodriguez-Valentin et al., 2006). However, our data implicate a more complex model in which each anatomical region of the reproductive tract is different and contraction can be initiated by both OA and glutamate in a state and region specific manner. There is additionally a distinct pattern of electrical activity underlying contraction in each region of the reproductive tract muscle, which is initiated and regulated by a yet undetermined set of receptors.

Glutamate and monoamines as neuromodulators

Neuromodulation is the process of modification, inhibition, stimulation or therapeutic alteration of electrical or chemical activity in neurons and neuronal networks. Neuromodulation underlies the flexibility of neural circuit function and animal behaviors (Nadim and Bucher, 2014). Multiple neuromodulators can act simultaneously on a neuron, and the intrinsic excitability and synaptic efficacy of neurons are constantly under neuromodulatory influence. While glutamate is the main excitatory neurotransmitter in mammals, aminergic neurotransmitters commonly interact with multiple signaling pathways such as those mediated by glutamate, and modulate most neuronal circuits. Glutamate can also act as a neuromodulator and amines can mediate fast excitatory signaling at some synapses depending on their post-synaptic receptors and other characteristics of each cell (Reiner and Levitz, 2018; Zhang et al., 2019). Diverse ionotropic and metabotropic glutamate receptor families signal in concert to enable the myriad roles of glutamate throughout the nervous system. In *Drosophila*, glutamate is the main peripheral excitatory neurotransmitter and can also act as an inhibitory transmitter through glutamate-gated chloride channels (Cully et al., 1996; L et al., 2004; DiAntonio, 2006). Similarly, a group of aminergic transmitters act on an array of receptor types, which depending on the location of the synapse, downstream biochemical processes, and state of the cell, also initiate a range of responses in neural networks. Several studies have investigated the function of aminergic neuronal clusters in invertebrates and vertebrates, but the function and interaction of each individual neuron that make up these clusters is not known. Recent studies in invertebrates and mammals demonstrate that aminergic cells, which were historically treated as homogeneous clusters that exert uniform effects on cells throughout the brain, have distinct roles in multiple different circuits (Chandler, 2014).

There are several glutamatergic receptors in the fly, broadly categorized into metabotropic and ionotropic receptors. The ionotropic glutamate receptors (iGluR) are ligand-gated channels that open on binding glutamate. Most of these channels conduct cations and so depolarize and excite the postsynaptic cell when opened. The metabotropic glutamate receptors (mGluR) are G-protein–coupled receptors that modulate a variety of second messenger signaling pathways on binding glutamate. Both classes of glutamate receptors are present in *Drosophila*, and both were shown to function at the larval NMJ. The ionotropic receptors mediate fast synaptic transmission at the *Drosophila* NMJ, leading to depolarization of the postsynaptic muscle (Jan and Jan, 1976). mGluRs appear to play a neuromodulatory role at the Drosophila NMJ, regulating the efficacy of short-term plasticity (Bogdanik et al., 2004). The vast majority of studies in Drosophila have focused on ionotropic receptors, as will this chapter.

Ionotropic glutamate receptors form as heteromeric tetramers. Three of these subunits, DGluRIII (also called GluRIIC), DGluRIID, and DGluRIIE, are essential for receptor formation and function. Each receptor also includes a fourth subunit, which can be either DGluRIIA or DGluRIIB. These two receptor subtypeshave different channel properties, synaptic currents, regulation by second messengers, and are localized to different areas (DiAntonio and Hicke, 2004). The B type channel desensitizes about ten times faster than the A type and animals expressing only the B type have a much faster decay time constant (Davis, 1998). In addition, the concentration of A versus B type channels at the NMJ is a key determinant of quantal size (the postsynaptic response to the spontaneous fusion of a single synaptic vesicle) and overexpression of the A type leads to a dose-dependent increase in quantal size. At the NMJ, each motoneuron innervated a postsynaptic site with a different set of glutamate receptor subunits (Marrus et al., 2004). The A type channel is present at the center of the puncta, while IIB is frequently expressed in a ring around each puncta (Peron et al., 2009).

Metabotropic glutamate receptors (mGluRs) are g-protein coupled receptors (GPCRs) that activate intracellular signaling cascades in order to modulate synaptic plasticity and neurotransmission (Conn and Pin, 1997). In mammals, mGluRs exist as 8 different subtypes that can be classified into 3 groups (type I, II, or III) based on their sequence and signal transduction pathways (Niswender and Conn, 2010). Drosophila express DmGluR which is most similar to mammalian Group II mGluRs, and is required for essential behaviors such as learning. There is widespread expression of DmGluR throughout the Drosophila central nervous system. DmGluRs are expressed at the motoneruon terminal the the larval NMJ but their presynaptic function has not been fully elucidated. Glutamate and mGluR agonists applied to the larval NMJ enhances spontaneous mini frequencies, while mGluR antagonists reduce spontaneous synaptic event frequencies, indicating that mGluR acts to increase NMJ synaptic function (Zhang, 2010). However, DmGluR mutants do not have significant changes to their basal transmission and have enhanced facilitation in response to high frequency stimulation (Bogdanik et al., 2004). Thus, DmGluR may be able to decrease glutamate mediated facilitation but this remains inconclusive. Some studies have suggested that Drosophila larval muscles also may express mGluRs, but this has not been demonstrated conclusively, and its role there is unknown.

Ziram and other pesticides

A defining property of neurons is the ability to integrate information, fire action potentials, and communicate with diverse cells to produce complex behaviors. Pesticides, namely those classified as insecticides, herbicides, and fungicides, have been shown to alter these properties in distinct ways in different cell types, which may underlie the epidemiological association between exposure to many of these chemicals and neurodegenerative disease risk (Mostafalou and Abdollahi, 2013; Palmer, 2013; Steenland, 2014). Insecticides frequently target the invertebrate nervous system but can also disrupt human neuronal function. The organochlorine

insecticides, such as dichloro-diphenyl-trichloroethane (DDT) and dieldrin, which remain in the environment despite being banned, cause acute toxicity at high concentration. DDT and another group of insecticides, the pyrethroids, keep Na channels open longer and block chloride channels, and thus are toxic because they cause neuronal hyper-excitability. These and another widely used organophosphate group of insecticides have also been associated with risk for neurodegeneration. Organophosphate pesticides have several neurotransmitter and synaptic enzyme targets that could underlie neurodegenerative diseases processes. Rotenone, a naturally occurring insecticide used in organic farming has been widely used as an animal model of parkinsonism and PD. It is a mitochondrial complex 1 inhibitor and induces oxidative stress and alpha-synuclein accumulation among other hallmarks of PD. Together with rotenone, the herbicide paraquat has been highly reported to enhance neurodegenerative disease risk in epidemiological studies, particularly with PD. Its mechanism of neurotoxicity is not fully understood, but mitochondrial dysfunction, oxidative stress, and inhibition of the ubiquitin-proteasome system have been proposed to play important roles in PD pathogenesis (Baltazar, 2014; Fitzmaurice et al., 2014; Martin et al., 2016; Matei and Trombetta, 2016).

Ziram is a dithiocarbamate fungicide that is widely used to protect crops including stone fruits and almonds from infection and to increase yield. However, ziram and other pesticides have been associated with neurotoxicity, including an increased risk for Parkinson's Disease (PD)-like pathology. Fungicides are derived from a variety of structures including simple inorganic compounds such as copper sulfate to complex organic compounds with sulfur as the most common active ingredient. They are considered to be of low toxicity to mammals and account for under 10% of pesticide application nationally, yet they account for the majority of dietary oncogenic and developmental risk from pesticides and for many severe poisoning epidemics worldwide. One class of fungicides are the dithiocarbamates including ziram, mancozeb, zineb, and maneb. In *Drosophila*, exposure to ziram altered vesicle recycling in glutamatergic and

aminergic synapses, and increased spontaneous calcium events in aminergic cells as measured with calcium and voltage fluorescent indicators. Ziram has several molecular targets, beyond its original known fungicidal action as a Kreb's cycle aconitase inhibitor, which may underlie its neurotoxicity. Ziram inhibits aldehyde dehydrogenase that detoxifies oxidative species and it broadly increases cellular oxidative stress. Other known actions of ziram are a disruption of calcium homeostasis through a sodium calcium exchanger and other cation channels, impairment of mitochondrial function, and a general reduction of sulfhydryl groups in cells. Importantly, ziram is an inhibitor of the ubiquitin activating enzyme, E1 ligase, which is the first step in the protein ubiquitination pathway. The Schweizer lab showed that in both hippocampal and cortical cultured cells, drug inhibitors of E1 ligase, the proteasome, and deubiquitinases all lead to an increase in mini frequency. Ziram, also an inhibitor of E1 ligase, mimicked these ubiquitination inhibitors as it also increased mini frequency, suggesting that one mechanism by which ziram may increase vesicle release is by altering the ubiquitination pattern of vesicle release proteins (Rinetti and Schweizer, 2010). Our aims examine the mechanisms by which ziram alters vesicle release and electrical activity of distinct cell types within a circuit to alter the output of different neuronal systems.

Ziram is a dithiocarbamate fungicide that is widely used to protect crops including stone fruits and almonds from infection and to increase yield. However, ziram and other pesticides have been associated with neurotoxicity, including an increased risk for Parkinson's Disease (PD)-like pathology. Most studies examining this link between pesticides and neurodegeneration focus on dopaminergic cell loss (Chou et al., 2008; Fitzmaurice et al., 2014; Jin et al., 2014; Dennis and Valentine, 2015; Martin et al., 2016; Cao et al., 2018). Ziram and other pesticides have indeed been shown to cause loss of dopaminergic cells. But the mechanisms by which neuronal function is disrupted before, and possibly leading to, major cell loss occurs is not clear.

Chapter 1: The effects of ziram on synaptic vesicle release and neuronal excitability

Abstract

Environmental toxicants have the potential to contribute to the pathophysiology of multiple complex diseases, but the underlying mechanisms remain obscure. One such toxicant is the widely used fungicide ziram, a dithiocarbamate known to have neurotoxic effects and to increase the risk of Parkinson's disease. We have used *Drosophila melanogaster* as an unbiased discovery tool to identify novel molecular pathways by which ziram may disrupt neuronal function. Consistent with previous results in mammalian cells, we find that ziram increases the probability of synaptic vesicle release by dysregulation of the ubiquitin signaling system. In addition, we find that ziram increases neuronal excitability. Using a combination of live imaging and electrophysiology, we find that ziram increases excitability in both aminergic and glutamatergic neurons. This increased excitability is phenocopied and occluded by null mutant animals of the *ether a-go-go* (*eag*) potassium channel. A pharmacological inhibitor of the temperature sensitive hERG (human *ether-a-go-go* related gene) phenocopies the excitability effects of ziram but only at elevated temperatures. *Seizure* (*sei*), a fly ortholog of hERG, is thus another candidate target of ziram. Taken together, the eag family of potassium channels emerges as a candidate for mediating some of the toxic effects of ziram. We propose that ziram may contribute to the risk of complex human diseases by blockade of human eag and sei orthologs, such as hERG.

Introduction

Environmental risk factors associated with an increased risk for complex human diseases include man-made toxicants such as pesticides (Parron et al., 2011; Mostafalou and Abdollahi, 2013; Stallones and Beseler, 2016). The mechanisms by which toxicants increase the risk for neurological disease include individual, well-characterized pathways such as the disruption of

the mitochondrial respiratory chain and increased oxidative stress (Cannon and Greenamyre, 2011; Mostafalou and Abdollahi, 2013; Nandipati and Litvan, 2016). However, toxicants can also initiate neurological disease states via other, less well-characterized pathways (Heinemann et al., 2016; Chen et al., 2018; Muddapu et al., 2019). Individual toxicants also may have more than one target and disruption of multiple pathways by the same toxicant could be required to increase the risk for disease (Sulzer, 2007). Therefore, to understand the mechanisms by which environmental toxicants contribute to neurological disease states it will be necessary to discover the array of potential pathways by which they can disrupt neuronal activity.

Parkinson's disease (PD) is the second most common neurodegenerative disease and produces devastating changes in cognition, mood, gastrointestinal function and motor activity (de Lau and Breteler, 2006; Ascherio and Schwarzschild, 2016). Risk factors for PD include genetic mutations as well as environmental toxicants (Goldman, 2014). Genetic mutations account for rare variants that are inherited primarily in a Mendelian fashion (Lotharius and Brundin, 2002; de Lau and Breteler, 2006; Bezard et al., 2013). Similarly, rare forms of parkinsonism can be caused by toxicants such as MPTP (Parron et al., 2011; Duda et al., 2016; Langston, 2017). In contrast to these clearly defined environmental and genetic causes, most clinical PD cases are idiopathic and develop in response to a combination of multiple factors, similar to other "complex" diseases such as cardiovascular disease (Sulzer, 2007; Cosselman et al., 2015). Each risk factor may have a relatively small influence on the disease phenotype and, in isolation, cause only small changes in cell physiology or circuit activity, but act together to cause pathophysiological effects (Cannon and Greenamyre, 2011; Wang et al., 2011; Goldman et al., 2012; Ascherio and Schwarzschild, 2016).

Model systems provide useful platforms to assess the mechanisms by which toxicants may compromise neuronal function (Bezard et al., 2013). Long-term exposures are particularly important to determine whether a toxicant or combination of toxicants will lead to cell death

and thus contribute to the clinical phase of neurodegenerative diseases (Cannon and Greenamyre, 2011; Parron et al., 2011; Ascherio and Schwarzschild, 2016). Long-term studies can reveal additional developmental and behavioral effects that precede or are distinct from later degenerative outcomes (Cao et al., 2019). Acute exposures on the other hand may be used to determine the more proximal targets of toxicants and the mechanisms by which toxicants initiate the disruption of neuronal activity (Cannon and Greenamyre, 2011; Heinemann et al., 2016). Importantly, a relatively acute cellular phase may be distinguishable from a later, more chronic clinical phase in neurodegenerative disease processes (De Strooper and Karran, 2016; Noyce et al., 2016).

Ziram is a widely used fungicide linked to a 3-fold increased risk of developing PD in both agricultural employees as well as people living adjacent to agricultural fields and chronically exposed to high concentrations of pesticides (Wang et al., 2011). While several cellular effects and molecular targets have been proposed, the mechanisms by which ziram disrupts neuronal activity and thereby increases the risk of human diseases are not known (Chou et al., 2008; Fitzmaurice et al., 2014; Martin et al., 2016). To address this question, we have taken an open-ended approach to determine how ziram affects neuronal activity in the model system *Drosophila melanogaster*. We used *Drosophila* in part because of the extensively developed genetic toolset that allows the use of mutations to explore mechanistic pathways (Ganetzky and Wu, 1986; Hales et al., 2015). Using live imaging and electrophysiological assays we show that ziram can disrupt neuronal activity via at least two pathways: 1) An increase in vesicle release probability mediated through the initial steps within the ubiquitin signaling system and; 2) an increase in excitability mediated by inhibition of evolutionarily conserved member(s) of the eag family of potassium channels. We propose that ziram acts via these and perhaps other pathways to increase the risk of human neurological disease,

especially during the early cellular phase of pathophysiology before overt neurodegeneration has begun (De Strooper and Karran, 2016; Noyce et al., 2016).

Methods

Drosophila Stocks and Husbandry

Flies were raised at 25°C under a 12 hour day/night cycle on a conventional cornmeal/molasses/yeast/agar medium. The GAL4-UAS system was employed for targeted expression of UAS-GCaMP6m (chromosome III insertion) in octopaminergic cells using Tdc2-GAL4 as described (Martin et al., 2016). eag^{sc29} is a null allele and eag^{1} is a hypomorphic allele of the *eag* potassium (K) channel (Xing and Wu, 2018). Additional K channel mutations used include $Shaker^{5}$ (Sh^{5}), a missense point mutation, and $Shaker^{KS133}$(Sh^{KS133}), a null allele of the *Shaker (Sh)* gene, and *slowpoke1* (slo^{1}), a null allele of the *slowpoke* (*slo*) gene. All lines are available from the Bloomington Stock Center unless otherwise noted. w^{1118} was used as a control line for K channel mutants and for all other experiments.

Dissection of *Drosophila* Larvae and Adults

Third instar wandering larvae were dissected to expose the muscles in the body wall in calcium free HL3.1 solution (Feng et al., 2004; Imlach and McCabe, 2009). For neuromuscular junction (NMJ) recordings, two dissections were used to differentiate the contribution of ziram to central versus peripheral nerves. To ablate all contributions of neurons and processes within the ventral nerve cord (VNC), the central nervous system (CNS) was removed and all processes at the base of the VNC were severed leaving only the free hanging nerves containing motoneuron axons (Fig. 5A). In a second preparation, a cut was made across segment A2 of the larval VNC, leaving the abdominal segments of the VNC intact and attached to the nerves that project to the body wall (Fig. 5B). For calcium imaging and electrophysiology of aminergic neurons in the adult

abdominal ganglion, female flies aged 3 to 7 days post-eclosion were used. The flies were pinned on a Sylgard platform or glued with UV-cured glue (Bondic) onto a glass coverslip and the cuticle was removed to expose the abdominal ganglion. For the “ventral” preparations a small window of cuticle was removed on the ventral surface of the animal to expose the ventral surface of the abdominal ganglion, which lies just below the cuticle. For “dorsal” dissections, the dorsal surface of the cuticle was cut and pinned back, and the overlying flight muscle was removed to expose the dorsal surface of the abdominal ganglion. The axons at the base of the abdominal ganglion were severed in “dorsal cut” preparations and were left intact in the dorsal and ventral “intact” preparations (Fig. 2A, E).

Solutions

Ziram stock solution (10 mM in DMSO) was prepared weekly and frozen (-20 C) as aliquots. Working dilutions from the aliquoted stock were prepared daily. KCl (3M) was used to fill sharp electrodes for intracellular recordings and HL3.1 (pH = 7.3; 70 mM NaCl, 5 mM KCl, 5 mM trehalose, 2 mM $CaCl_2$, 4 mM $MgCl_2$, 115 mM sucrose, 10 mM $NaHCO_3$) was used as external solution for all NMJ experiments as described in Feng et al. (2004). The internal solution for whole-cell patch clamp contained 140 mM potassium aspartate, 10 mM HEPES, 1 mM KCl, 4 mM Mg-ATP, 0.5 mM Na_3GTP, 1 mM EGTA (pH 7.3) and external solution was HL3.1 (see above). Ziram was purchased from ChemService Inc. and G5 was purchased from Santa Cruz Biotechnology. PYR 41, lactacystin, and NSC 624206, and disulfiram were purchased from Tocris/R&D Systems. Tetrodotoxin (TTX) was purchased from Alomone labs. Additional reagents were purchased from Sigma unless stated otherwise.

Electrophysiology

For intracellular recordings in larval abdominal wall muscle, recording pipettes with a resistance of 20–35 MΩ were pulled on a Sutter P-97 puller from 0.5mm ID, 1.0mm OD borosilicate glass (with filament; Sutter) and filled with 3M KCl. For miniature end junction potential (mini) post synaptic recordings, the electrode was inserted into muscle 6 in abdominal segments A3 or A4. Control solution was perfused (1 ml/min) during a five-minute baseline and then switched to another control or a test solution for the remainder of the experiment. To generate experimentally evoked excitatory junctional potentials (evoked potentials) at the larval NMJ, the relevant segmental nerve was sucked into a fire polished suction electrode (5-15 μm inner diameter), filled with calcium free HL3.1 and stimulated every 30 seconds to evoke action potentials (APs). The 1 ms stimulation current was adjusted to 1.5 times the threshold current to ensure AP initiation (30 μA-1mA).

The membrane potential in larval muscle was recorded using an Axoclamp 2B or a Multiclamp 700A (Molecular Devices) amplifier, amplified (100x) and low-pass filtered (Axoclamp: 3 kHz, Brownlees Instruments; Multiclamp: 4kHz). Data were digitized at 20 kHz using a National Instruments data acquisition board and software custom written in LabView (National Instruments, Inc). Recordings were analyzed offline using an event detection algorithm based on threshold crossings of the first derivative (LabView). Data normalization, graphing and further analysis were done using Origin (OriginLab Corporation).

For experiments conducted at elevated temperatures, a Warner SB TC-324B single channel temperature controller was used to elevate and maintain the perfusion solution temperature surrounding the larval preparation to 40°C. In addition, a Styrofoam enclosure was constructed around the recording microscope and a mini-space heater was used to elevate the ambient temperature within the enclosure to 32-38°C.

For electrophysiological recordings in the abdominal ganglion of adult female flies, Tdc2-positive octopaminergic neurons were recorded from a whole-cell patch clamp configuration. 1.5mm OD, 0.86mm ID Borosilicate glass electrodes (7-9 MΩ) were filled with the whole-cell patch clamp internal solution (see solutions above). The preparation was perfused with HL3.1 solution and continuously aerated with carbogen (95% O_2/5% CO_2). 3% Protease IV was puffed onto the preparation for 3-10 minutes prior to recording to remove the glial sheath that surrounds the ganglion (Ryglewski and Duch, 2012). Recordings were made using the current clamp mode of the whole-cell patch clamp technique. To measure AP threshold and AP number, a current was injected that ramped linearly over one second from a starting level of -50 pA to a maximal level of 0 pA. In the next trial the starting current was still -50 pA but ramped to a maximal current of +50 pA, then in the next trail to +100 pA, until a maximal current of +450 pA was reached. The number of APs for each ramp was divided by the number of APs obtained at +450 pA in the control condition to obtain the normalized values shown in Fig 3C. Recordings were made using a MultiClamp 700B Amplifier, filtered at 4 kHz, and sampled at 10 kHz with a Digidata 1300b under control of pClamp (Molecular Devices).

Calcium Imaging

To visualize intracellular calcium levels, UAS-GCaMP6m was expressed in octopaminergic cells using Tdc2-GAL4 (Cole et al., 2005; Chen et al., 2013). Third instar larval preparations were dissected as described previously in calcium free HL3.1 solution (see Solutions) and then washed 3x with chilled HL3.1 solution containing 2 mM Ca^{2+} prior to imaging (Martin et al., 2016). Control solution or a test drug was added via perfusion to the bath after a 1-2 minute baseline recording at ambient temperature. Nerve terminals and cells were imaged using a Zeiss Axio Examiner Z1 microscope and Zeiss Achroplan water immersion objective (40x, 1.0 N.A.) with a CCD camera (Andor iXon 897, Oxford Instruments, Oxfordshire, England) and a capture rate of 11.9 frames/s using Andor IQ2 software. A DG4 light source (Sutter, Novato,

CA) with a GFP Brightline® Filter Set (Semrock, Rochester, NY) was used for illumination. Segment A4 of muscle 13 was visualized for all experiments as previously described (Martin et al., 2016). For analysis of the GCaMP experiments, 3-5 individual boutons were selected per axon branch using ImageJ (NIH) and the Time Series Analyzer plugin. The individual boutons were background subtracted and then averaged per frame. ΔF/F was quantified as ΔF/F= [(F peak - F baseline)/ F baseline] as reported in Martin et al. (2016).

Experimental Design and Statistical Analysis

For each calcium imaging recording, 3-5 regions of interest from one preparation were imaged within a single 40x field of view and averaged to obtain a single observation with an n of 4-15 animals used for statistical analysis. For electrophysiology experiments, normalized frequency and amplitudes of minis and end junction potentials (EJP) were divided by their respective five-minute baseline interval before drug was added. The normalized and raw frequency and amplitudes were plotted over time or represented as scatterplots with mean ± SEM and used to quantify the effect of each mutant line and drug concentration. An effect was judged as statistically significant if $p<0.05$ in an ANOVA with a post-hoc Dunn-Sidak test for multiple comparisons, a Wilcoxon signed rank test, or a t-test when applicable. The analysis of the data in Figure 5K was made based on comparing means and differences in means using the bootstrap method implemented in Labview (Efron and Tibshirani, 1991; Efron and Hastie, 2016)

Results

Ziram dose-dependently increases excitability of octopaminergic neurons

We previously reported that a high concentration of ziram (20 μM) causes synchronized calcium events at octopaminergic processes and nerve terminals at the larval NMJ (Martin et al., 2016). Here, we expanded our dose response curve to include concentrations previously used to test

the toxicity of ziram (1-20 μM; Fig. 1 A-D) (Chou et al., 2008; Rinetti and Schweizer, 2010; Dennis and Valentine, 2015). Although concentrations as low as 1 μM induce synchronized calcium events in octopaminergic processes, higher concentrations generated more frequent events (Fig. 1B, D) and required a shorter incubation prior to the initiation of events (Fig. 1C). The time-period to the first calcium event differed between high (20 and 10 μM) versus low concentrations (1 and 2 μM) of ziram (Two-way ANOVA and post-hoc Dunn-Sidak: n=3-12, $p< 0.001$ per concentration). We also found that the *frequency* of calcium events at 25-30 minutes post-ziram addition was increased at higher concentrations, with 20 μM ziram significantly different from both 1 and 2 μM (One-way ANOVA and post-hoc Dunn-Sidak: n=4-14, $p=0.004$ and $p<0.001$, respectively).

To determine whether the effects of ziram would generalize to octopaminergic cells beyond those innervating the larval NMJ, we tested ziram at a well-defined cluster of midline neurons in the adult abdominal ganglion (Fig. 2A, E) (Rodriguez-Valentin et al., 2006; Rezaval et al., 2012). Application of 20 μM ziram either induced calcium events in octopaminergic cell bodies and processes within the ganglion in preparations with no baseline calcium activity or increased the frequency in preparations with spontaneous activity at baseline (Fig. 2C, F). Approximately half of these preparations showed spontaneous activity at baseline.

To help define ziram's site of action, we severed the nerves containing the distal axons and terminals of the octopaminergic neurons ("dorsal cut" dissection, see Fig. 2A). These preparations showed no spontaneous activity at baseline, and in contrast to dorsal "intact" preparations, ziram failed to increase calcium events in the cell bodies (Fig. 2A, D). This suggests that ziram's major site of action may be localized to or depend on factors in distal axonal processes or nerve terminals rather than somatodendritic sites (Fig. 2D).

Octopaminergic cell bodies within the abdominal ganglia localize to the ventral surface and are difficult to detect when visualized in dorsal preparations (“dorsal”, see Fig. 2A). To better visualize individual cells and distinguish fluorescence in somata versus their adjacent processes, we inverted our preparation so that the ventral surface of the ganglion was facing the objective (“ventral”, see Fig. 2E). Application of ziram increased the frequency of calcium signals in most if not all the visualized cells (Fig. 2E, F). Interestingly, calcium signals in individual octopaminergic neurons were not synchronized (Fig. 2E, F), suggesting heterogeneous excitability within the cluster of neurons.

To more directly test whether ziram increases electrophysiological excitability, we recorded from octopaminergic neurons in the abdominal ganglion of adult flies using whole-cell patch clamp. Increased excitability could manifest as a membrane potential depolarization, a decrease in the amount of current required to bring the neuron to threshold irrespective of membrane potential, or a combination of both mechanisms. Consistent with the first mechanism, perfusion of 10 μM ziram during a whole-cell current clamp recording depolarized the resting membrane potential by 8.2 ± 2.4 mV relative to controls (Fig. 3A; n=5, p=0.027; two-way t-test), thus bringing them closer to firing threshold. To test whether the amount of current required to elicit an AP might also be decreased, we used current ramp injections to measure threshold and AP number (see Methods). After application of ziram, less current was required to trigger an AP, consistent with a decreased AP threshold (Fig. 3B, C). To disambiguate depolarization and AP threshold, we kept the membrane potential hyperpolarized to -63 ± 1 mV by injecting bias current (Fig, 3B, C; black and red trace/curves). Ziram still decreased the minimum amount of current required to elicit an AP compared to controls and increased the mean number of APs at each current ramp injection (Fig 3B, C; black and red traces/curves). For example, the average number of APs elicited during a -50 pA to 300 pA ramp injection increased from 4.8 to 8 at -63 mV and from 6.8 to 13.4 at the cell’s resting potential (Wilcoxon nonparametric test, p=0.03 both at the cell’s

resting potential and at -63mV; Fig. 3B, C). Together these data demonstrate that ziram increases the excitability of octopaminergic neurons both by depolarizing the membrane potential and by lowering the threshold for AP firing.

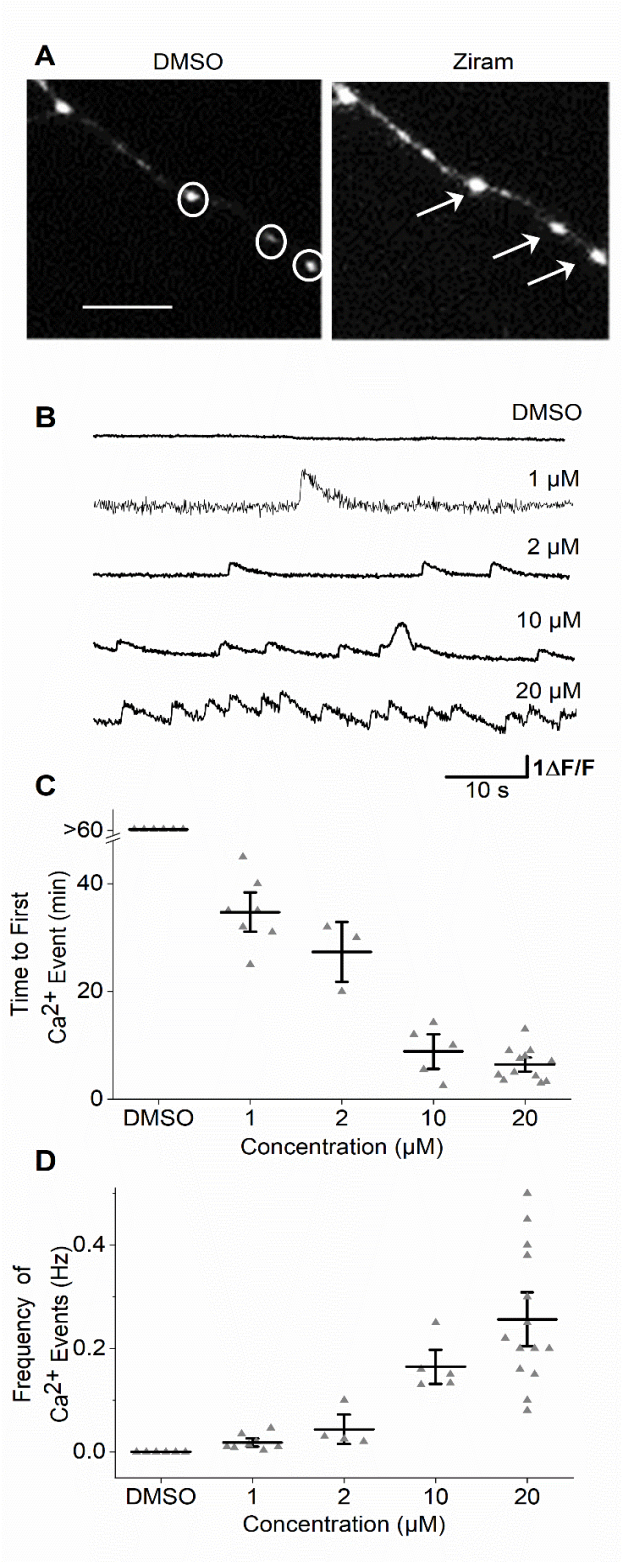

Figure 1. Exposure to ziram dose-dependently increases calcium events at octopaminergic terminals at the NMJ. A. GCaMP6m fluorescence in muscle 13 at

octopaminergic terminals exposed to control solution (left) and the same preparation in 20 µM ziram (right). Regions of interest (ROI) selected for analysis indicated as white circles (left). Note the increase in fluorescence (white arrows; right). Scale bar= 80 µm **B.** Representative ΔF/F traces show repetitive calcium events recorded from octopaminergic terminals after 25 minute exposure to control solution (n=6), 1 µM ziram (n=7), 2 µM ziram (n=4), 10 µM ziram (n=5), or 20 µM ziram (n=15). **C.** The time until the first calcium event decreases as the concentration of ziram increases with the onset of EJPs occurring earlier at the high doses. **D.** The mean frequency of calcium events at 25-30 minutes post-ziram at each concentration. Data shown as mean ± SEM.

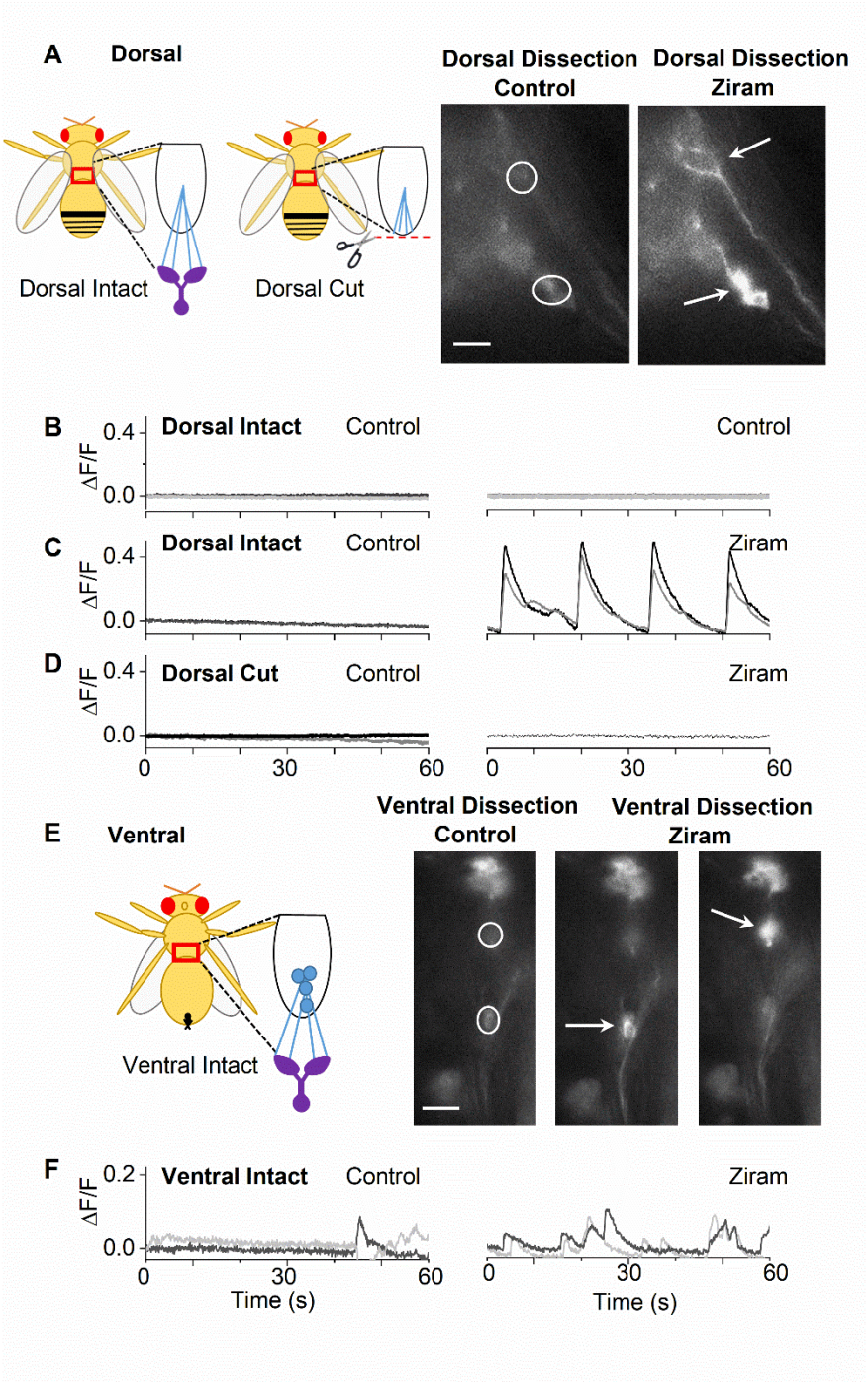

Figure 2. Ziram increases calcium events in octopaminergic projections and somata in the adult abdominal ganglion. A. Diagram of the dorsal intact and cut abdominal ganglion dissection (*left*): the area within the red square in the fly is shown magnified in the cartoon to the right of fly. Black half-oval: abdominal ganglion; blue lines: octopaminergic projections; purple:

target organs of projections. Images of octopaminergic neuronal projections in the dorsally dissected abdominal ganglion (*right*) in the of control period (*left micrograph*) and after application of 20 µM ziram (*right micrograph*). White circles indicate ROI. Note the synchronized calcium events at the octopaminergic projections indicated with white arrows. Scale bar is 160 µm. **B-C.** Representative ΔF/F traces of octopaminergic projections from two ROIs in an intact dorsal preparation in the presence of control at 2 minutes (*left*) and after a 25-minute control solution (B, *right,* n=5) or ziram (C, *right*, n=6) incubation. Each trace represents one ROI as indicated in the dorsal intact preparation shown in diagram A (white circles). **D.** Representative ΔF/F traces of octopaminergic projections from a dorsal cut preparation before (*left, n=5*) and after a 25-minute incubation in 20 µM ziram (*right*, n=5). Each trace represents one ROI in a dorsal cut preparation. Note that ziram no longer leads to synchronized calcium events. **E.** Diagram of the ventral intact abdominal ganglion dissection and fluorescent images of octopaminergic cell bodies in control solution (*left*) and after a 20-minute incubation in 20 µM ziram (*middle and right, images taken approximately 15 seconds apart).* White arrows indicate ziram-induced calcium events that occur in two different cell clusters at two different time points. Scale bar is 160 µm. **F.** Representative ΔF/F traces of calcium events at the indicated ROIs in control (*left*) and after a 20-minute incubation in 20 µM ziram (right, n=3) in a ventral intact preparation. Traces are from the indicated ROIs in diagram E (white circles).

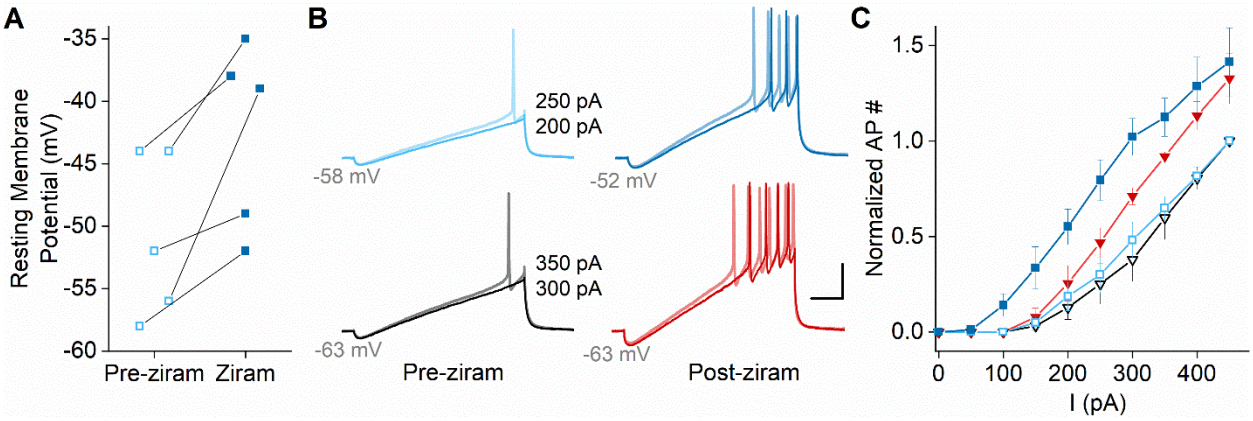

Figure 3. Ziram increases excitability of octopaminergic neurons via depolarization and lowering of AP threshold. Whole-cell current clamp recordings from octopaminergic neurons in the adult abdominal ganglia before and after perfusion of 10 µM ziram. **A.** Mean resting membrane potential (RP) is depolarized from -51 ± 3 mV to -43 ± 3 mV in the presence of ziram (open light blue squares: control; closed dark blue squares: ziram; n=5). **B.** Representative voltage traces from an individual cell in response to 1 second current ramp injections from -50 pA to 200 or 250 pA (top blue traces) and -50 pA to 300 or 350 pA (bottom black/red traces). Top traces at the cell's resting potential (RP; no bias current) and bottom traces at -63 mV (with bias current) in control (*left*) and 10 µm ziram (*right*). Note that ziram leads to both membrane depolarization and increased AP firing (*top*) and increased AP firing even when the cell is held at -63 mV (*bottom*). Scale bar is 200 ms and 20 mV. **C.** Normalized number of APs in response to 1 second ramp injections from -50 pA to the maximum current indicated on the x-axis. Data are normalized to the pre-ziram AP number for a ramp from -50pA to 450pA (13 APs for RP, 11APs at -63mV). Open symbols: control solution; closed symbols: ziram. Blue (corresponding to blue traces in panel B): neurons at intrinsic RP; Black/red (corresponding to red/black traces in panel B): neurons held at -63 mV with bias current. Mean ± SEM; data from the same 5 cells as shown in A and B. Note the leftward shifts in AP numbers when the cell is in ziram at its RP (light blue to dark blue) and when the potential is held at -63 mV (black to red).

Ziram increases the excitability of glutamatergic neurons

Using calcium imaging, we previously did not detect an increase in excitability in glutamatergic neurons innervating the larval NMJ (Martin et al., 2016). However, recent data show that calcium homeostasis differs between octopaminergic and glutaminergic neurons at the NMJ (Xing and Wu, 2018). Octopaminergic neurons show detectable calcium signals in response to a wide range of stimulation frequencies, but glutamatergic neurons, while responsive to stimulation, show a similarly robust calcium response only following high frequency stimulation and pharmacological inhibition of channel activity (Xing and Wu, 2018). We therefore reasoned that ziram might indeed stimulate *action potentials* in both glutamatergic and octopaminergic cells but fail to generate a *detectable calcium signal* in glutamatergic processes. To test this hypothesis, we performed sharp electrode electrophysiological recordings from muscle 6 at the larval NMJ (without VNC) (Imlach and McCabe, 2009).

Glutamatergic motoneuron APs elicit the exocytotic release of glutamate from *multiple* vesicles, triggering a large, ionotropic postsynaptic response, which can be measured in the postsynaptic muscle in the larval body wall as an excitatory end junction potential (EJP) of several millivolts in amplitude. These large EJPs, which occur in response to a presynaptic AP are easily distinguishable from the small, miniature end junction potentials (minis), which have an amplitude of $\leq$1 mV and occur in response to neurotransmitter released from a *single* vesicle. We can thus take the presence of these larger amplitude EJPs at the larval NMJ as an indicator of presynaptic APs, a proxy of increased neuronal excitability. If ziram increases the excitability of glutamatergic neurons to the point of AP firing, we expect to detect 'spontaneous' EJPs of several millivolts in amplitude. Indeed, when we measured the muscle membrane potential at the NMJ intracellularly, we observed 'spontaneous' EJPs following application of ziram in preparations without the VNC (Fig. 4A, B). Ziram-induced EJP events were sensitive to the sodium channel blocker tetrodotoxin (TTX; Fig. 4B, C). Since contraction-initiating APs in the muscles of the NMJ depend on calcium

channels rather than on TTX-sensitive sodium channels (Littleton and Ganetzky, 2000), we conclude that the large ziram-induced EJPs are triggered by presynaptic APs.

To further explore the electrophysiological response to ziram, we applied ziram at increasing concentrations and quantified the time to first EJP (Fig. 4D). In contrast to the modest but significant effects of $\leq$1 µM ziram on octopaminergic cells, we did not detect any EJPs in larval muscle at this low concentration in preparations without a VNC (Fig. 4D). Our data suggest that ziram may directly increase the excitability of both octopaminergic and glutamatergic neurons and that octopaminergic neurons may be more sensitive to the effects of ziram. However, previous reports show that octopamine can modulate glutamate release from glutamatergic (Type I) terminals and thus affect electrophysiological responses measured at the NMJ (Kutsukake et al., 2000; Nagaya et al., 2002). While muscle 6 is not a target for major octopaminergic innervation (Atwood et al., 1993; Monastirioti et al., 1995), we cannot rule out the possibility that the electrophysiological responses we observed were caused by the activation of octopaminergic (Type II) terminals by ziram, and the subsequent, indirect stimulation of Type I terminals by octopamine. Although we find that ziram concentrations as low as 1 µM can induce synchronized calcium events in octopaminergic processes, higher concentrations and more frequent events (Fig. 1B, D) might be required to release enough octopamine to stimulate Type I terminals.

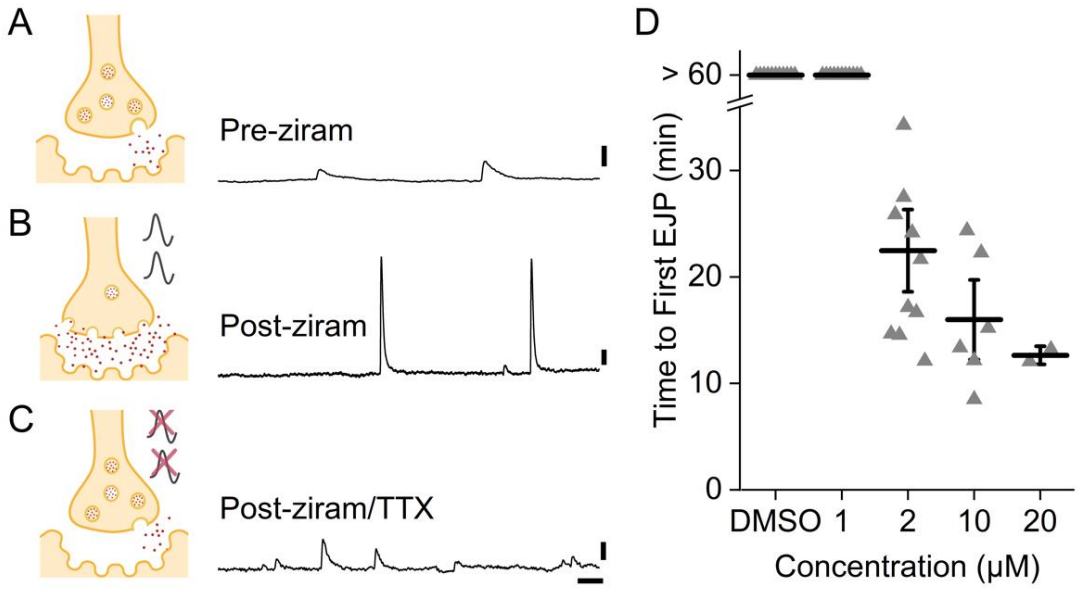

Figure 4. Ziram induces spontaneous, TTX sensitive EJPs at NMJ preparations without VNC. A- C. Representative trace in control (A, n=11), after addition of 2 μM ziram (B, n=11) and after addition of 1 μM TTX + 2 μM ziram (C, n=4) in preparations without VNC. **A- C.** Scale is 100 ms and 1 mV. **D.** Summary scatter graph of ziram induced EJPs. EJPs are induced at 2, 10, and 20 μM but not at 1 μM or in control solution. Dose of ziram is inversely related to the time to first EJP (Control n=11; 1 μM n=7; 2 μM n=11; 10 μM n=6; 20 μM n=2).

Differential effects of ziram across different sites of action

In addition to acting peripherally on Type I terminals (Kutsukake et al., 2000; Nagaya et al., 2002) octopamine can also act centrally on glutamatergic motoneurons to regulate their electrical activity and locomotor output (Saraswati et al., 2004; Fox et al., 2006; Simon et al., 2009; Koon and Budnik, 2012; Selcho et al., 2014). This suggests that ziram could have non-linear effects not only at the periphery but also centrally. To explore this idea, we compared the effects of ziram in two types of preparations in which the VNC was either completely severed

from the peripheral nerves or a portion of the VNC was left intact and attached to the peripheral nerves. For the intact VNC preparation, the descending inputs from the CNS to the VNC were severed to avoid contractions driven by CNS input. Consistent with previous reports that central octopaminergic cells can modulate motoneuron activity (Fox et al., 2006; Simon et al., 2009), we observe an increase in EJP frequency with octopamine bath application to preparations with the distal VNC left attached (data not shown). Similarly, we observe an increase in the fraction of experiments with detectable EJPs at 1 μM ziram and an increase in EJP frequency in preparations with the VNC attached (Fig. 5F, K). By contrast, when connections of the VNC to the body wall were severed, leaving only the free-hanging nerves (Fig. 5A), 1 μM ziram had no effect (Fig. 5E, K). Application of ziram at concentrations above 1 μM elicited EJPs in both preparations, but the frequency was higher in preparations with the VNC intact (Fig. 5K; 1μM n = 6 & 12, $p < 0.03$; 2μM: n=8 & 13, $p < 0.01$; 10 μM: n=9 & 14, $p < 0.001$ (see methods)). These data are consistent with the idea that depending on the site of action, the effects of ziram on excitability can differ. The similarity between the effect of ziram at 1 μM and the effect of octopamine in VNC-attached preparations suggest that the central site of action of 1 μM ziram could be octopaminergic processes that regulate motoneuron excitability; however, other pathways within the VNC that regulate motoneuron activity also represent potential targets.

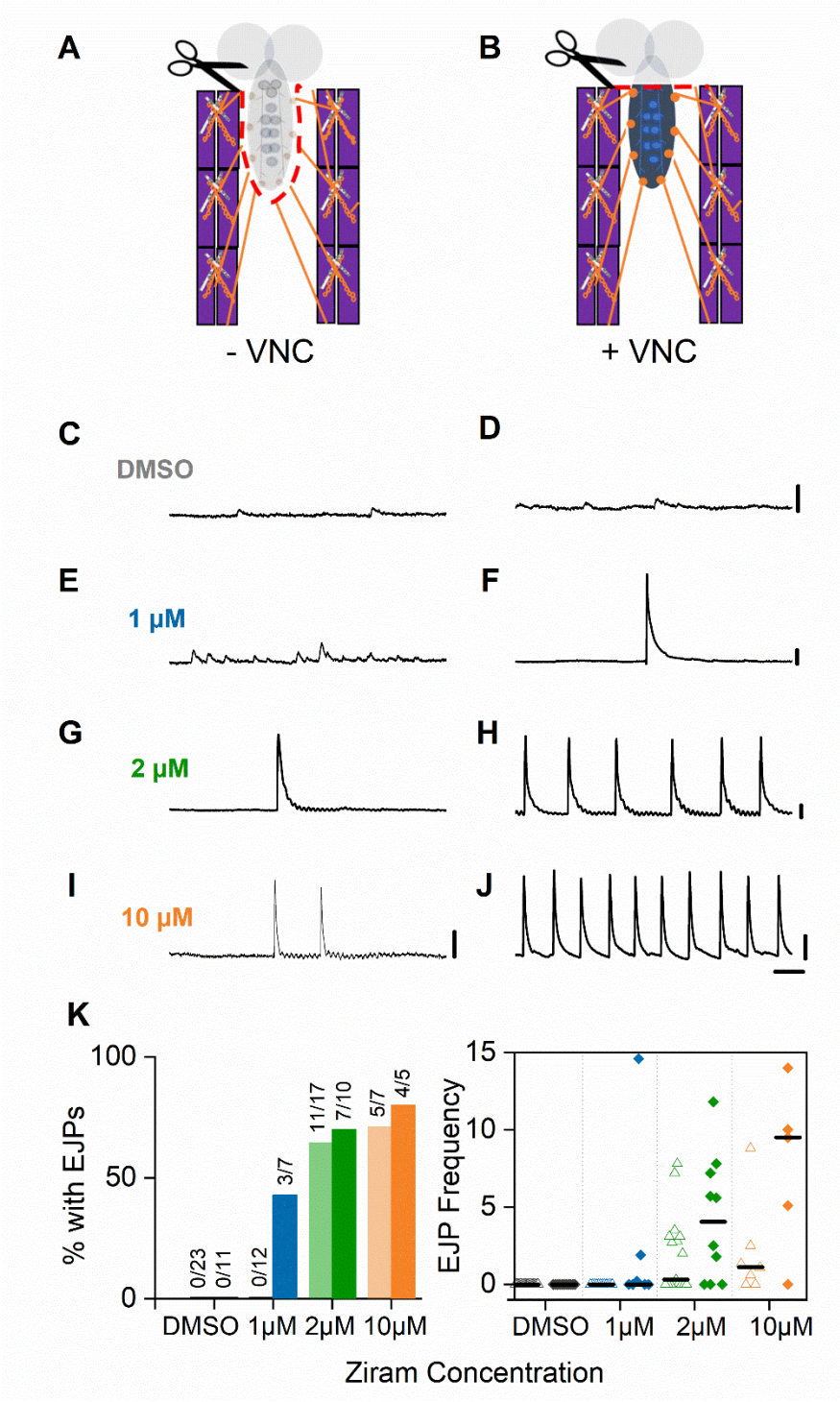

Figure 5. NMJ preparations containing octopaminergic and motor-neuron cell bodies in the VNC are more sensitive to ziram-induced excitability. A. Diagram depicting the NMJ preparation without the VNC (-VNC) and **B.** with the VNC intact (+VNC). Red dashed lines

indicate location of dissection cuts. Blue dots represent octopaminergic cells and orange dots represent glutamatergic motoneuron cell bodies. **C-J.** Representative traces of minis and EJPS in different conditions. **C, E, G: -VNC C.** Control (n=23); **E.** 1 µM ziram (n=12); **G.** 2 µM ziram (n=17); **I.** 10 µM ziram (n=7). **D, F, H: +VNC: D.** Control (n=11); **F.** 1 µM ziram (n=7); **H.** 2 µM ziram (n=10); **J.** 10 µM ziram (n=5). **K.** *Left*: Percentage of experiments with EJPs elicited by ziram during the recording period at each ziram concentration in preparations without (translucent color) and with (bold color) the VNC intact. Note that at 1 µM ziram, EJPs occur only in preparations with the VNC. *Right*: Median frequencies for each experiment in control (grey) and at each ziram dose (blue 1 µM, green 2 µM, orange 10 µM) in preparations with the VNC removed (open triangles) and VNC intact (filled diamonds). Difference of means and confidence interval [5%, 95%]: 1 µM 2.39 [0.03, 6.3]; 2 µM 2.32 [1.4, 4.6] 10 µM 6.24 [2.5, 9.8]; probability of means being equal: 1 µM $p < 0.03$, 2 µM $p < 0.01$, 10 µM $p < 0.001$ (see methods). Note the increase in frequency when ziram is applied to preparations with the VNC left intact. **C-J.** X scale is 100 ms. **C-F**. Y scale is 1 mV. **G-I.** Y scale is 5 mV**. J.** Y scale is 2 mV.

Ziram increases the probability of synaptic vesicle release

During our recordings of spontaneous EJPs we observed an increase in the frequency of mini events; however, this effect was partially obscured by ziram-induced spontaneous EJPs (Fig. 4B). Thus, we applied TTX to block the presynaptic APs required for EJPs to allow for the analysis of minis (Fig. 4C). We indeed observed a clear, ziram-induced increase in the frequency but not the amplitude of spontaneous minis, suggesting an increase in presynaptic vesicle release probability (Fig. 6A-C). The ziram-induced increase in mini frequency appeared to be independent of extracellular calcium concentration and occurred in HL3.1 solution containing calcium concentrations as low as 0.2 mM (n= 8; Fig. 6B).

Higher doses of ziram (10 μM and 20 μM) led to an increase in mini frequency (Fig. 6B), followed by a strong depolarization of the membrane potential (data not shown; see Fig. 3A for comparison). The concomitant decrease in driving force for currents through the glutamate receptors led to a decrease in mini amplitude, which made it progressively difficult to resolve low amplitude minis from noise. While this hindered the establishment of a rigorous dose-response relationship, higher doses elicited increases in frequency earlier during the experiment (Fig. 6B).

An increase in mini frequency is usually interpreted as an increase in the probability of the *spontaneous* release of individual synaptic vesicles. An increase in vesicle release probability might further reveal itself through an increased amplitude of the postsynaptic response to an experimentally triggered AP. These investigator-induced post synaptic events will be termed “evoked potentials” to differentiate them from the EJPs resulting from the spontaneous APs induced by ziram (see Fig. 4B). Thus, to determine whether ziram increases the probability of synchronous vesicle release, we measured the amplitude of evoked potentials following perfusion with ziram (Fig. 6D, F, G). We observe a consistent increase in the amplitude of evoked potentials, which peaked after 10 minutes in ziram and then declined (Fig. 6F). Quantification of evoked potential amplitudes at 10 minutes showed an increase as high as 3-fold in the presence of ziram relative to controls (Fig. 6D, F). These data are consistent with ziram increasing the probability of both spontaneous and synchronous evoked vesicle release.

We noted that the dose of ziram required to increase excitability was higher than the dose required to increase the probability of release. At a low dose of ziram (1 μM) both the evoked potential amplitude and mini frequency increased (Fig. 6B, G), however there was no detectable effect on the excitability of glutamatergic neurons at this dose (see Figs. 4D, 5E). These differences suggest that the mechanisms by which ziram increases the probability of vesicle release might be distinct from those responsible for increased excitability. To investigate the

pathways that lead to these two distinct neuronal effects, we tested compounds that share structural or toxicological properties with ziram.

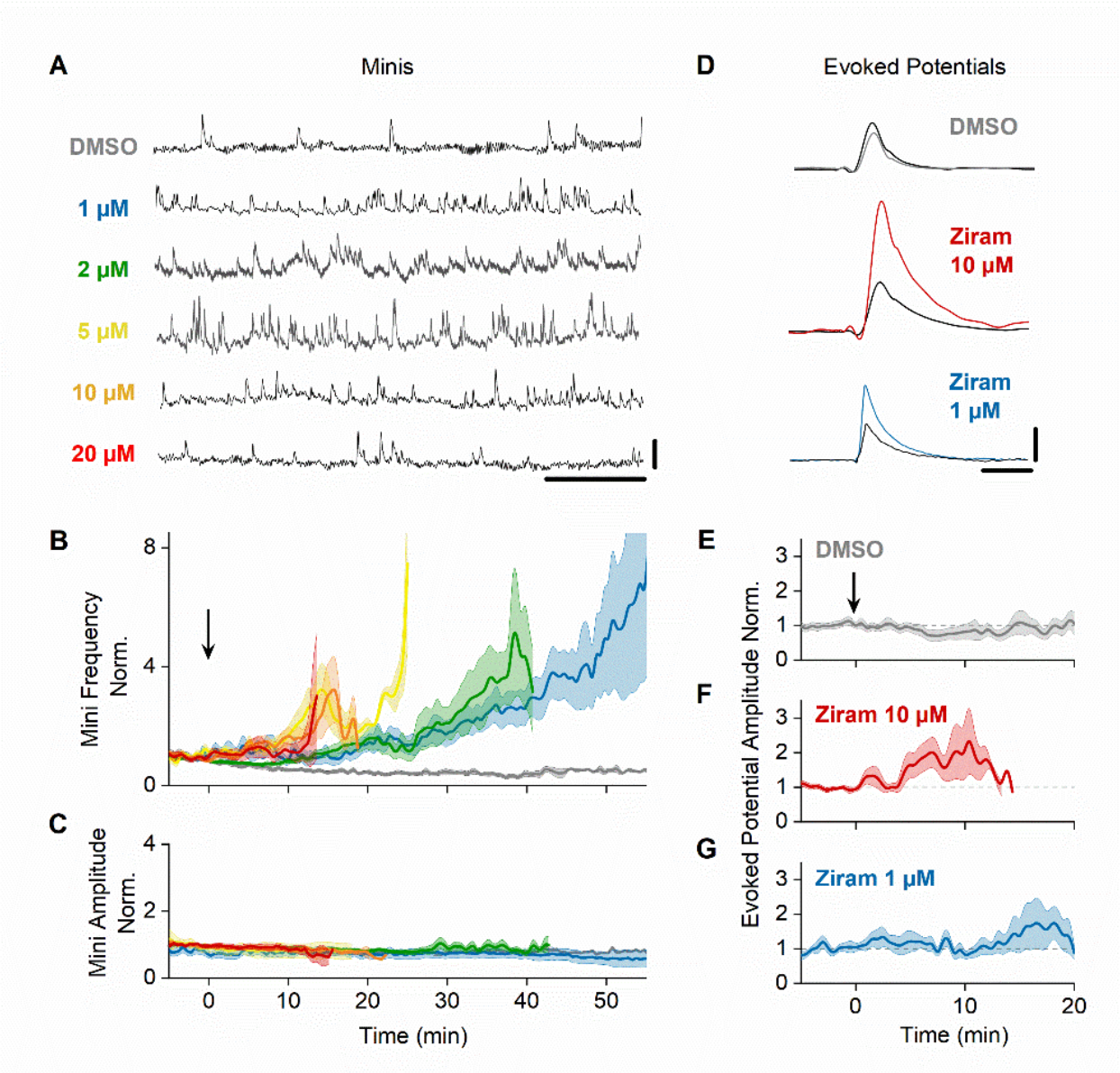

Figure 6. Ziram increases synaptic vesicle release probability. **A**. Representative traces of sharp electrode intracellular recordings at the *Drosophila* NMJ in control (grey, n=28) or ziram (blue 1 µM; green 2 µM; yellow 5 µM; orange 10 µM; red 20 µM; n=11-26). X scale is 1 s and Y scale is 0.5 mV. **B, C.** Mini frequency and amplitude measured over time and averaged across experiments in control and in various ziram concentrations. Mini frequencies at 10 µM and 1 µM

include experiments performed in both 2 mM and 0.2 mM calcium control solutions. Arrow indicates switch of perfusion from control to drug (or from control to control) solution after a five-minute baseline period. **D.** Sample traces of evoked responses during baseline and after control (grey), 10 µm ziram (red) or 1 µm ziram (blue). Scale is 100 ms and 5 mV. **E-G.** Normalized evoked potential amplitudes plotted over time in control solution (n=8), 10 µM (n=8), and 1 µM ziram (n=5) with addition of drug indicated by black arrow. All time traces are plotted as mean ± SE.

Other PD-associated pesticides, dithiocarbamates, and zinc do not mimic either of the neuronal effects caused by ziram at the NMJ

Ziram is composed of two identical, anionic dithiocarbamate molecules bound by a positively charged zinc atom raising the possibility that zinc alone might contribute to the effects of ziram (Fig. 7A). We tested zinc chloride at the NMJ and did not observe an increase in release probability or excitability at concentrations as high as 10 µM (Fig. 7B).

To determine whether dithiocarbamates as a class might increase excitability or release probability, we tested the effects of two structurally related chemicals, maneb, a PD associated fungicide (Wang et al., 2011), and disulfiram, an aldehyde dehydrogenase inhibitor used to treat alcoholism (Fig. 7A, B) (Fitzmaurice et al., 2014). We found that disulfuram, but not maneb, increased the probability of release (Fig. 7B; disulfiram: Dunn-Sidak p=<0.001; maneb: Dunn-Sidak p=0.15) and neither maneb nor disulfuram induced EJPs (data not shown). These data indicate that although features common to dithiocarbamates such as free cysteines may contribute to changes in release probability or excitability, neither effect is common to all dithiocarbamates. In addition, the differential effects of disulfuram on excitability and release probability support the hypothesis that ziram could act through two distinct pathways.

Exposure to two other pesticides, paraquat and rotenone (Fig. 7A), has been strongly associated with an increased risk of developing PD (McCormack et al., 2002; Wang et al., 2011; Cao et al., 2018). However, neither toxin increased the frequency of minis (Fig. 7B) nor triggered EJPs, indicating that the neuronal effects of ziram are not shared by all toxicants associated with PD.

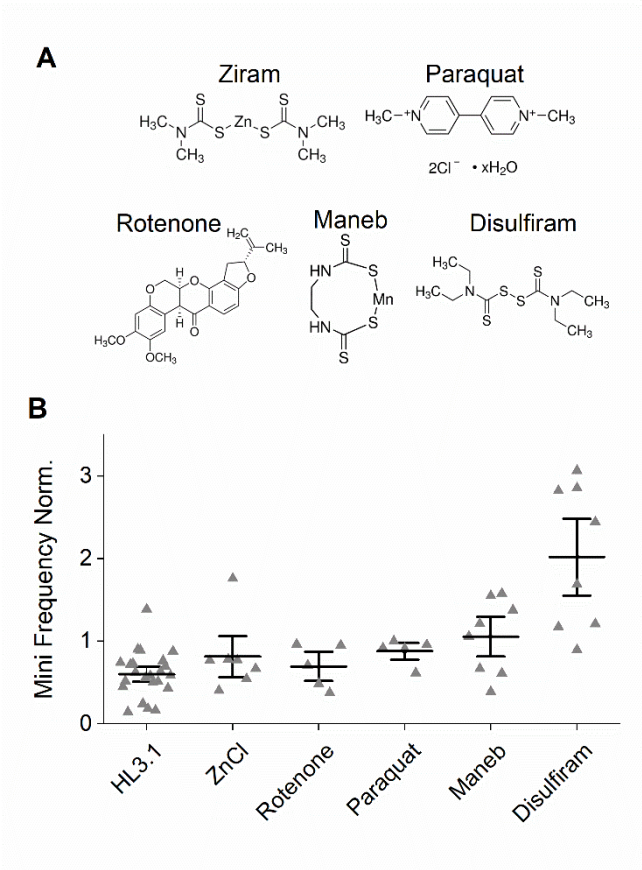

Figure 7. Other PD-associated pesticides, dithiocarbamates, and zinc do not mimic either of the neuronal effects caused by ziram at the NMJ

A. Chemical structures of compounds tested. **B.** Mean mini frequencies in control (n=26), zinc chloride (10 µM, n=8), rotenone (20 µM, n=5), paraquat (20 µM, n=5), maneb (10 µM, n=8) and disulfiram (10 µM, n=8). Disulfiram, and not the other compounds tested, increased mini frequency. None of the compounds tested induce EJPs.

Disruption of the ubiquitin signaling system enhances vesicle release probability

Ziram was previously reported to increase mini frequency in mammalian cell cultures via inhibition of E1 ligase, the first element of the ubiquitin signaling system (Rinetti & Schweizer, 2010; Fig. 8A). We therefore examined whether pharmacologic inhibition of E1 ligase would similarly increase mini frequency at the *Drosophila* NMJ, and whether this intervention would also increase excitability. Consistent with the results in mammals, we find that the E1 ligase inhibitors NSC and PYR41 increase mini frequency (Fig. 7B; one-way ANOVA and *post-hoc* Dunn-Sidak, PYR41: $p<0.001$; NSC: $p=0.012$). Consistent with an increase in release probability, PYR41 also increases evoked potential amplitude (one-way ANOVA and *post-hoc* Dunn-Sidak: $p=0.002$; Fig. 8D). Neither the proteasome inhibitor MG132 nor the deubiquitination inhibitor G5 showed a significant increase in mini frequency or evoked potential amplitude (Fig. 8B, D). Our results are in general agreement with previous work supporting the importance of the ubiquitin signaling system for synaptic transmission (DiAntonio and Hicke, 2004; Yi and Ehlers, 2005) and expand on those findings by suggesting that protein ubiquitination, rather than protein degradation, is crucial for the control of exocytosis.

We never observed spontaneous EJPs following perfusion with NSC, PYR41, MG132 or G5. This suggests that, unlike changes in the probability of release, the increase in excitability caused by ziram is not mediated via the ubiquitin signaling system (Fig. 8C). These results support the notion that the increase in excitability and vesicle fusion probability results from distinct molecular mechanisms.

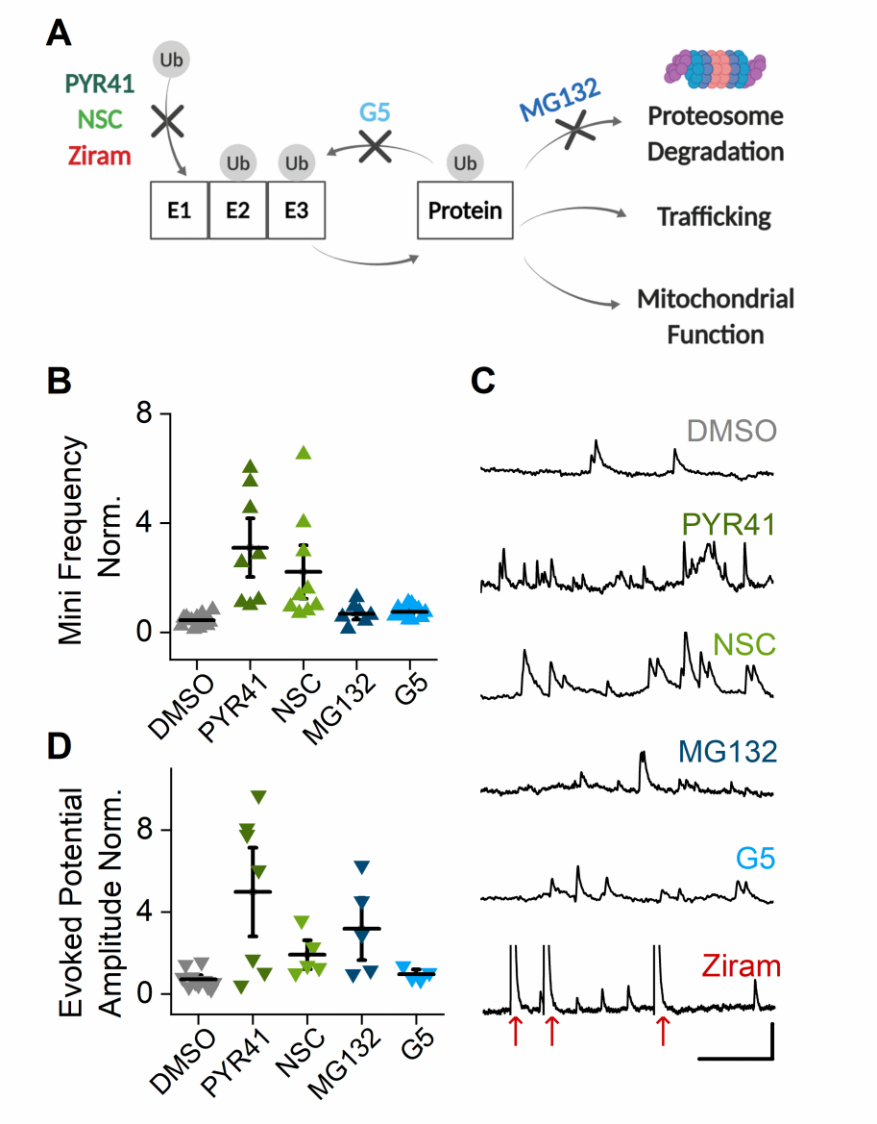

Figure 8. Disruption of the Ubiquitin Signaling System enhances vesicle release probability, but not excitability. A. Simplified diagram of the Ubiquitination Signaling System (USS) with sites of pharmacological inhibition indicated: E1 activating enzyme (PYR41, NSC, ziram), deubiquitinating enzyme (G5) and the proteasome (MG132). **B.** Normalized mini frequency in control (n=13), PYR41 (5 µM; n=8), NSC (20 µM; n=9), G5 (10 µM; n=12), and MG132 (10 µM; n=7) (mean ± SEM). **C.** Sample traces of minis following addition of control, PYR41, NSC, MG132, G5, and ziram. Note that unlike ziram, PYR41, NSC, MG132, and G5 do not induce EJPs (indicated by red arrows). Scale is 500 ms and 1 mV. **D.** Normalized evoked

potential amplitude following the addition of control (n=11), PYR41 (n=7), NSC (n=7), GS (n=4), and MG132 (n=5).

eag potassium channel mutants phenocopy and occlude ziram-induced excitability

We next explored mechanisms of ziram-induced excitability. Since K channels are critical regulators of neuronal excitability, we tested whether the broad-spectrum K channel blocker, tetraethylammonium (TEA), would replicate the effect of ziram on excitability. Indeed, TEA phenocopied ziram at octopaminergic terminals and induced spontaneous calcium signals (data not shown). We therefore hypothesized that ziram inhibits one or more K channels (Shieh et al., 2000; Bauer and Schwarz, 2018). In order to determine whether inhibition of K channels contribute to ziram-induced excitability, we tested for the presence of EJP activity in *eag*, *Shaker* and *slowpoke* K channel mutant animals (Pallanck and Ganetzky, 1994; Jan and Jan, 2012).

Consistent with previous reports that spontaneous EJPs occur at baseline in animals with a null mutation in the *ether-a-go-go* (*eag*) K channel (Ganetzky and Wu, 1983; Ganetzky et al., 1999; Frolov et al., 2012), we observed EJPs at baseline in *eag*, but not in *Shaker* nor *slowpoke* mutants (Fig. 9A-D). In both eag^{1} and eag^{sc29} mutants, we observed EJPs with amplitudes ranging from 9-25 mV and frequencies ranging from 1-10 Hz, both of which remained constant throughout the experiment (Fig. 9A, B). We next performed occlusion experiments similar to classical epistasis studies to determine whether mutations in *eag* might affect pathways similar to or divergent from ziram (Mackay, 2015). Addition of 10 μM ziram to larvae homozygous for either a hypomorphic or null allele of *eag* did not detectably increase (or decrease) the frequency of spontaneous EJPs over a 30-60 minute period (Figs. 9A-B, 11C). *eag* mutant animals thus both mimic and occlude the effects of ziram. These results suggest that eag channel blockade may be the primary mechanism of ziram's effect on excitability.

In contrast to *eag*, application of ziram to *Shaker* and *slowpoke* elicited EJPs (Fig. 9C, D). These data indicate that the target of ziram is still available for blockade in these mutants and supports the involvement of eag-type channels, but not other K channels, in the ziram-induced excitability increase. In addition, we note that in *Shaker* mutants, some of the EJPs occurring in response to ziram were slow depolarizing events, similar to those reported in *shaker* and *eag* double mutants (data not shown) (Ganetzky and Wu, 1983). We also observed slower repolarization of EJPs in the *slowpoke* mutants (Fig. 9D). These observations suggest that acute pharmacological block of eag channels by ziram acts akin to an *eag* null mutant in *modifying* the phenotype of *Shaker* and *slowpoke* mutants. In sum, our results support the hypothesis that increased neuronal excitability induced by ziram is likely due to disruption of a pathway involving eag or via direct inhibition of the eag channel.

eag mutations do not occlude ziram-induced mini frequency

To test the hypothesis that the mechanisms mediating ziram's effect on excitability and release probability are distinct, we examined the mini frequency of *eag*, *Shaker* and *slowpoke* mutant animals at baseline and following exposure to ziram (Fig. 9E, F). To allow for the quantification of minis in *eag* mutants, recordings were conducted in 1 µM TTX in order to block spontaneous EJPs. We did not observe a statistically significant difference in baseline mini frequency between wildtype and any of the K channel mutants (Fig. 9E). Application of 10 µM ziram elicited an increase in mini frequency in all K mutant lines tested, similar to the increase observed in wildtype animals (Fig. 9F). Two-way t-tests of each mutant showed that *eag*, *Shaker*, and *slowpoke* mutants have significantly increased mini frequencies in ziram relative to baseline (two-way t-tests: eag^{sc29} p=0.005; eag^{1} p= 0.03; Sh^{5} p=0.014; Sh^{KS133} p=0.03 (data not shown); $slowpoke^{1}$ p= 0.002; Fig 9F). Although the change in mini frequency in response to ziram appears less in *slowpoke* and *Shaker* animals than in *eag,* this difference in effect size

was not significant. These results support the hypothesis that inhibition of eag contributes to increased excitability but not to increased vesicle release.

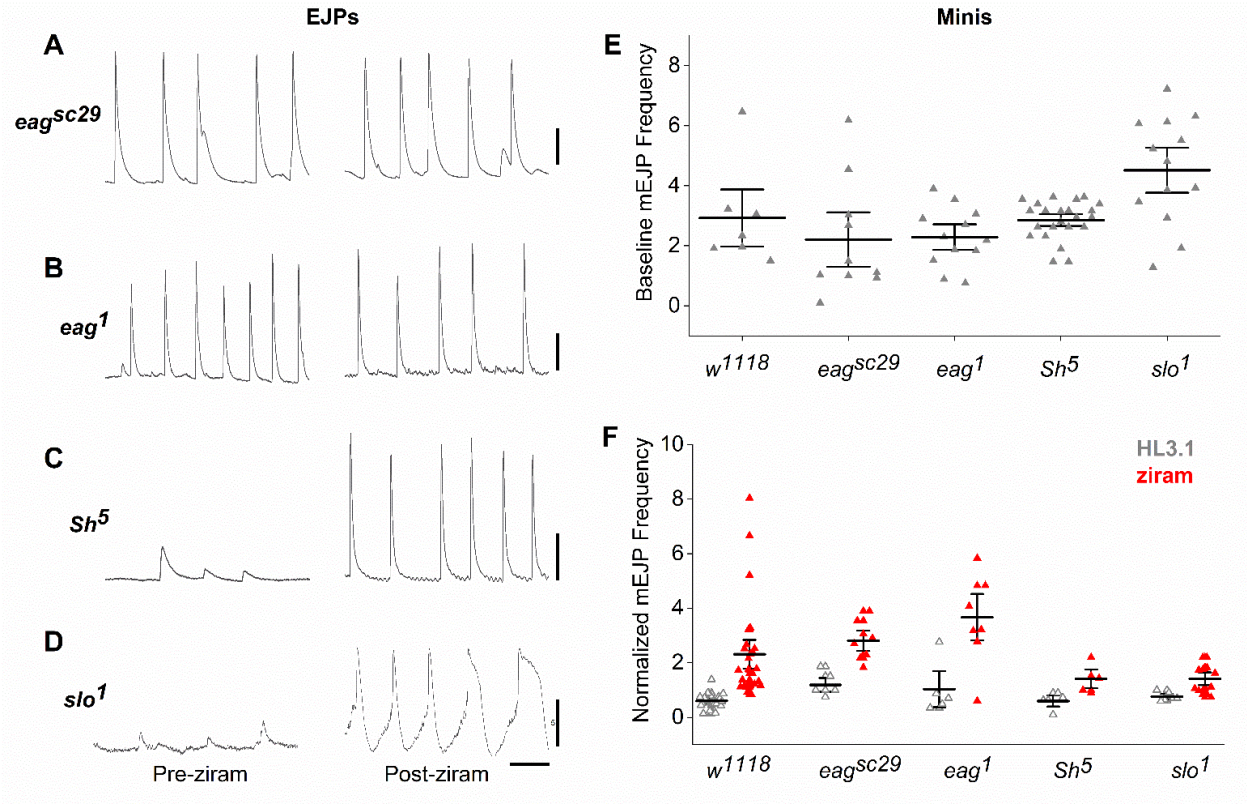

Figure 9. Ether-a-go-go potassium channel mutants phenocopy and occlude ziram-induced excitability, but not the ziram-induced changes in vesicle release probability. **A-D.** Representative traces of spontaneous EJPs in the eag^{sc29}, eag^{1}, Sh^{5}, and slo^{1} mutants in control (*left*) and after perfusion of 10 µM ziram (*right*, eag^{sc29} n=10, eag^{1} n=6, Sh^{5} n=5, and slo^{1} n=8). Scale is 200 ms and 5 mV. Ziram does not enhance EJP frequency in *eag* mutants. Ziram both increases mini frequency and elicits EJPs in *Shaker* and *slowpoke* mutants. **E.** Baseline mini frequencies during a five-minute recording period in wildtype and K channel mutants. **F.** Mini frequencies after perfusion of a second solution (control: grey open triangles; 10 µM ziram: red triangles). 1 µM TTX added to experiments using *eag* mutant animals. Mini frequencies were measured in wildtype and the following potassium channel mutants: eag^{sc29} (control n=5; ziram n=10), eag^{1} (control n=6; ziram n=6), Sh^{5} (control n=7; ziram n=5), Sh^{KS133} (control n=7;

ziram, n=7; data not shown), and *slo*^{1} (control n=5; ziram n=8). Note that ziram increases mini frequency independent of genotype.

The hERG inhibitor E4031 increases the excitability effect of ziram at elevated temperatures

Drosophila express three members of the eag-type family of K channels*: eag*, eag-like (*elk*), and an eag-related (*erg*) K channel called seizure (*sei*) (Titus et al., 1997). elk remains poorly characterized, especially in *Drosophila*, but the sei channel, an ortholog of the hERG channel in humans, was intriguing because it was previously shown to regulate synaptic function and excitability at the NMJ (Lee and Wu, 2010; Frolov et al., 2012; Hill et al., 2019). However, unlike eag, which maintains baseline excitability, the sei channel has been proposed to regulate neuronal excitability in response to heat stress (Jackson et al., 1984; Titus et al., 1997; Hill et al., 2019). At elevated temperatures s*ei* mutant larvae showed a decreased time to paralysis (Zheng et al., 2014), seizures (Hill et al., 2019) and increased branching at the NMJ (Lee and Wu, 2010). In the heart, sei seems to be active at room temperature and play a role similar to hERG (Ocorr et al., 2017). To determine whether we could detect the activity of sei in our preparation, we used the hERG channel inhibitor E4031, which phenocopies cardiac arrythmias (Ocorr et al., 2017) and the heat sensitivity phenotype (Zheng et al., 2014) of *sei* mutant flies. E4031 (100 μM) had no effect on neuronal excitability (n=6, see Fig 11B) at room temperature, consistent with the idea that although sei may be active in the heart at room temperature, it may be much less active at lower temperatures in neurons (Jackson et al., 1984; Titus et al., 1997; Hill et al., 2019) similar to hERG (Vandenberg et al., 2006; Vandenberg et al., 2012). Intriguingly, at elevated temperatures (40°C), E4031 elicited robust, spontaneous EJPs (Figs. 10A, 11B- C; Dunn-Sidak 40°C: 4.5±1.2, p= 0.006; 25°C: p= 0.07), consistent with E4031 inhibition of sei or another channel that only manifests itself at elevated temperatures.

Alternatively, based on these data alone we could not exclude the possibility E4031 only blocked eag channels but in a temperature dependent fashion. If so, E4031 should show little or no activity in an *eag* null mutant animal.

To begin to explore the relationship between E4031, ziram and the eag mutant, we first performed control experiments to test whether temperature alone would have any effects on excitability. We again elevated the temperature of the preparations to 40°C, and quantified EJP frequency in either wildtype animals or *eag* mutants in the absence of either ziram or E4031. We did not observe EJPs in wildtype flies at 40°C (Figs. 10A, 11B-C) and indeed observed a counterintuitive, two-fold *decrease* in EJP frequency at 40°C in *eag* mutants (*eag* 25°C: 1.0±0.34 Hz; *eag* 40°C: 0.47±0.06 Hz; p= 0.004; Figs. 10B, 11B-C). This decreased EJP frequency became more pronounced over time at 40°C and might reflect an adaptive engagement of sei or other temperature sensitive channels to counteract hyperexcitability.

To test whether ziram could inhibit other eag family members such as sei in addition to eag channels, we next recorded from wildtype and *eag* null mutants at elevated temperatures (40°C) in the presence of ziram. Application of ziram to wildtype animals at 40°C led to a larger increase in EJP frequency compared to room temperature (w^{1118} 25°C: 2.0±1.2 Hz; w^{1118} 40°C: 10.4±2.1 Hz; Dunn-Sidak: p=.001; Figs. 10A, 11B). The increased EJP frequency at elevated temperatures could be due to contributions from both eag and other temperature sensitive channels. We therefore recorded from *eag* null mutants at elevated temperatures. Ziram enhanced the EJP frequency in *eag* mutants relative to control solution at 40°C (control 40°C: 0.47±0.06 Hz; ziram 40°C: 7.9±1.76 Hz; n=12, Dunn-Sidak: p=0.003; Figs. 10B, 11C) but not at room temperature (Figs. 9A, 9B, 11C). These data indicate that at 40°C, ziram can increase excitability via blockade of a molecular target distinct from eag. Importantly, since eag^{sc29} is a null allele--, the increase in excitability is not due to further inhibition of eag.

To more specifically test whether the enhanced excitability effect of ziram at 40°C could be due to blockade of an E4031-sensitive channel such as sei, we applied E4031 to *eag* mutants at 25°C and 40°C. At 25°C, E4031 did not affect the EJP frequency in either w^{1118} or *eag* mutants (Fig. 11B, C). In contrast, E4031 did increase the EJP frequency in w^{1118} and *eag* mutants relative to control solution at 40°C (E4031 40°C: 7.13± 1.4 Hz; control 40°C: 0.47±0.06 Hz; Dunn-Sidak, p= 0.04; Figs. 10B, 11C). Our results are consistent with the idea that ziram inhibits both eag as well as a temperature and E4031 sensitive channel such as the sei ortholog hERG (Fig. 11A).

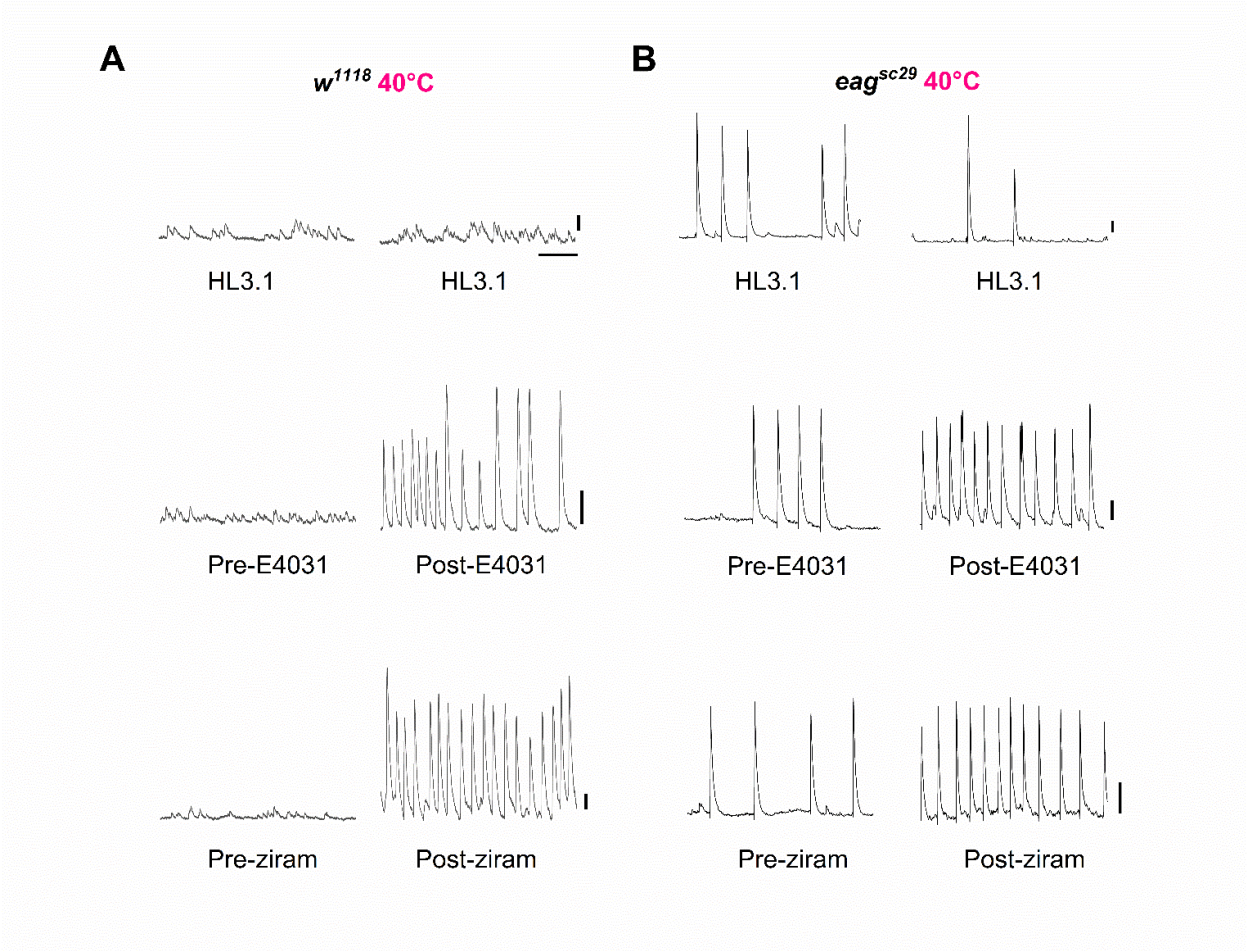

Figure 10. Ziram and E4031 enhance excitability at elevated temperature. A. Representative traces of minis in wildtype (w^{1118}) animals at baseline (*left*) and with control, 100

µM E4031, or 10 µM ziram (*right*) recorded at 40°C (control n=7, E4031 n=8; ziram n=9). Scale bar is 200 ms and 5 mV. **B.** Representative traces of EJP Frequency in *eag*^{sc29} null mutants at baseline (*left*) and with control, 100 µM E4031, or 10 µM ziram solution recorded at 40°C (control n=19, E4031 n=8, ziram n=12). Scale bar is 200 ms and 5 mV.

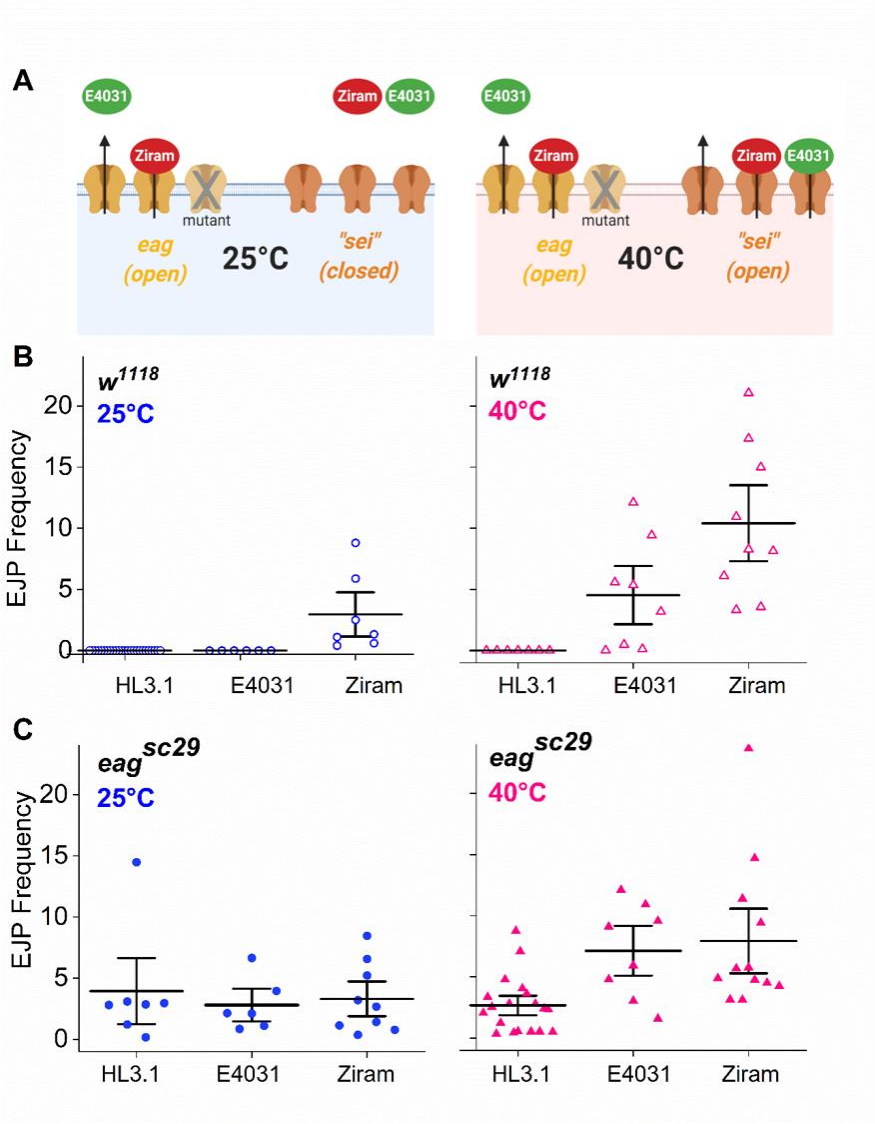

Figure 11. At 40°C ziram blocks both eag and "sei" potassium channels. A. Proposed mechanism: at 25°C, ziram inhibits the eag K channel to increase excitability and *eag* null mutants also show enhanced excitability. E4031, a hERG channel blocker, has no effect since

most sei channels are closed (*left).* At 40°C, sei channels are thought to be active. Both ziram and E4031 inhibit “sei” to drive excitability in wildtype and *eag* mutants. Ziram increases excitability by blocking both “sei” and eag (*right)*. **B.** EJP frequency in wildtype at 25°C (*left*) in control (n=25), E4031 (n=6) and ziram (n=7) and in experiments performed at 40°C (*right;* control, n=7, E4031, n=8; ziram, n=9). **C**. EJP frequency in eag^{sc29} null mutants at 25°C (*left)* in control (n=7 E4031 (n=6), and ziram (n=9) and in experiments performed at 40°C (*right;* control, n=19*;* E4031 n=8; ziram n=12). Since the target of the E4031 is not unequivocally sei and could potentially be another temperature sensitive channel, the name is depicted in quotation marks (“sei,” see main text for discussion).

Discussion

A combination of genetic susceptibilities and environmental factors are thought to contribute to complex diseases such as cardiovascular disease and neurological conditions such as idiopathic PD and Alzheimer’s disease (AD) (Szot, 2012; Baltazar et al., 2014; Yegambaram et al., 2015). While chronic exposure paradigms using a combination of chemicals will be essential to determine how toxicants cause cell death in neurodegenerative diseases, acute exposure will pinpoint the initial targets of each toxicant that might be compromised long before the manifestation of clinical symptoms (Carvey et al., 2006; Heinemann et al., 2016). Ziram inhibits several biochemical pathways *in vitro* and *in vivo* (ALDH, E1 ligase, sodium-calcium exchanger, mitochondrial functions) but the relationship between these and other putative targets and human disease remains unclear (Rinetti and Schweizer, 2010; Fitzmaurice et al., 2014; Jin et al., 2014; Matei and Trombetta, 2016). We have used an open-ended approach in *Drosophila melanogaster* to investigate how ziram changes neuronal activity and identified a novel molecular pathway through which ziram can increase neuronal excitability.

Inhibition of E1 ligase increases synaptic vesicle release in cultured mammalian neurons, however the mechanisms remain unclear (Rinetti and Schweizer, 2010). Protein degradation via the proteasome is one possible pathway and has been suggested to regulate both the fly NMJ and mammalian synaptic activity (Speese et al., 2003; Rinetti and Schweizer, 2010; Ramachandran and Margolis, 2017; Ramachandran et al., 2018). However, the effects of proteasome inhibitors in our experiments differ from the effects of E1 ligase inhibitors. Ubiquitination can alter protein function in several ways that are distinct from proteasome dependent degradation, including the regulation of mitochondrial function, membrane trafficking, and endocytosis (DiAntonio and Hicke, 2004). Using ziram and other toxicants in combination with *Drosophila* genetics may help uncover the relevance of these non-degradative ubiquitin signaling system pathways to synaptic function and the early stages of complex diseases.

We previously reported that ziram causes an increase in the excitability of octopaminergic processes at the fly NMJ as observed through an increase in spontaneous calcium signals (Martin et al., 2016). However, an increase in calcium signals in presynaptic glutamatergic processes was not detected, possibly due to differences in calcium homeostasis between octopaminergic and glutamatergic axons (Xing and Wu, 2018). It thus seemed possible that ziram could elicit spontaneous APs in glutamatergic processes without causing detectable calcium transients. Hence, we re-examined the effects of ziram in glutamatergic neurons using electrophysiological methods. Indeed, ziram induces EJPs, suggesting that excitability of not only aminergic but also glutamatergic neurons is increased. We cannot rule out the possibility that ziram acts on octopaminergic neurons and that the release of octopamine, or indeed another transmitter, affects the changes in the glutamatergic neurons (Nagaya et al., 2002)

In addition to peripheral octopaminergic neuronal processes (Fig. 1A-D), we show that ziram increases the excitability of octopaminergic neurons in the adult CNS through a decrease in AP threshold and an increase in resting membrane potential (Fig. 3A-C). In the larval CNS,

octopaminergic neurons regulate the activity of glutamatergic motoneurons that project peripherally to the NMJ (Simon et al., 2009; Selcho et al., 2014). Taking advantage of this locomotion circuit, we show that 1 μM ziram only elicits motoneuron APs if the distal portion of the VNC is left intact, but not when the VNC is completely severed and only the peripheral axons are present (Fig. 5B, F). This central interaction could be elicited through octopaminergic neurons, but additional pathways that regulate motoneuron output might contribute to the increased excitability as well. These data support the idea that ziram may differentially affect some neuronal processes within a circuit, and that the effects of ziram on excitability can influence downstream outputs.

Ziram-induced increases in excitability of glutamatergic and octopaminergic neurons could propagate through circuits and thus indirectly affect other classes of neurons in the CNS in flies and perhaps mammals. We note that changes in the excitability of glutamatergic processes have been suggested to contribute to the pathophysiology of PD and the death of norepinephrine (NE) and dopaminergic (DA) neurons (Calabresi et al., 1993; Ridding et al., 1995; Ambrosi et al., 2014).

Potassium channels are exquisite regulators of neuronal activity that have been implicated in both the neuroprotective and pathophysiological effects of neurodegenerative diseases including both AD and PD (Dragicevic et al., 2015; Duda et al., 2016; Chen et al., 2018; Zott et al., 2018). For example, inactivation of K-ATP channels as well as inhibition of SK channels have been shown to block DA cell activity and cell death in rodent models (Liss et al., 2005; Duda et al., 2016). Similarly, overexpression of mutant alpha-synuclein increases DA neuron firing frequency by inhibiting A-type K channels (Subramaniam et al., 2014). In animal models of AD, ablation of the AD-linked β-secretase BACE1 reduces the amount of the m-current mediating Kv7.2/KCNQ2 (Lehnert et al., 2016) and decreased surface expression of the A-type K channel Kv3.4, both leading to enhanced excitability (Hartmann et al., 2018). Here we report

that ziram acutely alters neuronal excitability by inhibiting members of the *ether-a-go-go* channel family, eag itself and possibly sei. A third member of this family, *elk*, remains poorly characterized in flies, and mutants do not show any apparent phenotype (Ganetzky et al., 1999). E4031 has been shown to inhibit hERG channels, but its actions on sei channels are not well characterized and are mostly inferred by E4031 mimicking and interacting with behavior observed in *sei* mutants (Zheng et al., 2014; Ocorr et al., 2017). Thus, while the sequence similarity between hERG and *sei* and the temperature dependent action of E4031 (Zheng et al., 2014; Ocorr et al., 2017) support the notion that E4031 blocks sei, additional channels could also serve as targets of ziram, and more direct experiments using sei mutants will be necessary to distinguish between these possibilities. It is also conceivable that ziram may act via a common upstream regulatory pathway rather than direct inhibition of K channels in the eag family and experiments using heterologously expressed cDNAs representing each channel will be necessary to address this question.

Eag and *sei* were discovered in *Drosophila* as hyperexcitability mutants at baseline and under heat stress, respectively, and *eag* led to the discovery of the eag family of channels in mammals (Ganetzky and Wu, 1983, 1986). Later the fly *seizure* locus was shown to encode the *Drosophila* homolog of hERG (Wang et al., 1997). Humans express eight orthologs of eag, originally classified as the KCNH family of K channels, which are grouped into the Kv10 (hEAG), Kv11 (hERG) and Kv12 (ELK) channels (Ganetzky et al., 1999). eag channels were previously reported to preferentially localize to neuronal axons and terminals rather than the somatodendritic compartment (Sun et al., 2004; Bronk et al., 2018). Similarly, sei channels were shown to be enriched in axonal projections in glutamatergic and octopaminergic neurons (Hill et al., 2019). Consistent with this, our results indicate that ziram affects axonal projections more strongly than cell bodies (Fig. 2C, D). However, the increased firing threshold in adult abdominal

ganglion cell bodies detected by whole-cell recordings indicates a possible direct effect on cell bodies (Fig. 3B, C).

We hypothesize that ziram will also inhibit eag orthologs in mammalian neurons. Our attention has been particularly drawn to the channel encoded by human *eag*-related gene 1 (hERG1/KCNH2/Kv11.1) because of its relevance to human disease, especially cardiac arrhythmias (Vandenberg et al., 2012). Disruption of hERG1 activity caused by either genetic mutations or drugs is a major cause of long QT syndrome that increases the risk of potentially fatal arrhythmias (Perrin and Gollob, 2013; Perry et al., 2015). Interestingly, the prevalence of long QT syndrome is also elevated in PD patients (Deguchi et al., 2002) and emerging evidence indicates an interaction between arrhythmias and AD (Ihara and Washida, 2018), but the potential relevance of hERG to PD or AD has not been explored. hERG1 is inhibited by an unusually large number of structurally diverse drugs including commonly prescribed drugs and our findings suggest that ziram might be added to this list (Suessbrich et al., 1997; Thomas et al., 2002; Lee et al., 2012; Kratz et al., 2017).

A majority of studies on inhibition of eag orthologs have focused on its physiology in the context of cardiac conditions, but all members of this family are widely expressed in the nervous system (Jeng et al., 2005; Ferreira et al., 2012; Perrin and Gollob, 2013; Perry et al., 2015). We speculate that inhibition of human eag orthologs by ziram and by other compounds increases neuronal excitability and contributes to the initiation of disease and possibly early progression of neurotoxicity (Duda et al., 2016). ERG channels are highly expressed in the striatum, globus pallidus, and SN, and hERG inhibitors (E4031 and rBeKm-1) directly increase the rate of spontaneous firing in midbrain DA neurons (Ferreira et al., 2012; Ji et al., 2012). *eag* orthologs are also expressed in CNS glutamatergic neurons (Jeng et al., 2005; Vandenberg et al., 2012). It is possible that inhibition of a subset of human *eag* channels by ziram could indirectly and directly affect DA neurons by increasing excitatory glutamatergic drive and by increasing DA

neuron activity, thus increasing metabolic load (Blandini, 2010; Ji et al., 2012). *eag* orthologs are also expressed in NE neurons and contribute to physiological functions such as heart rate, sleep, arousal, and stress (Gullo et al., 2003; Schwarz and Luo, 2015). We note that in flies, *sei* and *eag* mutants exhibit neuropathology and reduced longevity, suggesting their potential relevance to neurodegenerative diseases (Fergestad et al., 2006). Although the mechanisms underlying these effects remain unclear, these data suggest that additional studies in the fly might be used to dissect the relationship between the eag family and downstream pathophysiological processes.

We have used *Drosophila* molecular genetics in combination with calcium imaging and electrophysiology to identify target pathways, which may contribute to neurophysiological effects of ziram. If dysfunction of the eag channel family in humans does indeed play a role in human neuropathology, it will necessitate the evaluation of mutations as risk factors, and of additional environmental and pharmaceutical compounds that act on these channels. Our data further suggest that patients exposed to ziram should be examined for evidence of cardiac hyperexcitability, a known risk of drugs that target the eag family of K channels.

Summary

Complex diseases such as idiopathic PD are thought to be caused by the interaction of multiple genetic and environmental factors. While the study of genetic risk factors has contributed enormously to our mechanistic understanding of complex diseases, environmental toxicants have received much less attention. We propose that examination of the acute effects of disease-linked environmental factors will expose potentially novel molecular pathways involved in complex diseases. Using *Drosophila*, we show that the widely used agricultural fungicide ziram alters both glutamatergic and aminergic neuronal function via two distinct mechanisms: i) increasing the probability of vesicle release through an E1-ligase dependent pathway and, ii),

increasing electrophysiological excitability. Null mutants of the potassium channel *ether a-go-go* phenocopy and occlude the ziram-induced increase in excitability. Moreover, E4031, an inhibitor of the hERG (human *eag* related gene) channel, an ortholog of sei, also phenocopies and occludes ziram-induced excitability increases, but only at elevated temperatures. Sei or a related channel may thus be an additional target of ziram at elevated temperatures. Taken together, our data raise the novel possibility that ziram could inhibit human eag channel orthologs such as hERG and thereby contribute to human disease states such as PD.

References

Ambrosi G, Cerri S, Blandini F (2014) A further update on the role of excitotoxicity in the pathogenesis of Parkinson's disease. J Neural Transm (Vienna) 121:849-859.

Ascherio A, Schwarzschild MA (2016) The epidemiology of Parkinson's disease: risk factors and prevention. Lancet Neurol 15:1257-1272.

Atwood HL, Govind CK, Wu CF (1993) Differential ultrastructure of synaptic terminals on ventral longitudinal abdominal muscles in Drosophila larvae. J Neurobiol 24:1008-1024.

Baltazar MT, Dinis-Oliveira RJ, de Lourdes Bastos M, Tsatsakis AM, Duarte JA, Carvalho F (2014) Pesticides exposure as etiological factors of Parkinson's disease and other neurodegenerative diseases--a mechanistic approach. Toxicol Lett 230:85-103.

Bauer CK, Schwarz JR (2018) Ether-a-go-go K(+) channels: effective modulators of neuronal excitability. J Physiol 596:769-783.

Bezard E, Yue Z, Kirik D, Spillantini MG (2013) Animal models of Parkinson's disease: limits and relevance to neuroprotection studies. Mov Disord 28:61-70.

Blandini F (2010) An update on the potential role of excitotoxicity in the pathogenesis of Parkinson's disease. Funct Neurol 25:65-71.

Bronk P, Kuklin EA, Gorur-Shandilya S, Liu C, Wiggin TD, Reed ML, Marder E, Griffith LC (2018) Regulation of Eag by Ca(2+)/calmodulin controls presynaptic excitability in Drosophila. J Neurophysiol 119:1665-1680.

Calabresi P, Mercuri NB, Sancesario G, Bernardi G (1993) Electrophysiology of dopamine-denervated striatal neurons. Implications for Parkinson's disease. Brain 116 (Pt 2):433-452.

Cannon JR, Greenamyre JT (2011) The role of environmental exposures in neurodegeneration and neurodegenerative diseases. Toxicol Sci 124:225-250.

Cao F, Souders Ii CL, Perez-Rodriguez V, Martyniuk CJ (2018) Elucidating Conserved Transcriptional Networks Underlying Pesticide Exposure and Parkinson's Disease: A Focus on Chemicals of Epidemiological Relevance. Front Genet 9:701.

Cao F, Souders CL, Li P, Adamovsky O, Pang S, Qiu L, Martyniuk CJ (2019) Developmental toxicity of the fungicide ziram in zebrafish (Danio rerio). Chemosphere 214:303-313.

Carvey PM, Punati A, Newman MB (2006) Progressive dopamine neuron loss in Parkinson's disease: the multiple hit hypothesis. Cell Transplant 15:239-250.

Chen TW, Wardill TJ, Sun Y, Pulver SR, Renninger SL, Baohan A, Schreiter ER, Kerr RA, Orger MB, Jayaraman V, Looger LL, Svoboda K, Kim DS (2013) Ultrasensitive fluorescent proteins for imaging neuronal activity. Nature 499:295-300.

Chen X, Xue B, Wang J, Liu H, Shi L, Xie J (2018) Potassium Channels: A Potential Therapeutic Target for Parkinson's Disease. Neurosci Bull 34:341-348.

Chou AP, Maidment N, Klintenberg R, Casida JE, Li S, Fitzmaurice AG, Fernagut PO, Mortazavi F, Chesselet MF, Bronstein JM (2008) Ziram causes dopaminergic cell damage by inhibiting E1 ligase of the proteasome. J Biol Chem 283:34696-34703.

Cole SH, Carney GE, McClung CA, Willard SS, Taylor BJ, Hirsh J (2005) Two functional but noncomplementing Drosophila tyrosine decarboxylase genes: distinct roles for neural tyramine and octopamine in female fertility. J Biol Chem 280:14948-14955.

Cosselman KE, Navas-Acien A, Kaufman JD (2015) Environmental factors in cardiovascular disease. Nat Rev Cardiol 12:627-642.

de Lau LM, Breteler MM (2006) Epidemiology of Parkinson's disease. Lancet Neurol 5:525-535.

De Strooper B, Karran E (2016) The Cellular Phase of Alzheimer's Disease. Cell 164:603-615.

Deguchi K, Sasaki I, Tsukaguchi M, Kamoda M, Touge T, Takeuchi H, Kuriyama S (2002) Abnormalities of rate-corrected QT intervals in Parkinson's disease-a comparison with multiple system atrophy and progressive supranuclear palsy. J Neurol Sci 199:31-37.

Dennis KE, Valentine WM (2015) Ziram and sodium N,N-dimethyldithiocarbamate inhibit ubiquitin activation through intracellular metal transport and increased oxidative stress in HEK293 cells. Chem Res Toxicol 28:682-690.

DiAntonio A, Hicke L (2004) Ubiquitin-dependent regulation of the synapse. Annu Rev Neurosci 27:223-246.

Dragicevic E, Schiemann J, Liss B (2015) Dopamine midbrain neurons in health and Parkinson's disease: emerging roles of voltage-gated calcium channels and ATP-sensitive potassium channels. Neuroscience 284:798-814.

Duda J, Potschke C, Liss B (2016) Converging roles of ion channels, calcium, metabolic stress, and activity pattern of Substantia nigra dopaminergic neurons in health and Parkinson's disease. J Neurochem 139 Suppl 1:156-178.

Efron B, Tibshirani R (1991) Statistical data analysis in the computer age. Science 253:390-395.

Efron B, Hastie T (2016) *Computer Age Statistical Inference: Algorithms, Evidence, and Data Science* Cambridge Univ. Press.

Feng Y, Ueda A, Wu CF (2004) A modified minimal hemolymph-like solution, HL3.1, for physiological recordings at the neuromuscular junctions of normal and mutant Drosophila larvae. J Neurogenet 18:377-402.

Fergestad T, Ganetzky B, Palladino M (2006) Neuropathology in Drosophila Membrane Excitability Mutants. Genetics 172:1031-1042.

Ferreira NR, Mitkovski M, Stuhmer W, Pardo LA, Del Bel EA (2012) Ether-a-go-go 1 (Eag1) potassium channel expression in dopaminergic neurons of basal ganglia is modulated by 6-hydroxydopamine lesion. Neurotoxicity research 21:317-333.

Fitzmaurice AG, Rhodes SL, Cockburn M, Ritz B, Bronstein JM (2014) Aldehyde dehydrogenase variation enhances effect of pesticides associated with Parkinson disease. Neurology 82:419-426.

Fox LE, Soll DR, Wu CF (2006) Coordination and modulation of locomotion pattern generators in Drosophila larvae: effects of altered biogenic amine levels by the tyramine beta hydroxlyase mutation. J Neurosci 26:1486-1498.

Frolov RV, Bagati A, Casino B, Singh S (2012) Potassium channels in Drosophila: historical breakthroughs, significance, and perspectives. J Neurogenet 26:275-290.

Ganetzky B, Wu CF (1983) Neurogenetic analysis of potassium currents in Drosophila: synergistic effects on neuromuscular transmission in double mutants. J Neurogenet 1:17-28.

Ganetzky B, Wu CF (1986) Neurogenetics of membrane excitability in Drosophila. Annu Rev Genet 20:13-44.

Ganetzky B, Robertson GA, Wilson GF, Trudeau MC, Titus SA (1999) The eag family of K+ channels in Drosophila and mammals. Ann N Y Acad Sci 868:356-369.

Goldman SM (2014) Environmental toxins and Parkinson's disease. Annual review of pharmacology and toxicology 54:141--164.

Goldman SM, Kamel F, Ross GW, Bhudhikanok GS, Hoppin JA, Korell M, Marras C, Meng C, Umbach DM, Kasten M, Chade AR, Comyns K, Richards MB, Sandler DP, Blair A, Langston JW, Tanner CM (2012) Genetic modification of the association of paraquat and Parkinson's disease. Mov Disord 27:1652-1658.

Gullo F, Ales E, Rosati B, Lecchi M, Masi A, Guasti L, Cano-Abad MF, Arcangeli A, Lopez MG, Wanke E (2003) ERG K+ channel blockade enhances firing and epinephrine secretion in rat chromaffin cells: the missing link to LQT2-related sudden death? FASEB J 17:330-332.

Hales KG, Korey CA, Larracuente AM, Roberts DM (2015) Genetics on the Fly: A Primer on the Drosophila Model System. Genetics 201:815-842.

Hartmann S, Zheng F, Kyncl MC, Karch S, Voelkl K, Zott B, D'Avanzo C, Lomoio S, Tesco G, Kim DY, Alzheimer C, Huth T (2018) beta-Secretase BACE1 Promotes Surface

Expression and Function of Kv3.4 at Hippocampal Mossy Fiber Synapses. J Neurosci 38:3480-3494.

Heinemann SD, Posimo JM, Mason DM, Hutchison DF, Leak RK (2016) Synergistic stress exacerbation in hippocampal neurons: Evidence favoring the dual-hit hypothesis of neurodegeneration. Hippocampus 26:980-994.

Hill AS, Jain P, Folan NE, Ben-Shahar Y (2019) The Drosophila ERG channel seizure plays a role in the neuronal homeostatic stress response. PLoS Genet 15:e1008288.

Ihara M, Washida K (2018) Linking Atrial Fibrillation with Alzheimer's Disease: Epidemiological, Pathological, and Mechanistic Evidence. J Alzheimers Dis 62:61-72.

Imlach W, McCabe BD (2009) Electrophysiological Methods for Recording Synaptic Potentials from the NMJ of Drosophila Larvae. JoVE:e1109.

Jackson FR, Wilson SD, Strichartz GR, Hall LM (1984) Two types of mutants affecting voltage-sensitive sodium channels in Drosophila melanogaster. Nature 308:189-191.

Jan LY, Jan YN (2012) Voltage-gated potassium channels and the diversity of electrical signalling. J Physiol 590:2591-2599.

Jeng CJ, Chang CC, Tang CY (2005) Differential localization of rat Eag1 and Eag2 K+ channels in hippocampal neurons. Neuroreport 16:229-233.

Ji H, Tucker KR, Putzier I, Huertas MA, Horn JP, Canavier CC, Levitan ES, Shepard PD (2012) Functional characterization of ether-a-go-go-related gene potassium channels in midbrain dopamine neurons - implications for a role in depolarization block. Eur J Neurosci 36:2906-2916.

Jin J, Lao AJ, Katsura M, Caputo A, Schweizer FE, Sokolow S (2014) Involvement of the sodium-calcium exchanger 3 (NCX3) in ziram-induced calcium dysregulation and toxicity. Neurotoxicology 45:56-66.

Koon AC, Budnik V (2012) Inhibitory control of synaptic and behavioral plasticity by octopaminergic signaling. J Neurosci 32:6312-6322.

Kratz JM, Grienke U, Scheel O, Mann SA, Rollinger JM (2017) Natural products modulating the hERG channel: heartaches and hope. Nat Prod Rep 34:957-980.

Kutsukake M, Komatsu A, Yamamoto D, Ishiwa-Chigusa S (2000) A tyramine receptor gene mutation causes a defective olfactory behavior in Drosophila melanogaster. Gene 245:31-42.

Langston JW (2017) The MPTP Story. J Parkinsons Dis 7:S11-s19.

Lee J, Wu CF (2010) Orchestration of Stepwise Synaptic Growth by K+ and Ca2+ Channels in Drosophila. J Neurosci 30(47):15821-15833.

Lee SH, Sung MJ, Hahn SJ, Kim J, Min G, Jo SH, Choe H, Choi BH (2012) Blockade of human HERG K(+) channels by rosiglitazone, an antidiabetic drug. Arch Pharm Res 35:1655-1664.

Lehnert S, Hartmann S, Hessler S, Adelsberger H, Huth T, Alzheimer C (2016) Ion channel regulation by beta-secretase BACE1 - enzymatic and non-enzymatic effects beyond Alzheimer's disease. Channels (Austin) 10:365-378.

Liss B, Haeckel O, Wildmann J, Miki T, Seino S, Roeper J (2005) K-ATP channels promote the differential degeneration of dopaminergic midbrain neurons. Nat Neurosci 8:1742-1751.

Littleton JT, Ganetzky B (2000) Ion channels and synaptic organization: analysis of the Drosophila genome. Neuron 26:35-43.

Lotharius J, Brundin P (2002) Pathogenesis of Parkinson's disease: dopamine, vesicles and alpha-synuclein. Nat Rev Neurosci 3:932-942.

Mackay TF (2015) Epistasis for quantitative traits in Drosophila. Methods Mol Biol 1253:47-70.

Martin CA, Myers KM, Chen A, Martin NT, Barajas A, Schweizer FE, Krantz DE (2016) Ziram, a pesticide associated with increased risk for Parkinson's disease, differentially affects the presynaptic function of aminergic and glutamatergic nerve terminals at the Drosophila neuromuscular junction. Exp Neurol 275 Pt 1:232-241.

Matei AM, Trombetta LD (2016) Exposure of rat hippocampal astrocytes to Ziram increases oxidative stress. Toxicol Ind Health 32:579-588.

Mauerhöfer M, Bauer CK (2016) Effects of Temperature on Heteromeric Kv11.1a/1b and Kv11.3 Channels. Biophys J 111:504-523.

McCormack AL, Thiruchelvam M, Manning-Bog AB, Thiffault C, Langston JW, Cory-Slechta DA, Di Monte DA (2002) Environmental risk factors and Parkinson's disease: selective degeneration of nigral dopaminergic neurons caused by the herbicide paraquat. Neurobiol Dis 10:119-127.

Monastirioti M, Gorczyca M, Rapus J, Eckert M, White K, Budnik V (1995) Octopamine immunoreactivity in the fruit fly Drosophila melanogaster. J Comp Neurol 356:275-287.

Mostafalou S, Abdollahi M (2013) Pesticides and human chronic diseases: evidences, mechanisms, and perspectives. Toxicol Appl Pharmacol 268:157-177.

Muddapu VR, Mandali A, Chakravarthy VS, Ramaswamy S (2019) A Computational Model of Loss of Dopaminergic Cells in Parkinson's Disease Due to Glutamate-Induced Excitotoxicity. Front Neural Circuits 13:11.

Nagaya Y, Kutsukake M, Chigusa SI, Komatsu A (2002) A trace amine, tyramine, functions as a neuromodulator in Drosophila melanogaster. Neurosci Lett 329:324-328.

Nandipati S, Litvan I (2016) Environmental Exposures and Parkinson's Disease. Int J Environ Res Public Health 13.

Noyce AJ, Lees AJ, Schrag A-E (2016) The prediagnostic phase of Parkinson's disease. Journal of Neurology, Neurosurgery & Psychiatry 87:871-878.

Ocorr K, Zambon A, Nudell Y, Pineda S, Diop S, Tang M, Akasaka T, Taylor E (2017) Age-dependent electrical and morphological remodeling of the Drosophila heart caused by hERG/seizure mutations. In: PLoS Genet.

Pallanck L, Ganetzky B (1994) Cloning and characterization of human and mouse homologs of the Drosophila calcium-activated potassium channel gene, slowpoke. Hum Mol Genet 3:1239-1243.

Parron T, Requena M, Hernandez AF, Alarcon R (2011) Association between environmental exposure to pesticides and neurodegenerative diseases. Toxicol Appl Pharmacol 256:379-385.

Perrin MJ, Gollob MH (2013) Genetics of cardiac electrical disease. Can J Cardiol 29:89-99.

Perry MD, Ng CA, Mann SA, Sadrieh A, Imtiaz M, Hill AP, Vandenberg JI (2015) Getting to the heart of hERG K(+) channel gating. The Journal of physiology 593:2575-2585.

Ramachandran KV, Margolis SS (2017) A mammalian nervous-system-specific plasma membrane proteasome complex that modulates neuronal function. Nat Struct Mol Biol 24:419-430.

Ramachandran KV, Fu JM, Schaffer TB, Na CH, Delannoy M, Margolis SS (2018) Activity-Dependent Degradation of the Nascentome by the Neuronal Membrane Proteasome. Mol Cell 71:169-177.e166.

Rezaval C, Pavlou HJ, Dornan AJ, Chan YB, Kravitz EA, Goodwin SF (2012) Neural circuitry underlying Drosophila female postmating behavioral responses. Curr Biol 22:1155-1165.

Ridding MC, Inzelberg R, Rothwell JC (1995) Changes in excitability of motor cortical circuitry in patients with Parkinson's disease. Ann Neurol 37:181-188.

Rinetti GV, Schweizer FE (2010) Ubiquitination acutely regulates presynaptic neurotransmitter release in mammalian neurons. J Neurosci 30:3157-3166.

Rodriguez-Valentin R, Lopez-Gonzalez I, Jorquera R, Labarca P, Zurita M, Reynaud E (2006) Oviduct contraction in Drosophila is modulated by a neural network that is both, octopaminergic and glutamatergic. J Cell Physiol 209:183-198.

Ryglewski S, Duch C (2012) Preparation of Drosophila Central Neurons for in situ Patch Clamping. In: J Vis Exp.

Saraswati S, Fox LE, Soll DR, Wu CF (2004) Tyramine and octopamine have opposite effects on the locomotion of Drosophila larvae. J Neurobiol 58:425-441.

Schwarz LA, Luo L (2015) Organization of the Locus Coeruleus-Norepinephrine System. Curr Biol 25:R1051-R1056.

Selcho M, Pauls D, Huser A, Stocker RF, Thum AS (2014) Characterization of the octopaminergic and tyraminergic neurons in the central brain of Drosophila larvae. J Comp Neurol 522:3485-3500.

Shieh CC, Coghlan M, Sullivan JP, Gopalakrishnan M (2000) Potassium channels: molecular defects, diseases, and therapeutic opportunities. Pharmacol Rev 52:557-594.

Simon AF, Daniels R, Romero-Calderón R, Grygoruk A, Chang HY, Najibi R, Shamouelian D, Salazar E, Solomon M, Ackerson LC, Maidment NT, DiAntonio A, Krantz DE (2009) Drosophila Vesicular Monoamine Transporter Mutants Can Adapt to Reduced or Eliminated Vesicular Stores of Dopamine and Serotonin. In: Genetics, pp 525-541.

Speese SD, Trotta N, Rodesch CK, Aravamudan B, Broadie K (2003) The ubiquitin proteasome system acutely regulates presynaptic protein turnover and synaptic efficacy. Curr Biol 13:899-910.

Stallones L, Beseler CL (2016) Assessing the connection between organophosphate pesticide poisoning and mental health: A comparison of neuropsychological symptoms from clinical observations, animal models and epidemiological studies. Cortex 74:405-416.

Subramaniam M, Althof D, Gispert S, Schwenk J, Auburger G, Kulik A, Fakler B, Roeper J (2014) Mutant alpha-synuclein enhances firing frequencies in dopamine substantia nigra neurons by oxidative impairment of A-type potassium channels. J Neurosci 34:13586-13599.

Suessbrich H, Schonherr R, Heinemann SH, Attali B, Lang F, Busch AE (1997) The inhibitory effect of the antipsychotic drug haloperidol on HERG potassium channels expressed in Xenopus oocytes. Br J Pharmacol 120:968-974.

Sulzer D (2007) Multiple hit hypotheses for dopamine neuron loss in Parkinson's disease. Trends Neurosci 30:244-250.

Sun XX, Hodge JJ, Zhou Y, Nguyen M, Griffith LC (2004) The eag potassium channel binds and locally activates calcium/calmodulin-dependent protein kinase II. J Biol Chem 279:10206-10214.

Szot P (2012) Common factors among Alzheimer's disease, Parkinson's disease, and epilepsy: Possible role of the noradrenergic nervous system. Epilepsia 53:61--66.

Thomas D, Gut B, Wendt-Nordahl G, Kiehn J (2002) The antidepressant drug fluoxetine is an inhibitor of human ether-a-go-go-related gene (HERG) potassium channels. J Pharmacol Exp Ther 300:543-548.

Titus SA, Warmke JW, Ganetzky B (1997) The Drosophila erg K+ channel polypeptide is encoded by the seizure locus. J Neurosci 17:875-881.

Vandenberg JI, Varghese A, Lu Y, Bursill JA, Mahaut-Smith MP, Huang CL (2006) Temperature dependence of human ether-a-go-go-related gene K+ currents. Am J Physiol Cell Physiol 291:C165-175.

Vandenberg JI, Perry MD, Perrin MJ, Mann SA, Ke Y, Hill AP (2012) hERG K(+) channels: structure, function, and clinical significance. Physiol Rev 92:1393-1478.

Wang A, Costello S, Cockburn M, Zhang X, Bronstein J, Ritz B (2011) Parkinson's disease risk from ambient exposure to pesticides. Eur J Epidemiol 26:547-555.

Wang XJ, Reynolds ER, Deak P, Hall LM (1997) The seizure locus encodes the Drosophila homolog of the HERG potassium channel. J Neurosci 17:882-890.

Xing X, Wu CF (2018) Unraveling Synaptic GCaMP Signals: Differential Excitability and Clearance Mechanisms Underlying Distinct Ca2+ Dynamics in Tonic and Phasic Excitatory, and Aminergic Modulatory Motor Terminals in Drosophila. In: eNeuro.

Yegambaram M, Manivannan B, Beach TG, Halden RU (2015) Role of environmental contaminants in the etiology of Alzheimer's disease: a review. Curr Alzheimer Res 12:116-146.

Yi JJ, Ehlers MD (2005) Ubiquitin and protein turnover in synapse function. Neuron 47:629-632.

Zheng X, Valakh V, Diantonio A, Ben-Shahar Y (2014) Natural antisense transcripts regulate the neuronal stress response and excitability. Elife 3:e01849.

Zott B, Busche MA, Sperling RA, Konnerth A (2018) What Happens with the Circuit in Alzheimer's Disease in Mice and Humans? Annu Rev Neurosci 41:277-297.

Chapter 2: Glutamatergic regulation of *Drosophila* oviduct muscle physiology

Abstract

Visceral muscle contraction and its regulation by neuronal activity is critical for the survival and reproduction of animals and thus it is important to understand the neuronal circuits underlying visceral muscle physiology. The *Drosophila melanogaster* reproductive tract represents a simple model of the regulation of visceral muscle function by aminergic and glutamatergic circuits. We show that the excitatory neurotransmitter L-glutamate (LGA) causes a pattern of depolarizations and rhythmic electrical activity that underlies muscle contractions in the common oviduct of the reproductive tract. Consistent with the mechanisms of mammalian visceral contraction, the metabotropic glutamate receptor (mGluR) are expressed in local neurons and processes but not in the contractile muscle cells. mGluR is necessary for the repetitive membrane potential activity in the common oviduct muscle. These data indicate that mGluR-expressing cells play a critical role as regulators of electrical activity in the reproductive tract muscle and have important implications for visceral muscle motility.

Introduction

The regulation of visceral muscle contraction and its underlying rhythmic activity is crucial for survival and reproduction of both insects and mammals. Thus, it is important to understand the neuronal circuits governing visceral muscle physiology. The *Drosophila* reproductive circuit is a useful model to explore the regulation of visceral muscle contractions and the mechanisms by which glutamatergic receptors interact with each other to coordinate essential behaviors. We use this neuromuscular circuit to investigate the regulation of visceral muscle by glutamate. In mammalian visceral smooth muscle, peristaltic contractions can occur independently of central neuronal innervation and rely on intermediary, non-contractile cells near muscle, some of which are called Interstitial Cells of Cajal (ICC). Interstitial Cells of Cajal and other functionally similar

cells orchestrate rhythmic activity in the gastrointestinal tract and other smooth muscles by relaying signals from the CNS to muscle (Klein et al., 2013). Muscle cell activity is also modulated indirectly via receptors on local neurons and interstitial cells. By contrast, regulation of visceral muscles in invertebrates is thought to be coordinated by direct central nervous system innervation and the concept that visceral muscles in *Drosophila* might be regulated indirectly has received little attention (Kiss et al., 1984; Rodriguez-Valentin et al., 2006; Garner et al., 2018). It remains unknown whether there are local cells with different markers that act as mediators between neural circuits and the muscle and may contribute to the coordination of myogenic rhythms at the *Drosophila* reproductive tract.

A previously reported model for the regulation of *Drosophila* female reproductive tract muscle contraction showed that central innervation by octopaminergic and glutamatergic neurons lead to relaxation and contraction of the muscle as a whole, respectively (Rodriguez-Valentin et al., 2006). Glutamate acts as the main excitatory neurotransmitter in mammalian central nervous systems. In insects it has been shown to be the major excitatory neurotransmitter in both visceral muscles and “skeletal” muscles and increases contractions in the oviducts of several species, including locusts. In addition to direct contraction, glutamate can modulate neuronal function through activation of metabotropic glutamate receptors in both insects and mammals or inhibit neurons through the glutamate-gated chloride channel in insects (Bogdanik et al., 2004; Garner et al., 2018).

We identify the location and role of specific glutamatergic receptors at the *Drosophila* reproductive tract neuromuscular junction. Cells expressing metabotropic glutamate receptors lie in the oviduct lumen and outside of the visceral muscle rather than within the muscle membranes where the ionotropic glutamate receptors have been reported to be localized (DiAntonio, 2006; 2020a). The long thin processes of these cells surround nuclei and project in

between the muscle cells, around neuronal terminals. Additionally, our data show that glutamate indeed causes contraction in the reproductive tract oviduct muscle, but we also observe an underlying rhythmic pattern of electrical activity extending beyond the initial muscle contraction. Using pharmacology and genetics, we show that muscle rhythmic activity only occurs when metabotropic glutamate receptors are stimulated, whereas the ionotropic receptors cause an immediate membrane depolarization. Our results contribute to the idea that similar to mammalian smooth muscles, insect visceral muscles are modulated at least in part by receptors extrinsic to the muscle cells themselves. We propose that there are cells at *Drosophila* reproductive tract muscle which express mGluR and are important for rhythmic electrical activity in *Drosophila* visceral muscle.

Materials

Drosophila Stocks and Husbandry

Flies were raised under a 12 hr day/night cycle at 25°C on a conventional cornmeal/ molasses/ yeast/ agar medium and 50-70% humidity. UAS-RCaMP1b (chromosome III insertion), 24b-GAL4, and UAS-ChR2 in muscle (using 24b- GAL4), mGluR-T2A- GAL4, and ILP7-GAL4 were obtained from Bloomington Stock Center. MiMIC GAL4 lines were obtained from Dr. Hugo Bellen. Adult females aged 3-6 days post-eclosion were used for each experiment.

Dissections

For all experiments, 3-6 day old mated female adults were used. Flies were anesthesized on ice and dissected on Sylgard in a cold calcium free HL3.1 solution. For channelrhodopsin experiments, the thorax and abdominal cuticle was cut to expose the abdominal ganglia and reproductive tract. Insect pins were used on the tip of the abdomen, and on the thorax and abdomen cuticle and the gut was removed to visualize the abdominal ganglion and reproductive tract. In isolated preparations, the head and thorax, the gut, the abdominal cuticle and all local

and central processes were removed from the reproductive tract and pins were placed on both ovaries and the tip of the uterus to stabilize the preparation under the microscope. In fillet preparations, reproductive tracts and local neuronal cell bodies and processes were left intact as well as the abdominal cuticle. Pins were placed on both sides of the cuticle and the gut was removed for visualization.

Immunohistochemistry

All samples were dissected in phosphate buffered saline and stained using a standard staining protocol. Briefly, samples were fixed in 4% paraformaldehyde for 30 minutes and blocked in 5% normal goat serum for 30 minutes. After 3 washes in PBST (0.3% Triton X 100 in PBS), samples were stained with primary antibody overnight and then in secondary antibody for 2-3 hours. Samples were then washed in PBST and PBS and cleared with 25% glycerol. Antibodies reactive against the drosophila metabotropic glutamate receptor, and the glutamate receptor II D, C, and A subunits were gifts from the Dickman laboratory (Kiragasi et al., 2017). Phalloidin and HorseRadish Peroxidase were purchased from Sigma and were used to locate muscle and neurons, respectively. Tissues were mounted on bridged slides using Fluormount-G with DAPI (SouthernBiotech 0100-20) or Diamond Prolong mounting media (Thermofisher 36966). Images were then processed using publicly ImageJ software. All antibodies used with their sources and concentrations are listed in chapter 2 table 1.

Electron Microscopy

UAS-NES-APEX2 fly lines were crossed to the mGluR-T2A-GAL4 line for visualization of mGluR-expressing cells in the reproductive tract. Animals were dissected as described above and then fixed in 4% paraformaldehyde and 2.5% glutaraldehyde for 20 minutes. Following fixation, tissues were washed in PBS, reacted with DAB to reveal sites of peroxidase activity, and washed again. Samples were then post-fixed in 0.5% osmium tetroxide in 0.1MPB for

30min, and dehydrated through a graded series of ethanol concentrations. After infiltration with Eponate 12 resin, the sections were flat embedded in fresh Eponate 12 resin and polymerized at 60°C for 24 hours. Then the sections in resin were attached to a pre-polymerized Epon 12 resin capsule by fresh Epon 12 resin and polymerized for 24 hours at 60°C. Ultrathin sections of 77 nm thickness were prepared and placed on formvar coated copper grids. Some grids were stained with uranyl acetate and Reynolds' lead citrate. Grids with or without counterstaining were examined using a JEOL 100CX transmission electron microscope at 60 kV and images were captured by an AMT digital camera (Advanced Microscopy Techniques Corporation, model XR611) (Electron Microscopy Core Facility, UCLA Brain Research Institute). Sodium-cacodylate (cat. no. 12300), glutaraldehyde (16220 and 16120), paraformaldehyde (15710), osmium tetraoxide (19190), 3,3'-diaminobenzidine (DAB; D5905), potassium hexacyanoferrate (II) (P9387), thiocarbohydrazide (88535), sodium hydrosulfite (157953) and durcopan resin (44610) were purchased at Sigma-Aldrich.

Solutions

Glutamate stock was prepared prepared on the same day as experiments and diluted for experiments. KCl (3M) was used as internal solution to fill electrodes for sharp electrode intracellular recordings and HL3.1 (pH = 7.3; 70 mM NaCl, 5 mM KCl, 5 mM trehalose, 2 mM $CaCl_2$, 4 mM $MgCl_2$, 115 mM sucrose, 10 mM $NaHCO_3$) was used as external solution for all NMJ experiments as described in Feng et al. (2004). The mGluR agonist and antagonist LY354740 (3246) and LY341495 (4062) was purchased from Tocris. Additional reagents were purchased from Sigma unless stated otherwise.

Electrophysiology

For intracellular recordings in adult *Drosophila* reproductive tract muscle, recording pipettes with a resistance of 20–30 MΩ were pulled on a Sutter P-97 puller from 0.5mm ID, 1.0mm OD

borosilicate glass (with filament; Sutter) and filled with 3M KCl. Electrodes were inserted into the common oviduct muscle (see diagram). Preparations were incubated in control HL3.1 solution during a 2 to 20 minute baseline recording and then bath application of second HL3.1 solution or a test solution was washed in for the remainder of the experiment.

Optical Stimulation and Calcium Imaging

Flies were dissected as described above. To visualize intracellular calcium levels, UAS-RCaMP1b was expressed in muscle using 24b-GAL4. Adult flies were dissected as described previously in calcium free HL3.1 solution (see “semi-intact” in Dissections) and then washed 3x with chilled HL3.1 solution containing 2 mM Ca2+ prior to imaging. HL3.1 control solution or a test drug was added via perfusion to the bath after a 1-2 minute baseline recording at ambient temperature. Muscles were imaged using a Zeiss Achroplan water immersion objective (10x, 1.0 N.A.) on a Zeiss Axio Examiner Z1 microscope with a CCD camera (Andor iXon 897, Oxford Instruments, Oxfordshire, England) and a capture rate of 12 frames/s using Andor IQ2 software. A DG4 light source (Sutter, Novato, CA) with a RFP Brightline® Filter Set (Semrock, Rochester, NY) was used for illumination. For analysis of the GCaMP experiments, 3-5 individual regions of the common oviduct muscle or cell processes were selected ImageJ (NIH) and the Time Series Analyzer plugin. The individual regions of interest were background subtracted and then averaged per frame. ΔF/F was quantified as ΔF/F= [(F peak - F baseline)/ F baseline] as reported in Martin et al. (Martin et al., 2016).

Experimental Design and Statistical Analysis

For each calcium imaging recording, the regions of interest in the oviducts from one preparation were imaged within a single 10x field of view and averaged to obtain a single observation with an n of 9 animals used for statistical analysis. All electrophysiological data was analyzed using custom software in Labview from Felix Schweizer. An effect was judged as statistically

significant if $p<0.05$ in an ANOVA with a post-hoc Dunn-Sidak test for multiple comparisons or a two-way t-test when applicable.

Ch. 2 Table 1.

Antibody	**Experiment**	**Concentration**	**Source**	**Ref#**
Rabbit anti GFP – 488 preconjugated.	Receptor Expression	1:500	Invitrogen	A-21311
Phalloidin – 555	Muscle Costain	1:500	Invitrogen	A34055
HRP – 568	Neural Costain	1:500	Invitrogen	
GluRIIA, C, D	Receptor Expression	1:20	Dion Dickman Lab	

Results

Glutamate stimulates oviduct muscle contraction and a distinct pattern of rhythmic electrical activity

Similar to mammalian skeletal muscle, the model for muscle contraction in insects is that an excitatory neurotransmitter causes depolarization of the muscle membrane and contraction upon binding to receptors localized to the contractile muscle cells. However, in mammals the regulation and pattern of activity in visceral muscle differs in important ways from skeletal muscle: in skeletal muscle there is a single depolarization while visceral smooth muscles have

rhythmic bouts of depolarizations. It was previously shown in *Drosophila* that glutamate, as the primary excitatory neurotransmitter at the oviduct visceral muscle, causes vigorous global contraction (Garner et al., 2018). It was also reported that stimulation of ILP7 glutamatergic neurons in the abdominal ganglion causes contraction in the oviduct muscle. However, in the prior studies that demonstrated this effect, the electrical activity underlying the contraction in response to glutamate was not investigated (Rodriguez-Valentin et al., 2006).

To determine whether fly visceral muscles, like mammalian smooth muscles, have an underlying rhythmicity that contributes to the regulation of visceral muscle contraction, we stimulated the previously described ILP7 glutamatergic neurons in the abdominal ganglion which innervate the reproductive tract and cause contraction of the common oviduct. We then used electrophysiology to record electrical activity in the common oviduct. As previously reported, we observed a common oviduct muscle contraction upon stimulation. An initial membrane depolarization occurred in all animals (2.2 ± 0.5 mV) with rhythmic depolarizations occurring in 5 out of 6 animals in the posterior common oviduct muscle (Fig. 1; frequency within bursts: 8 ± 0.9 Hz, burst duration: 0.85 ± 0.05 s). This was surprising since glutamate causes one short (~10 s) contraction event, and at the well-studied larval NMJ muscle glutamate stimulates a single end junction potential rather than a series of depolarizations (Jan and Jan, 1976). This ongoing burst activity is characteristic of smooth visceral muscles rather than the "skeletal" type muscle at the NMJ, which have a unique regulatory system and set of receptors.

While previous studies identified a dorsal and ventral glutamatergic ILP7 neurons projecting from the abdominal ganglion to the reproductive tract and which cause oviduct contraction, they did not delineate the projection pattern of these cells on the reproductive tract or which post-synaptic receptors were stimulated to allow for muscle contraction. It has previously been shown that GluRII is the major glutamate receptor in *Drosophila* skeletal muscle that leads to

contraction, but *Drosophila* express several ionotropic and metabotropic glutamate receptor subtypes which may regulate visceral muscle (see Fig. 3). To assess the contribution of all glutamatergic inputs and post-synaptic receptors on contraction in the common oviduct, we bath applied glutamate to the isolated preparation and recorded activity in the common oviduct. Miniature depolarization events (minis) were observed at baseline in glutamate experiments and before and after addition of HL3.1 control solution, indicating the presence of a synapse with ionotropic receptors (Fig. 2C; control baseline mini frequency= 3.1**±** 0.6 Hz, n= 9; control addition mini frequency= 2.8 **±** 1 Hz, n=6; glut addition mini frequency= 3.89 **±** 0.5 Hz, n= 30). Mini frequencies were not significantly different in each treatment group or after addition of control solution (HL3.1 control: p=0.99; glut: p=0.86). Similar to ILP7 stimulation, glutamate caused a membrane depolarization with a burst of depolarization events, however glutamate also led to multiple bursts of events in 38 out of 60 animals which we never observed with 30 s of ILP7 cell stimulation. Glutamate caused a large initial depolarization compared to control solution (Control membrane depolarization= 1 **±** 2 mV, n=13; Glut addition: membrane depolarization= 12.1 **±** 1.6; p=0.005). At least one burst of events upon glutamate addition occurred in 41 of 60 animals, which were not observed in animals treated with control solution alone (Fig. 2B; burst frequency= 1.4 **±** 0.2 Hz; burst duration= 28 ± 3.4 s; interburst interval= 37.7 ± 3.4 s).

The rhythmic electrical activity in the common oviduct lasting for several minutes after the initial contraction was unexpected since the initial calcium event in this muscle lasts approximately 30 seconds (see Deshpande et al., 2021). This behavior is consistent with myogenic electrophysiological rhythms seen in most visceral muscles and is distinct from the glutamate-induced events that tightly correlate with muscle contraction (see Fig. 2B). The differences between the effects of bath application compared to optogenetic stimulation of ILP7 cells suggested that at least some of the elements required for all of the effects of glutamate on the

CO might be absent when this small selection of glutamatergic cells and their corresponding postsynaptic receptors are activated. This may include additional inputs from the local glutamatergic neurons and glutamatergic receptors that were stimulated with the less specific higher concentration of glutamate or due to the longer time duration of receptor stimulation with bath application. In addition, the difference in burst frequency and change in membrane potential with these two setups may be due to the artificial stimulation of glutamatergic neurons with channel-rhodopsin, such as the time duration and pattern of stimulation.

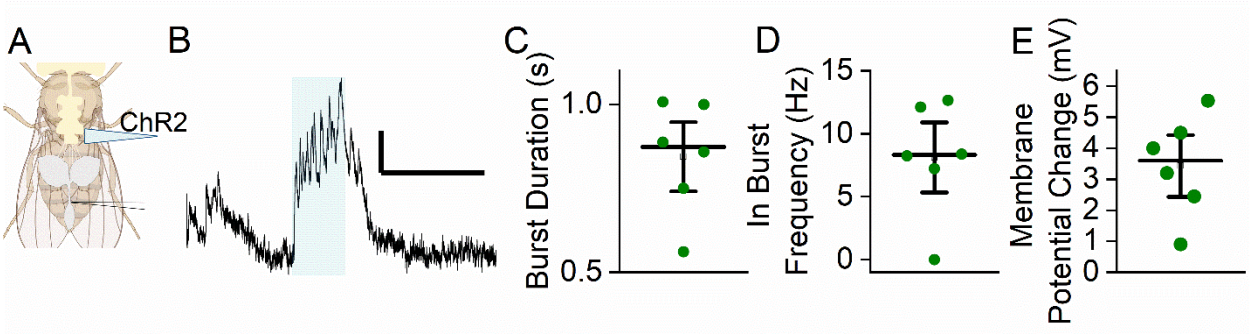

Figure 1. Stimulation of central glutamatergic lLP7 neurons causes membrane depolarization and a burst of rhythmic depolarizations in the common oviduct.

A. Schematic depicting experimental setup. Light stimulation of channelrhodopsin2- expressing ILP7 cells in the abdominal ganglion and sharp electrode recordings from the lower common oviduct muscle in female *Drosophila*. **B**. Representative trace recorded from the common oviduct using an *ILP7-T2A-gal4* line to drive expression of *UAS-ChR2*. Light stimulation indicated time with the blue rectangle (30s stimulation). **C**. Mean duration of depolarization events during light stimulation from each experiment. Scale bar X= 1 s, Y= 5 mV.

D. Mean frequency of events upon light stimulation from each experiment. **E**. Mean baseline membrane depolarization from each experiment (measured from 30 s baseline potential to peak potential).

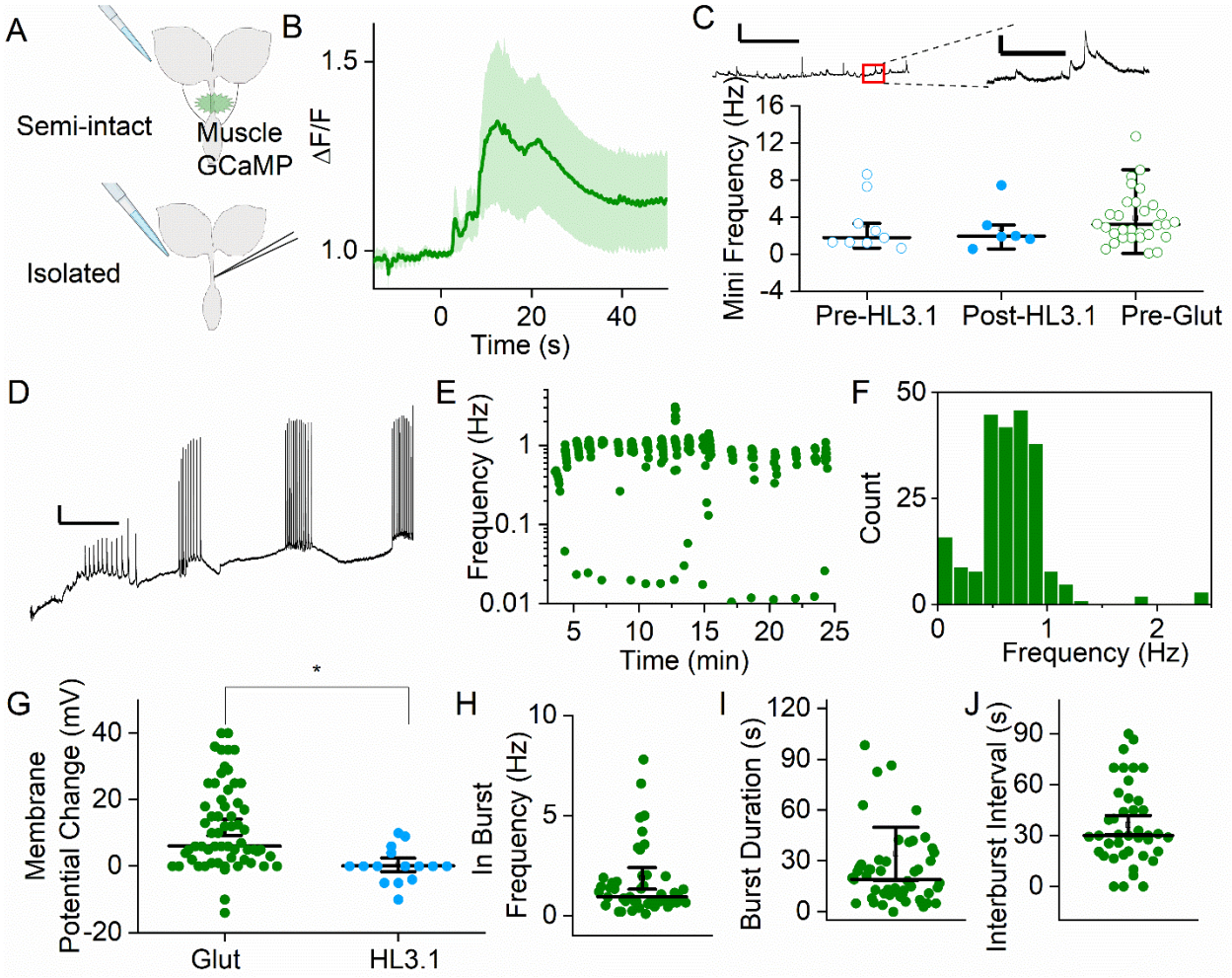

Figure 2. Glutamate causes a membrane depolarization and a series of rhythmic depolarization bursts

A.Cartoons showing each dissection and experimental setups. *Top*: A “semi-intact” preparation was used for measuring calcium flux in the oviduct muscle using a UAS-RCaMPib line to drive expression of 24b-Gal4 in the muscle and glutamate was bath applied. *Bottom*: An “isolated” preparation was used for electrophysiological recordings and glutamate was bath applied. **B**. Mean calcium flux measured from the common oviduct muscle. 8mM glutamate bath applied at time 0 (n=9). **C**. *Top*: Representative trace from a sharp electrode recording at the common oviduct muscle in an isolated preparation post-HL3.1 control solution showing miniature events and an expanded view of individual events from that trace. *Bottom*: Mean frequency of miniature

events recorded from the common oviducts before (blue open circles; n=9) and after HL3.1 control solution (blue closed circles; n=6) was added to each preparation and before glutamate was added to the bath (green open circles; n=30). Scale bar (left): X= 30 s, Y= 5 mV. Scale bar (right): X= 2 s, Y= 1 mV. **D**. Representative trace from a sharp electrode recording at the common oviduct muscle in an isolated preparation after 8mM glutamate was added to the bath (n=51). Glutamate leads to an initial membrane depolarization and multiple bursts of depolarization events following glutamate (8mM) addition. **E**. Frequency of depolarization event bursts over time post-glutamate addition from the recording shown in D. **F**. Number of depolarization events occurring at each interevent interval from the preparation in D. **G.** Baseline membrane potential of oviduct muscle before and after addition of glutamate of HL3.1 control solution (open green triangle: HL3.1 solution, closed green triangle: glutamate addition, open blue circle: HL3.1 solution, closed blue circle: HL3.1 addition) quantified as the mean potential from a 1 minute pre-glutamate/HL3.1 and the potential at the first event. **H.** Mean frequency of events from all bursts post-glutamate. *Center*: Mean time duration of each burst post-glutamate. **I**. Mean interval between bursts of events post-glutamate. Each triangle represents one preparation.

Metabotropic and ionotropic glutamate receptors are differentially expressed in the reproductive tract

The multiple actions of glutamate on the oviduct muscles in addition to its direct stimulation of muscle contraction is consistent with glutamate acting via several receptor types at visceral muscle. At the *Drosophila* reproductive tract there are glutamatergic processes projecting to the calyces and uterus (Fig. 3A-i). Glutamate may activate one or more of several ionotropic glutamate receptor subtypes and a metabotropic glutamate receptor that are expressed in

Drosophila and which may have inhibitory or modulatory effects in addition to directly inducing muscle contraction. However, it is not known which subtypes are expressed at the reproductive tract visceral muscle and local cells. To determine which glutamatergic receptors are located at the reproductive tract we used a GAL4 MIMIC mGluR and Glu-Cl lines and GluRII antibodies to visualize the metabotropic and ionotropic receptors in the muscle and local cells at the reproductive tract. We see mGluR-expressing cells located directly adjacent to the uterus muscle, there is a local mGluR-expressing neuron detached from the muscle but with projections toward the uterus and ovaries (Fig.3Ci-Civ). In addition, there are five mGluR-expressing cells on the left and right sides of the uterus adjacent to the seminal receptacle (right uterus n=6, left uterus n=5; Fig. 3Bi-Bvii). mGluR-expressing cell processes extend throughout the common oviduct, the seminal receptacle, spermatheca, and the anterior uterus (Fig. 3Di-Diii). mGluR-expressing processes co-label with the neuronal marker HRP (Fig. 3Ei- Eiii) and interdigitate between the muscle cells, between muscle cells and in the lumen of the common oviduct and uterus.

Drosophila also have several ionotropic glutamate receptors including a glutamate gated chloride channel. We used GluRIID, A, and C receptor antibodies to show that in contrast to mGluR expression the ionotropic GluRII D and C receptor subunits are expressed throughout the reproductive tract in the muscle layer and it does not co-label with mGluR-positive cells (Fig. 3Fi- Fiii). Using the GluRIIA and C antibodies, we do not see expression of these receptors at the reproductive tract muscle. However, using the Glu-Cl line we show that there is expression of the Glu-Cl ionotropic receptor in neuronal processes on the lateral and common oviducts, and ovaries that project from the abdominal ganglion as well as in local neuronal processes (Fig. 3Gi- Hii). Similar to mGluR, Glu-Cl receptors are not seen in the muscle (Fig. 3Gii) but instead are expressed in processes on the muscle (Fig. 3Ii-Iiii). Thus, glutamate may directly cause contraction of the oviduct via GluRII ionotropic receptors and modulate contraction indirectly

through mGlu and Glu-Cl receptors expressed on local neurons, analogous to the actions of neuromodulators at mammalian visceral muscles.

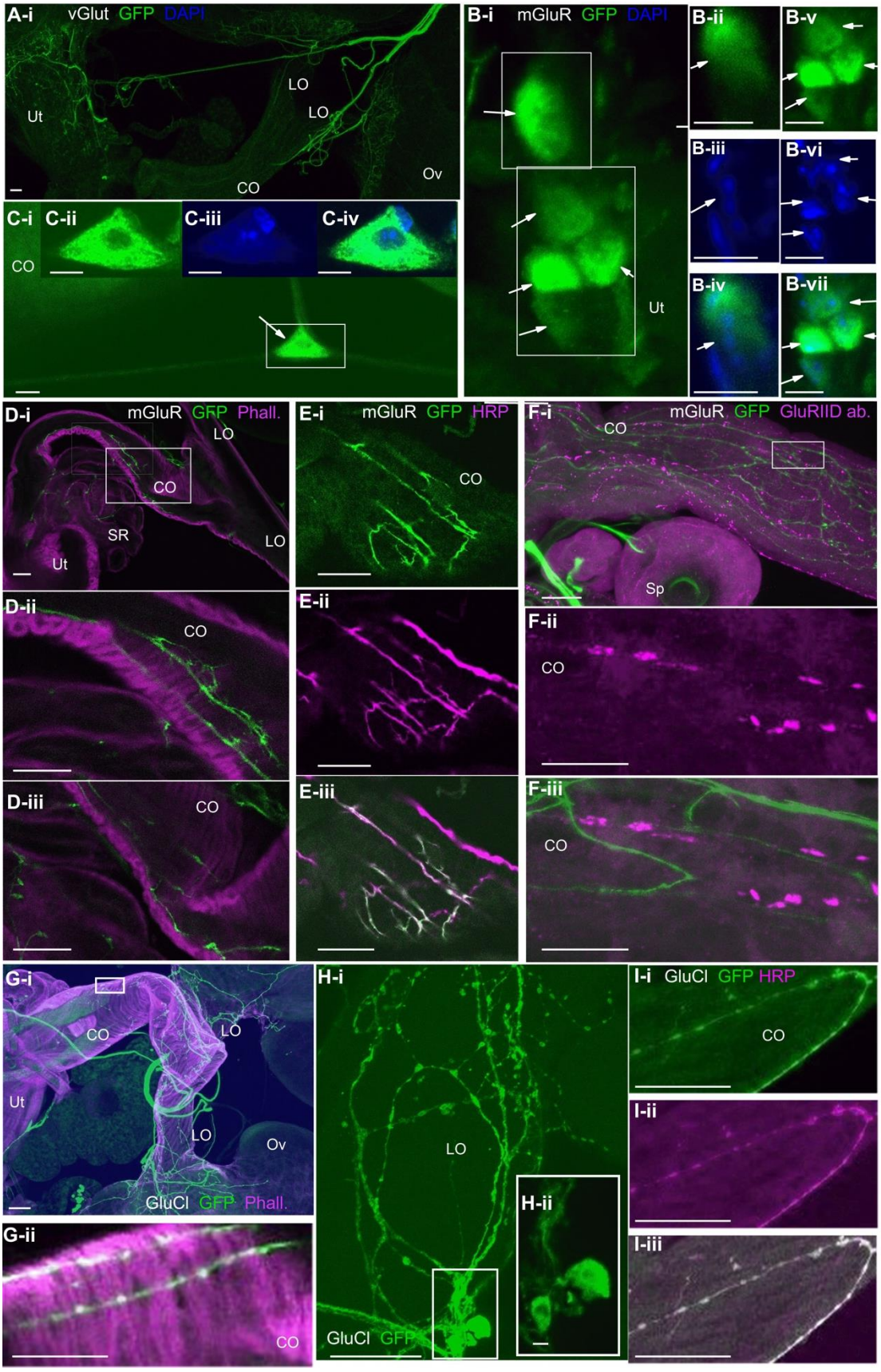
A-i vGlut GFP DAPI
LO
LO
Ut
CO
Ov
B-i mGluR GFP DAPI
Ut
B-ii
B-v
B-iii
B-vi
B-iv
B-vii
C-i C-ii C-iii C-iv
CO
D-i mGluR GFP Phall.
LO
CO
SR
LO
Ut
D-ii
CO
D-iii
CO
E-i mGluR GFP HRP
CO
E-ii
E-iii
F-i mGluR GFP GluRIID ab.
CO
Sp
F-ii
CO
F-iii
CO
G-i
CO
LO
Ut
LO
Ov
GluCl GFP Phall.
G-ii
CO
H-i
LO
H-ii
GluCl GFP
I-i GluCl GFP HRP
CO
I-ii
I-iii

Figure 3. **Glutamatergic receptors are differentially expressed in the reproductive tract**

A-i Overview of glutamatergic neuronal expression in the whole reproductive tract using *dVGluT-Gal4* to express UAS-mcd8-GFP (anti GFP-488**,** green). **B-i.** *mGlu receptor* expression using *mGluR-T2A-Gal4* to express UAS-mcd8-GFP (i, vi, vii: anti GFP-488**,** green) or UAS-nls-GFP (ii, iv: anti GFP-488, green) and co-labeled with DAPI (iv, v: blue). Expression of five mGluR-positive cells in the uterus of the reproductive system. **B-ii, B-v**. Nuclear GFP (left), **B-iii, B-vi**. DAPI (middle), and **B-iv, B-vii**. co-labelled GFP and DAPI expression in 5 cells in the uterus of the preparation in B-i. **C-i.** Expression of *mGluR* in a local peripheral cell and projections toward the uterus and the left and right ovaries. **C-ii.** mGluR expression, **C-iii**. DAPI expression, and **C-iv**. co-labelled GFP and DAPI expression in the peripheral mGluR-positive cell shown in C-i. **D-i, D-ii.** Overview of the expression of mGluR projections in the uterus (Ut), Seminal Receptacle (SR), and Common Oviduct (CO) co-labeled with phalloidin ("phall.", magenta). **D-iii.** The projection pattern of mGluR-positive cells interdigitated on the inside and outside of the muscle cell layer of the common oviduct from the dissection shown in D-ii. **E-i.** *mGlu* receptor expression using *mGluR-T2A-Gal4* to express UAS-mcd8-GFP (anti GFP-488**,** green) and neuronal expression using horseradish peroxidase (HRP, magenta). mGluR-positive cell projections in the common oviduct. **E-ii.** Expression of HRP in the common oviduct. **E-iii.** Co-expression of mGluR and HRP in the common oviduct. **F-i.** *mGlu receptor* expression using *mGluR-T2A-Gal4* to express UAS-mcd8-GFP (anti GFP-488**,** green). Overview of the expression pattern of mGluR and GluRIID antibody in the common oviduct. **F-ii.** Expression of GluRIID receptor in the common oviduct and **F-iii.** GluRIID receptor expression co-labelled with mGluR in the common oviduct. mGluR-positive cell projections do not overlap with the expression of ionotropic GluRIID receptors (GluRIID antibody, magenta). **G-i.** GluCl receptors throughout the reproductive tract and expression in local neuronal processes. **G-ii.** GluCl receptor expression co-labelled with phalloidin in the common oviduct showing GluCl-expressing processes on top of the muscle. **H-i.** Local GluCl cell bodies and processes and

processes projecting from the abdominal ganglion at the lateral oviduct. **H-ii.** GluCl-expressing cell bodies in the lateral oviduct preparation shown in H-i. **I-i.** GluCl expression **I-ii.** and HRP neuronal stain in the common oviduct showing **I-iii.** Co-labelled GluCl receptor-expressing neuronal processes. **Scale bars:** A-i, D-i, D-ii, D-iii, E-I, E-ii, E-iii, F-i, F-ii, G-I, G-ii, H-i, I-i, I-ii, I-iii = 50µm; B-i, B-ii, B-iii, B-iv, B-v, B-vi, B-vii, C-i, C-ii, C-iii, C-iv, H-i = 5µm. (Panel H Credit: Ethan Rohrbach)

Metabotropic glutamate receptor- expressing cells interdigitate muscle cells in the reproductive tract and surround neuronal terminals

Our attention was directed towards the metabotropic receptor since rather than being expressed in the contractile muscle cells, mGluR-expressing processes appear to lie extrinsic to the muscle and within the lumen of the common oviduct where we see a response to glutamate in isolated tissues (Fig. 3D-F). The “web-like” appearance of mGluR-expressing cells is similar to some of the interstitial cell types found in mammalian smooth muscle which form electrical connectivity with muscle cells to regulate membrane potentials and allow for contraction. Since interstitial cells are characterized by their unique ultrastructure with fine processes between muscle cell layers and drive rhythmic activity in muscle, we hypothesized that the mGluR-expressing cells in the oviduct have common characteristics to mammalian interstitial cells. To more precisely locate these cells within the context of oviduct and uterus muscle and determine their ultrastructural morphology, we expressed ascorbate peroxidase (APEX2) in mGluR-positive cells and imaged the reproductive tract sections. We observe fine mGluR-positive processes (~0.1 µM) interdigitating the muscle cells in the oviduct and uterus and surrounding some nuclei which may be the cell bodies that we observed in the uterus using fluorescent microscopy (Fig. 4C-i, C-ii, 3B). mGluR- positive cells also partially surround neuronal terminals, which may belong to mGluR-expressing cells themselves or to descending CNS neurons which

are in close proximity to and possibly contacting mGluR-expressing cells on the muscle (Fig. 4B-i, B-ii). Since a major function of interstitial cells is to make contacts with both neurons and muscle cells to relay information to modulate muscle activity, the proximity and morphology of the mGluR staining between terminals and muscle cells may indicate that these cells have a similar function to interstitial types of cells in mammalian smooth muscle.

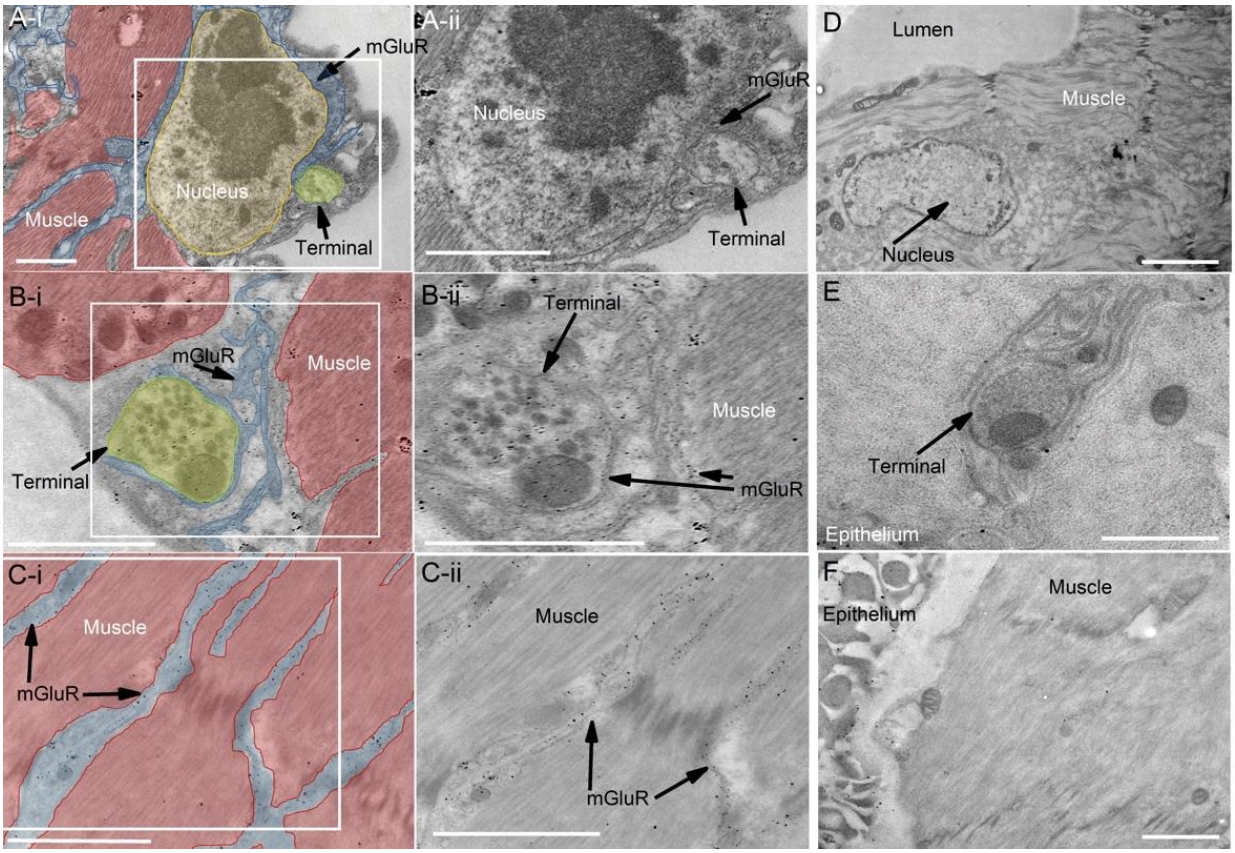

Figure 4. Metabotropic glutamate receptor- expressing cells interdigitate muscle cells in the reproductive tract and surround neuronal terminals

A-i. Electron micrograph of a cross section of the reproductive tract to show an overview of the outer muscular layer and metabotropic glutamate receptor expression using *mGluR-T2A-Gal4* to express *UAS-NES-APEX2* (nuclear export signal ascorbate peroxidase 2). An mGluR

expressing cell with its nucleus interdigitating the muscle cells and closely apposed to a neuronal terminal (muscle=red; terminal=green; nucleus=yellow; APEX2=blue). **A-ii**. APEX2 expression in mGluR-positive processes surrounding a nucleus from the preparation in A-i. **B-i.** Electron micrograph of mGluR-positive thin cell processes that surround a terminal and muscle (muscle=red; terminal=orange). **B-ii**. APEX2 expression in mGluR-positive processes surrounding a terminal from the preparation in B-i. **C-i.** Electron micrograph with the *mGluR-T2A-Gal4* line driving expression of *UAS-NES-APEX2* and showing expression of mGluR-positive cells interdigitating the muscular layer (muscle-red; APEX2=blue). **C-ii**. APEX2 expression in mGluR-positive processes surrounding muscle cells from the preparation in C-i. **D**. Electron micrograph from an mGluR-T2A-Gal4 line showing a nucleus and the muscular layer and lack of APEX2 expression. **E**. Electron micrograph from a UAS-NES-APEX2 line depicting a neuronal terminal and the epithelium layer adjacent to the muscular layer. **F**. Electron micrograph from a UAS-NES-APEX2 line showing the muscular layer adjacent to the epithelium layer and lack of APEX2 expression. **A- F**. Scale bar = 1 µM.

Metabotropic glutamate receptor stimulation causes rhythmic electrical activity

To determine the functional role of ionotropic and metabotropic receptors that we identified at the common oviduct and how they each influence muscle response to glutamate, we applied mGluR agonist and antagonist drugs to activate metabotropic or ionotropic receptors in isolation. Surprisingly, a 5-10 minute incubation in the mGluR antagonist (1µM) followed by 8mM glutamate addition causes a sharp membrane depolarization initially, similar to glutamate alone, but the rhythmic depolarization bursts of activity seen with glutamate alone were not observed (Fig. 5B-C; membrane depolarization= 17.3 **±** 3.5 mV, glut: $p=0.14$, agonist: $p<0.001$; $n=14$). By contrast, the mGluR agonist (1µM) causes rhythmic events similar to glutamate addition but without a substantial change in the initial membrane potential (Fig. 5D-J; membrane depolarization= -3.2 **±** 3.6 mV, glut: p=<0.001; burst frequency= 3 **±** 1.4 Hz, glut: p=0.2; burst

duration= 28.6 ± 7 s, glut: p=0.8; interburst interval= 29.8 ± 5.5 s, p=0.42; n=15). This may indicate that the metabotropic receptors contribute the rhythmic depolarizations component of the muscle response to glutamate in the common oviduct while the ionotropic receptors contribute the initial membrane depolarization component. Together with the receptor localization experiments, these data indicate that activation of specific glutamatergic receptors can induce distinct patterns of electrical activity, in contrast to the suggestion that the oviduct's response to glutamate in *Drosophila* may be limited to acute muscle contractions alone (Rodriguez-Valentin, 2006). The rhythmic pattern of activity caused by stimulation of mGlu receptors suggests that there may be cells in the reproductive tract which express mGluR and act as rhythm-generating cells, regulating the contractile behavior of the oviduct. In this way, a new model of muscle contraction in *Drosophila* may be that activation of GluRII in the common oviduct muscle causes contraction while mGluR in cells external to the muscle integrate neurotransmission from local and central neurons through regulation of the muscle membrane potential.

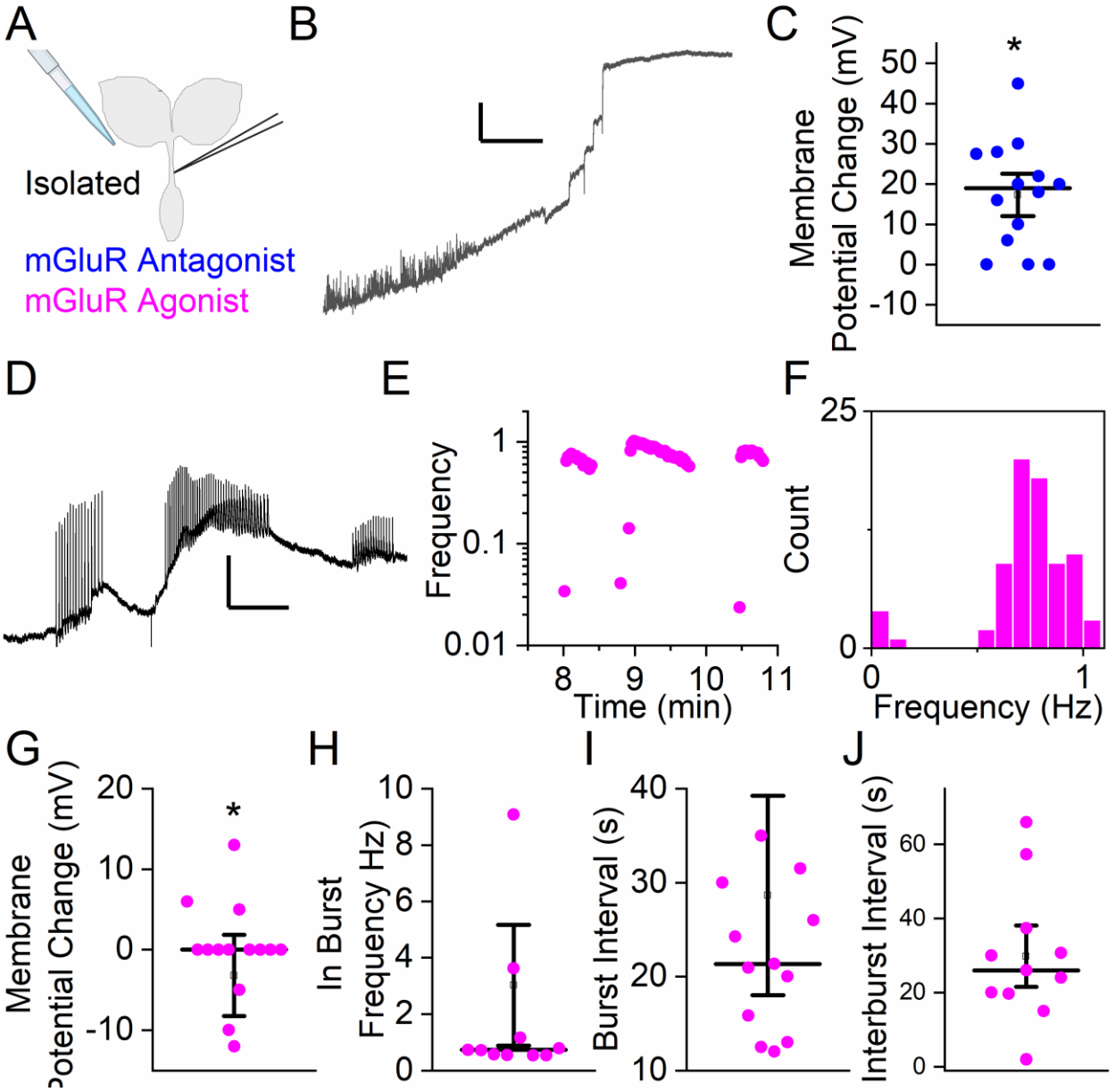

Figure 5. Stimulation of metabotropic receptors causes rhythmic electrical activity without membrane depolarization

A. Cartoon depicting experimental setup. Recordings were taken from the lower common oviduct using sharp electrode electrophysiology. 1uM of mGluR agonist was added to “isolated” preparations or 8mM glutamate was added to “isolated” preparations incubated in 1uM mGluR antagonist drug. **B**. Representative trace after addition of the mGluR antagonist LY341495 (1 µM) followed by addition of glutamate (8 mM) in an isolated oviduct preparation. Scale bar: X=

30 s, Y= 5 mV. **C.** Mean change in membrane potential after incubation in the mGluR antagonist LY341495 (1 µM) followed by addition of glutamate (8 mM) in isolated reproductive tract preparations (n=13). **D**. Representative trace after addition of the mGluR agonist LY354740 (1 µM, n=14) in an isolated oviduct preparation. Scale bar: X= 30 s, Y= 5 mV. **E.** Frequency of depolarization events post-LY354740 from the recording shown in D. **F.** Number of depolarization events occurring at each frequency from the preparation in D. **G.** Mean change in membrane potential post-LY354740 in isolated reproductive tract preparations (quantified as the difference in potential from a 1 minute pre-LY354740.1 to the potential at the first event). **H.** Mean frequency of events from all bursts post-glutamate. **I**. Mean time duration of each burst post-glutamate. **J**. Mean interval between bursts of events post-glutamate. Each triangle represents one preparation.

Ch. 2 Table 2: Oviduct electrophysiology summary table

	Glutamate	Agonist	Antagonist + Glutamate	control solution	TTX+Glutamate
Total experiments	60	15	14	15	2
Slow membrane depolarization and single burst of rhythmic events	5	0	0	0	0
Slow membrane depolarization and multiple rhythmic bursts	36	1	0	0	0
Slow membrane depolarization	6	1	13	0	0

only					
Rhythmic bursts only	1	12	0	0	2
Slow membrane hyperpolarization and rhythmic bursts	1	1	0	0	0
Hyperpolarizations only	1	0	0	0	0
Minis only	0	0	1	9	0

Discussion

Smooth muscles in visceral organs differ from skeletal muscle in several ways including the ability to be controlled involuntarily, to form spontaneous slow oscillations of the membrane potential which allow the visceral smooth muscle to remain tonic without contraction, and to contract rhythmically (Webb, 2003; Klein et al., 2013). Recent work has identified cells outside of vertebrate smooth muscle that relay signals from neuronal circuits to maintain this slow wave potential and rhythmic activity (Klein et al., 2013; Pasternak et al., 2016). The mechanisms by which these rhythmic activity generating cells interact with central and local neurons to regulate neuromuscular junction activity is not fully understood and invertebrate models would be useful to investigate the mechanisms involved. Molecular studies of visceral muscle in insects have been limited compared to work in models of skeletal muscle contraction, particularly at the larval NMJ (DiAntonio, 2006; Zhang, 2010). There is evidence of myogenic rhythms in insects from earlier electrophysiological studies in visceral tissue, but whether there are pacemaker slow waves and a rhythm generating intrinsic cell type as seen in vertebrates is unclear. We have

used the *Drosophila* reproductive tract circuit to elucidate the location and role of specific glutamatergic receptors involved in rhythmic activity initiation and visceral muscle contraction.

While acetylcholine is the main excitatory neurotransmitter at mammalian neuromuscular junctions, *Drosophila* and other insects use glutamate (DiAntonio, 2006). In addition to contraction initiation, acetylcholine can act as a neuromodulator through the metabotropic acetylcholine receptor in mammalian visceral organs. Due to our historical view of muscle function in *Drosophila*, we had expected glutamate would cause a depolarization that corresponds with muscle contraction and that all of the glutamatergic receptors relevant to oviduct contractions would localize to contractile muscle cells (Jan and Jan, 1976). We instead found that stimulation of glutamatergic cells in the abdominal ganglia caused both a baseline membrane depolarization and a burst of fast depolarization events in the common oviduct muscle (Fig. 2D). This “wave” of membrane potential change with a burst of depolarizations pattern closely resembles the bursts of peristaltic activity observed in mammalian smooth muscle, such as the gastrointestinal tract muscle, which is regulated by receptors on cells external to muscle (Pasternak et al., 2016). In addition, we found that central neuronal innervation was not necessary since we observed both types of electrical events in isolated preparations after bath application of glutamate, indicating that the contraction is either myogenic or initiated by peripheral cells. Interestingly, when we stimulated all peripheral glutamatergic receptors with bath applied glutamate we saw multiple bursts of fast depolarization events, further suggesting that the electrical activity and signaling mechanisms regulating muscle function might parallel that of mammalian visceral muscle.

The continuous rhythmic pattern of muscle activity following an initial change in membrane potential indicates that multiple types of glutamatergic receptors are involved in the regulation of muscle contraction. Similar to mammals, flies express both ionotropic and metabotropic

glutamate receptors in addition to a glutamate gated chloride channel not found in mammals (DiAntonio, 2006). It was previously shown that the GluRIIC, GluRIIA and GluRIIB subunits of the ionotropic glutamate receptor GluRII all cluster at Ilp7 boutons at the oviduct and were reported to be responsible for the ILP7 stimulation induced contraction in this muscle (Garner et al., 2018). Consistent with previous reports, we observe expression of GluRII C (not shown) and D subunits throughout the reproductive tract localized to the muscle rather than cells extrinsic to the muscle. Together with the previously reported role of GluRII in other invertebrate systems, this suggests that GluRII initiates contraction directly. By contrast, we observe expression of both GluCl and the fly orthologue of metabotropic glutamate receptors, mGluR, in local neuronal processes and they do not appear to be expressed by the contractile muscle cells in the oviducts (Fig. 3D-I). The extrinsic localization of GluCl suggests that it may modulate muscle contraction and it may be inhibitory since its activation would most likely lead to a hyperpolarization of the membrane. The distinct pattern of mGluR expression in the common oviduct was atypical and appeared morphologically similar to some types of interstitial cells previously identified in mammalian viscera. Some of the mGluR expression is likely in the nerve terminals and may contribute to the modulation of neurotransmitter release at presynaptic sites as reported in prior studies at the larval NMJ (Bogdanik et al., 2004). The *Drosophila* mGluR regulates several circuits in the central nervous system, but the possibility that it may have additional roles in the periphery has not been fully explored.

Our finding that mGluR-expressing cells have a distinct morphology, branching out within the lumen and outside of muscle cells, seemed to suggest that there may be another type of cell other than muscle and neurons at the oviduct. Further, the ultrastructure of the oviduct showed expression of mGluR in thin membrane-bound processes in between muscle cells, around nuclei and surrounding neuronal terminals position them to relay signals between neurons and the muscle. In the vertebrate gut, signal between central neuronal inputs and muscle are

mediated by Interstitial Cells of Cajal (ICC), often via gap junctions. ICCs, and other cells with different markers that have been characterized in various vertebrate visceral organs including the oviducts, are responsible for the generation of rhythmic contractions. These ICCs and interstitial cell-like cells are activated by NOS, ADP, adrenergic and cholinergic neurons including metabotropic acetylcholine receptors (Klein et al., 2013). We hypothesized that the mGluR may be a marker for a functionally similar interstitial like cell in flies and that these cells in the uterus and common oviduct can similarly indirectly signal to and modulate muscle rhythmic activity upon activation by glutamate.

In support for this hypothesis, we observe rhythmic activity in the common oviduct muscle without an initial membrane depolarization when we pharmacologically activate the mGluR in isolation. The other component of electrical activity caused by glutamate, the initial membrane depolarization, appears to be triggered by the ionotropic receptors in the muscle. Thus, together with the morphological findings, mGluR-expressing cells may represent a type of cell in insects that plays similar functional roles to interstitial cells in mammalian muscle. Exact analogs of ICCs with the typical genetic markers such as c-kit or interstitial cell-like cells have not been identified in any invertebrate. While it is possible that rather than local peripheral cells in insects driving rhythmic contractions, all the rhythms we observe are stimulated by well characterized central pattern generators, our data strongly suggest that mammalian and insect viscera may be similarly regulated. Our results indicate that glutamate may be responsible for the regulation of the visceral muscles of the fly oviducts via signaling pathways within local, non-contractile mGluR-expressing cells that then indirectly communicate to muscle cells. To determine whether these local cells indeed impart electrical rhythmicity to muscle it will be important to test whether they show intrinsic rhythmic activity by recording their electrical activity at baseline and in response to glutamate. In addition, stimulation of each of the local mGluR cells specifically in the uterus and local processes will be a critical experiment to pinpoint which cells are

responsible for the rhythmic muscle activity. This would allow us to fully understand the role of these local cells versus the role of central glutamatergic inputs. Critical future experiments will also include localization of gap junctions from the local rhythm generating cells or sites of synaptic connections between neurons, these cells, and the muscle to elucidate how these cells signal to the muscle.

Our results reveal an unanticipated level of complexity in the neuronal activity underlying muscle contraction and in the arrangement of glutamatergic receptors that regulate oviduct contractions at the reproductive tract circuit. Our findings also support the idea that insect visceral muscles may undergo neuro-modulatory regulation mainly by stimulation of receptors extrinsic to the muscle cells themselves. While the mGluR-expressing local cells need to be fully characterized, we propose that these and similar cells with different markers in other visceral tissues have a similar function in insect visceral muscle to the recently recognized interstitial cells in vertebrate smooth muscle.

References

Ainsley J (2003) Enhanced locomotion caused by loss of the Drosophila DEG/ENaC protein Pickpocket1. Current biology : CB 13:1557--1563.

Akerboom J (2012) Optimization of a GCaMP calcium indicator for neural activity imaging. J Neurosci 32:13819-13840.

Atwood HL, Govind CK, Wu CF (1993) Differential ultrastructure of synaptic terminals on ventral longitudinal abdominal muscles in Drosophila larvae. J Neurobiol 24:1008-1024.

Baltazar MT, Dinis-Oliveira RJ, Bastos M, Tsatsakis AM, Duarte JA, Carvalho F (2014) Pesticides exposure as etiological factors of Parkinson's disease and other neurodegenerative diseases—A mechanistic approach. Toxicology Letters 230:85--103.

Barker BS (2017) Ion Channels. Conn's Translational Neuroscience:11--43.

Barnett MW, Larkman PM (2007) The action potential. Pract Neurol 7:192-197.

Bogdanik L, Mohrmann R, Ramaekers A, Bockaert J, Grau Y, Broadie K, Parmentier M (2004) The Drosophila metabotropic glutamate receptor DmGluRA regulates activity-dependent synaptic facilitation and fine synaptic morphology. The Journal of neuroscience : the official journal of the Society for Neuroscience 24.

Brent J, Werner K, McCabe BD (2009) Drosophila larval NMJ immunohistochemistry. J Vis Exp.

Cao F, Souders Ii CL, Perez-Rodriguez V, Martyniuk CJ (2018) Elucidating Conserved Transcriptional Networks Underlying Pesticide Exposure and Parkinson's Disease: A Focus on Chemicals of Epidemiological Relevance. Front Genet 9:701.

Chandler DJ (2014) Heterogeneous organization of the locus coeruleus projections to prefrontal and motor cortices. Proceedings of the National Academy of Sciences of the United States of America 111:6816--6821.

Chen X, Xue B, Wang J, Liu H, Shi L, Xie J (2018) Potassium Channels: A Potential Therapeutic Target for Parkinson's Disease. Neurosci Bull 34:341-348.

Chou AP, Maidment N, Klintenberg R, Casida JE, Li S, Fitzmaurice AG, Fernagut PO, Mortazavi F, Chesselet MF, Bronstein JM (2008) Ziram causes dopaminergic cell damage by inhibiting E1 ligase of the proteasome. J Biol Chem 283:34696-34703.

Conn P, Pin J (1997) Pharmacology and functions of metabotropic glutamate receptors. Annual review of pharmacology and toxicology 37.

Cully D, Paress P, Liu K, Schaeffer J, Arena J (1996) Identification of a Drosophila melanogaster glutamate-gated chloride channel sensitive to the antiparasitic agent avermectin. The Journal of biological chemistry 271.

Davis R (1998) Neurophysiology of glutamatergic signalling and anthelmintic action in Ascaris suum: pharmacological evidence for a kainate receptor. Parasitology 116 (Pt 5).

Dennis KE, Valentine WM (2015) Ziram and sodium N,N-dimethyldithiocarbamate inhibit ubiquitin activation through intracellular metal transport and increased oxidative stress in HEK293 cells. Chem Res Toxicol 28:682-690.

DiAntonio A (2006) Glutamate Receptors At The Drosophila Neuromuscular Junction. International Review of Neurobiology 75:165--179.

DiAntonio A, Hicke L (2004) Ubiquitin-dependent regulation of the synapse. Annu Rev Neurosci 27:223-246.

Fitzmaurice AG, Rhodes SL, Cockburn M, Ritz B, Bronstein JM (2014) Aldehyde dehydrogenase variation enhances effect of pesticides associated with Parkinson disease. Neurology 82:419-426.

Fox LE, Soll DR, Wu CF (2006) Coordination and modulation of locomotion pattern generators in Drosophila larvae: effects of altered biogenic amine levels by the tyramine beta hydroxlyase mutation. J Neurosci 26:1486-1498.

Fox LE (2006) Coordination and Modulation of Locomotion Pattern Generators in Drosophila Larvae: Effects of Altered Biogenic Amine Levels by the Tyramine beta Hydroxlyase Mutation. Journal of Neuroscience 26:1486--1498.

Frolov RV (2012) Potassium Channels in \textless i \textgreater Drosophila \textless /i \textgreater : Historical Breakthroughs, Significance, and Perspectives. Journal of Neurogenetics 26:275--290.

Garner S, Castellanos M, Baillie K, Lian T, Allan D (2018) Drosophila female-specific Ilp7 motoneurons are generated by Fruitless-dependent cell death in males and by a double-assurance survival role for Transformer in females. Development (Cambridge, England) 145.

Gorczyca, D (2014) Identification of Ppk26, a DEG/ENaC Channel Functioning with Ppk1 in a Mutually Dependent Manner to Guide Locomotion Behavior in Drosophila. Cell Reports 9:1446--1458.

Jan L, Jan Y (1976) Properties of the larval neuromuscular junction in Drosophila melanogaster. The Journal of physiology 262.

Jan LY, Jan YN (2012) Voltage-gated potassium channels and the diversity of electrical signalling. J Physiol 590:2591-2599.

Jia XX, Gorczyca M, Budnik V (1993) Ultrastructure of neuromuscular junctions in Drosophila: comparison of wild type and mutants with increased excitability. J Neurobiol 24:1025-1044.

Jin J, Lao AJ, Katsura M, Caputo A, Schweizer FE, Sokolow S (2014) Involvement of the sodium-calcium exchanger 3 (NCX3) in ziram-induced calcium dysregulation and toxicity. Neurotoxicology 45:56-66.

Kiragasi B, Wondolowski J, Li Y, Dickman D (2017) A Presynaptic Glutamate Receptor Subunit Confers Robustness to Neurotransmission and Homeostatic Potentiation. Cell reports 19.

Kiss T, Varanka I, Benedeczky I (1984) Neuromuscular transmission in the visceral muscle of locust oviduct. Neuroscience 12.

Klein S, Seidler B, Kettenberger A, Sibaev A, Rohn M, Feil R, Allescher H, Vanderwinden J, Hofmann F, Schemann M, Schmid R, Schneider G, Saur D (2013) Interstitial cells of Cajal integrate excitatory and inhibitory neurotransmission with intestinal slow-wave activity. Nature communications 4.

Lee H, Choi H, Zhang C, Park Z, Kim Y (2016) A Pair of Oviduct-Born Pickpocket Neurons Important for Egg-Laying in Drosophila melanogaster. Molecules and cells 39.

Marrus S, Portman S, Allen M, Moffat K, DiAntonio A (2004) Differential localization of glutamate receptor subunits at the Drosophila neuromuscular junction. The Journal of neuroscience : the official journal of the Society for Neuroscience 24.

Martin CA, Myers KM, Chen A, Martin NT, Barajas A, Schweizer FE, Krantz DE (2016) Ziram, a pesticide associated with increased risk for Parkinson's disease, differentially affects the presynaptic function of aminergic and glutamatergic nerve terminals at the Drosophila neuromuscular junction. Exp Neurol 275 Pt 1:232-241.

Matei AM, Trombetta LD (2016) Exposure of rat hippocampal astrocytes to Ziram increases oxidative stress. Toxicol Ind Health 32:579-588.

Vannucchi M (2020) The Telocytes: Ten Years after Their Introduction in the Scientific Literature. An Update on Their Morphology, Distribution, and Potential Roles in the Gut. International journal of molecular sciences 21.

Middleton C, Nongthomba U, Parry K, Sweeney S, Sparrow J, Elliott C (2006) Neuromuscular organization and aminergic modulation of contractions in the Drosophila ovary. BMC biology 4.

Miller T (1975) Neurosecretion and the control of visceral organs in insects. Annual Review of Entomology 20:133-149.

Mostafalou S, Abdollahi M (2013) Pesticides and human chronic diseases: evidences, mechanisms, and perspectives. Toxicol Appl Pharmacol 268:157-177.

Nadim F, Bucher D (2014) Neuromodulation of neurons and synapses. Current opinion in neurobiology 29.

Niswender C, Conn P (2010) Metabotropic glutamate receptors: physiology, pharmacology, and disease. Annual review of pharmacology and toxicology 50.

Palmer MJ (2013) Cholinergic pesticides cause mushroom body neuronal inactivation in honeybees. Nature Communications 4:1634.

Pasternak A, Szura M, Gil K, Matyja A (2016) Interstitial cells of Cajal - systematic review. Folia morphologica 75.

Peron S, Zordan M, Magnabosco A, Reggiani C, Megighian A (2009) From Action Potential to Contraction: Neural Control and Excitation-Contraction Coupling in Larval Muscles of Drosophila. Comparative biochemistry and physiology Part A, Molecular & integrative physiology 154.

Reiner A, Levitz J (2018) Glutamatergic Signaling in the Central Nervous System: Ionotropic and Metabotropic Receptors in Concert. Neuron 98.

Rinetti GV, Schweizer FE (2010) Ubiquitination acutely regulates presynaptic neurotransmitter release in mammalian neurons. J Neurosci 30:3157-3166.

Rodriguez-Valentin R, Lopez-Gonzalez I, Jorquera R, Labarca P, Zurita M, Reynaud E (2006) Oviduct contraction in Drosophila is modulated by a neural network that is both, octopaminergic and glutamatergic. J Cell Physiol 209:183-198.

Steenland K (2014) Organochlorine chemicals and neurodegeneration among elderly subjects in Costa Rica. Environmental Research 134:205--209.

Sudhof TC (2013) Neurotransmitter release: the last millisecond in the life of a synaptic vesicle. Neuron 80:675-690.

Sudhof TC, Rizo J (2011) Synaptic vesicle exocytosis. Cold Spring Harb Perspect Biol 3.

Webb R (2003) Smooth muscle contraction and relaxation. Advances in physiology education 27.

Wicher D, Walther C, Wicher C (2001) Non-synaptic ion channels in insects--basic properties of currents and their modulation in neurons and skeletal muscles. Prog Neurobiol 64:431-525.

Xing X, Wu CF (2018) Unraveling Synaptic GCaMP Signals: Differential Excitability and Clearance Mechanisms Underlying Distinct Ca2+ Dynamics in Tonic and Phasic Excitatory, and Aminergic Modulatory Motor Terminals in Drosophila. In: eNeuro.

Yoshikawa S (2016) A subset of interneurons required for Drosophila larval locomotion. Molecular and Cellular Neuroscience 70.

Zhang B (2010) Electrophysiological recording from Drosophila larval body-wall muscles. Cold Spring Harbor protocols 2010:pdb.prot5487.

Zhang Z, Zhang S, Fu P, Lin K, Ko JK, Yung KK (2019) Roles of Glutamate Receptors in Parkinson's Disease. Int J Mol Sci 20.

Conclusions and Future Directions

In my doctoral dissertation I aimed to examine the modulation of neuronal and muscle function by the endogenous neurotransmitter glutamate and by the environmental toxicant ziram using two neuromuscular junction models in *Drosophila melanogaster*. The genetic accessibility, short lifespan, large numbers and low cost of Drosophila make them an especially good model to investigate toxicants linked to Parkinson's Disease (PD). Parkinson's Disease is less than 10% familial, highlighting the importance of environmental factors and there are likely many "hits" over the long course of the disease. While there are several proposed cell autonomous mechanisms such as mitochondrial dysfunction and oxidative stress by which toxicants may lead to PD, non-autonomous processes such as excitotoxicity are likely important pathways as well. We focused on ziram to investigate mechanisms important for Parkinson's Disease pathogenesis because it was shown in studies conducted by Dr. Ritz and colleagues at UCLA to be a risk factor for PD and our lab previously showed that ziram causes an increase in excitability at the larval NMJ aminergic terminals. We used ziram to explore both heavily studied and potentially new pathways that contribute to PD pathogenesis.

We found, using a combination of pharmacology and electrophysiology, that ziram increases spontaneous synaptic vesicle release, which is mimicked by inhibitors of the E1 ubiquitin activating enzyme, but not by proteasome inhibition. This result indicates that ziram disrupts protein ubiquitination pattern to alter the function of proteins rather than alter protein degradation. Experiments to test whether altering the pool of free versus bound ubiquitin leads to the same outcome will show whether this is a specific protein ubiquitination pattern effect or a broader ubiquitin cycle effect. Current experiments in the lab are examining the effect of mutations that block the ubiquitination of the synaptic protein VAMP2 to test for occlusion of ziram-induced increase in exocytosis. Further experiments screening for ubiquitin mutations in this and other synaptic proteins will help to determine the targets of ziram. It remains unclear

which aspect of the vesicle release process is disrupted; there are several steps required for synaptic vesicles to properly fuse upon stimulus, and vesicle recycling may influence synaptic release as well. These experiments would help elucidate the importance of ubiquitination in the modulation of synaptic release probability and how this process can be affected by toxicants.

While our findings indicate that ubiquitination is one process by which ziram increases minis, we did not rule out other mechanisms and the ubiquitin pathway drugs may not have had the same magnitude of effect as ziram. While these experiments are consistent with findings from cell cultures, it will also be important to use E1 ligase and other ubiquitination mutants to rule out off-target effects of the pharmacological agents we used, particularly because many of the drugs have been characterized in mammals rather than invertebrates. There may be multiple targets of ziram leading to increased minis and more experiments are needed to examine these mechanisms. Current experiments include screening other mutant lines that also alter mini frequency and testing for occlusion of ziram's effect, which will allow us to identify different pathways that may also be involved. While the other toxicants we tested did not have the same effect as ziram on synaptic release, it will be critical to determine what differentiates these compounds so that we may be able to predict other toxicants that do have similar effects.

At both the larval NMJ and adult CNS, ziram increased excitability at aminergic and glutamatergic neurons. While we found that eag mutants block and occlude this effect at glutamatergic synapses, it remains to be tested whether eag is also the excitability target in aminergic neurons. We hypothesize that ziram targets this same family of channels in all cells, and future experiments should use eag and sei mutants with a GCaMP or Arclight indicator to confirm this hypothesis. Critically, while our results strongly suggest that sei is blocked by ziram, we did not use the sei mutant to show occlusion of ziram and this remains to be tested. It is also unclear that ziram directly targets eag and sei channels or different proteins in the same

pathway, and we will need to test what its mechanism of block is as well. To answer these questions, current experiments in our lab use whole cell patch electrophysiology in cells expressing hEAG and hERG. These tests will help bridge the gap from fly to human channels. Further experiments in mammalian model animals and in other cell types such as cardiomyocytes will help us to understand the importance of ziram, and other compounds with similar targets, as risk factors for cardiovascular events, particularly in agricultural workers exposed to large quantities. Other follow up questions include looking at the risk for PD in human populations with mutations in hERG or related channels, which may help identify populations that are at a higher risk for toxicity. The incidence of arrhythmias or other heart conditions in populations working with ziram is another important question since hERG mutations are known to cause these conditions.

While we show that ziram acts on two separate pathways, there may still be overlap. One idea is that increased calcium in the cell leads to both increased vesicle release and eag channel inhibition, since the eag channel is known to be calcium sensitive in both mammals and flies. Although we observed an increase in excitability without mini frequency increase in mutant animals, the influence of calcium flux is on both of these processes remains to be tested with experiments that, for example, use calcium caging and calcium binding proteins.

Finally, I found that glutamate triggers a pattern of electrical activity in the common oviduct consisting of an initial depolarization and multiple bursts of depolarization events. Using pharmacology and electrophysiology, I observed that these two events can be separated out by blocking either metabotropic or ionotropic glutamate receptors, showing that these receptors interact to regulate common oviduct contraction. Since mGluR was found only in cells outside the muscle, and is expressed in a unique pattern that differentiates it from other neuronal processes present at the reproductive tract, we postulated that these cells have a unique role in

modulating muscle activity and integrate signals from neurons to the muscle. It remains to be determined whether the local mGluR cells have their own baseline rhythmic activity or become rhythmic in response to glutamate. Future experiments recording from these cells as well as stimulating them and recording the electrical activity in muscle are critical for determining the function of these local cells.

Importantly, we assumed that we were recording from the thin muscle cell layer because muscles are known to be electrically excitable similar to neurons and in the common oviduct we measured an increased calcium response. However, we need to test whether the activity we observe may actually be from recordings in the epithelial layer on the inside of the muscle layer since it was difficult to tell which layer the pipette tip was in. These two layers may also be electrically coupled or interact in an undefined way. To test this, we will use RNAi to inhibit either the epithelial or muscle cells and record from the oviduct. We can also record with a dye so that we can visualize where the pipette was localized. Further experiments ongoing in the lab will identify the cell type that mGluR is expressed in, which we predict will be glutamatergic or cholinergic, as these are excitatory transmitters with ionotropic receptors in flies. We also need to understand how the mGluR-expressing cells may be signaling to the muscle if these are indeed the repetitive activity- generating cells, and thus future experiments include testing for gap junctions and synaptic partners. This will help us to characterize the local mGluR cells, their presynaptic partners and how they signal to the muscle to regulate is activity. Identifying the markers and function of these cells may allow this system to model visceral muscle regulation in insects and perhaps vertebrates.

In conclusion, in this dissertation I have identified a unique target of the widely used pesticide ziram which may contribute to PD disease initiation or progression and may be an important target of several pharmaceutical and environmental compounds. Although the true importance

of hERG and other eag homologues in relation to PD remains to be elucidated, the data presented here provides a strong target to investigate, especially for patients prescribed drugs that interact with this channel and who may be at increased risk for PD. We also present a strategy to use toxicants like ziram as tools to identify complex disease mechanisms in an unbiased manner. In my second project, I suggest that there is an unexpected conservation of visceral muscle regulation by indirect signaling mediated via receptors in local neurons in *Drosophila*. While several critical experiments remain, these results are a crucial starting point for a more complete understanding of visceral muscle regulation in Drosophila and mammals.